MOUSE GENETIC MODELS OF COXSACKIEVIRUS B3 INFECTION

Sean Andrew Wiltshire,

DEPARTMENT OF HUMAN GENETICS,

MCGILL UNIVERSITY, MONTREAL

JANUARY 31ST, 2014

A thesis submitted to McGill University in partial fulfillment of the requirements of the degree of Doctor of Philosophy

ACKNOWLEDGMENTS

I would like to begin by thanking my supervisor Dr. Silvia Vidal for her mentorship and the opportunity to develop the work described within this thesis. I am profoundly grateful for her guidance, friendship and vision during the years spent in her laboratory.

I would also like to thank my supervisory committee composed of Dr. Philippe Gros, and Dr. Jamie Engert for their contributions over the years. I am indebted to Dr. J-C Loredo-Osti for introducing me to R, genetic analysis and statistics head first. And to Dr. Emil Skamene who was also a mentor and took his role to heart.

I am also grateful to have enjoyed the guidance and friendship of Dr. Agnieszka Kielczewska, Dr. Nassima Fodil-Cornu and Danica Albert; who taught me all the basics. I would like to especially thank Jennifer Marton for the many hours of collaboration, sharing ideas, sharing reagents, and for her unfailing humour and optimism. In particular, Jennifer is also recognized for her help in proof-reading much of this thesis. To Gregory Boivin for sharing an office space, and so many ideas. I am also grateful to Gabriel Leiva-Torres for his professionalism and his work in the CSS3 project. I must thank Benoit Charbonneau for his contributions beyond counting to various projects (and of course, friendship) throughout the years.

Special recognition is deserved by the animal health technicians who helped in managing all of the myriad strains and families of mice necessary to conduct this research. In particular: Patricia D'Arcy, Geneviève Perreault, Nadia Prud'homme, Vanessa Guay, Leigh Piercey-Brunet, Chantal Lacroix, Cynthia Villeda-Herrera, and Kathy Aubé.

I would like to thank the Honour students I have mentored over the years for their specific contributions to projects, and for providing me an opportunity to pass on some of what I have learned. In chronological order they were: Dr. Jessica Thoma, Dr. Han Yao and Dr. Emeric Bojarski, Jennifer Marton and Kenry Chiu.

I would like to express my appreciation for every other lab mate so far unmentioned, who were motivating, insightful and made the laboratory a home away from home. In no

particular order they were Dr. Michal Pyzik, Dr. Gregory Caignard, Dr. Julien Pothlichet, Peter Moussa, Maya Corminboeuf, Anne Dumaine and Eve-Marie Gendron-Pontbriand.

I was fortunate to receive technical assistance and expertise in histology from the Morphology Unit at the University of Ottawa, from Melina Narlis, Julie Hinsinger and Micheline Fortin at the Institute for Research in Immunology and Cancer (IRIC)at the Université de Montréal, and from Jo-Ann Bader at the McGill Cancer Centre.

Outside of McGill I was fortunate to collaborate with Dr. Kirk Knowlton, Dr. Toshitaka Yajima and Dr. Michinari Nakamura from the University of California at San Diego. I was also fortunate to collaborate with Dr. Douglas Marchuk and Dr. Hao Tang from Duke University. Last and not least, I was fortunate to work on the Recombinant Congenic Strains (RCS) with the many scientists of Emerillion Therapeutics including Dr. Eduardo Diez and Dr. Anny Fortin.

I would also like to thank my family. My parents and sister for supporting my efforts every step of the way. To my wife Amelia and to my dear little boy Felix: thank you for giving me the motivation to get through to the end, you both mean everything to me.

TABLE OF CONTENTS

LIST OF FIGURES

LIST OF TABLES

ABSTRACT

Coxsackievirus B3 (CVB3) is a relatively common cause of infection. Infection by coxsackieviruses is typically mild and resolves quickly without lasting complications. In a subset of individuals, coxsackievirus infection can be severe, leading to permanent damage of vital organs or even death. The mouse presents an ideal model to study natural variation in response CVB3 infection as human isolates of CVB3 productively infect the mouse, and lead to similar pathologies as found in humans. Inbred strains of mice respond differently to CVB3 infection, therefore the genetic background of the host can determine susceptibility to CVB3 infection. We hypothesize that interrogation of genetically determined susceptibility to CVB3 infection will help to identify genes whose direct involvement in control of CVB3 was previously unsuspected.

To characterize the contribution of host genetics to coxsackievirus, we screened a panel of recombinant congenic strains (RCS) generated from susceptible A/J and C57BL/6 progenitors. While most C57BL/6 background (BcA) strains were more susceptible than C57BL/6, BcA86 in particular was particularly susceptible to early lethality and hepatic necrosis. A segregating [BcA86xC57BL/10]F_2 mapping cross led to the identification of a locus on distal chromosome 13 controlling liver damage during coxsackieviral hepatitis. Previously through the analysis of a segregating we detected the *Vms1* (viral myocarditis susceptibility) locus on distal chromosome 3. *Vms1* controls viral replication, inflammation and necrosis within the heart during CVB3 infection. We have further refined this locus in additional mapping crosses and congenic lines of mice. We have also determined that *Vms1* controls viral replication before inflammation becomes evident within the heart. The cardiac specific kinase *Tnni3k* is a candidate gene for *Vms1*. We found that overexpression of TNNI3K greatly enhanced necrosis and inflammation in the heart following CVB3 infection. Furthermore, we found increased viral replication and gene expression and changes within isolated cardiomyocytes, indicating TNNI3K is implicated in a heart specific immune pathway. Altogether, our results provide new functional insight into the host determinants of pathogenesis following infection with coxsackievirus B3.

RÉSUMÉ

Les virus Coxsackie du groupe B3 (CVB3) sont retrouvés partout dans le monde et il y a une prévalence saisonnière. L'infection par CVB3 se manifeste de manière différente selon les personnes. Certains individus ne développent pas de maladies cliniquement apparentes et guérissent spontanément, tandis que d'autres risquent de développer des complications plus sévères comme des affections cardiaques, des hépatites où des atteintes du système nerveux central. Les cas les plus graves peuvent entraîner la mort du sujet. La souris de laboratoire constitue un modèle idéal pour étudier les mécanismes inhérents à ces formes diverses des maladies induites par l'infection. En effet, des lignées des souris consanguines peuvent être infectées expérimentalement avec des souches humaines du virus CVB3. Les lignés des souris présentant un large spectre des signes cliniques indique que la constitution génétique des individus infectés est un facteur déterminant dans la gravité de l'infection. Nous avons donc formulé l'hypothèse que l'investigation des facteurs génétiques étant à l'origine de la réponse de l'hôte à l'infection par CVB3 devrait nous conduire à identifier des gènes et des mécanismes moléculaires directement impliqués dans le contrôle de cette infection dont on n'aurait pas eu connaissance dans le passé.

Dans le but de mieux cerner la contribution des facteurs génétiques de l'hôte dans l'évolution de l'infection par CVB3, nous avons utilisé une approche de cartographie génétique. En ce sens, nous avons examiné une collection des lignées de souris recombinantes consanguines (RCS) issues des lignées parentales A/J et C57BL/6. Nous avons constaté que la plupart des lignées BcA (dont le fonds génétique est majoritairement issu de la lignée C57BL/6) présentaient une susceptibilité accrue en comparaison à C57BL/6. Dû à son taux précoce de mortalité, la lignée BcA86 a été particulièrement visée. En ayant recours à un croisement (BcA86 x C57BL/10)F_2 il nous a été possible de détecter un locus dans la région distale du chromosome 13 liée à la sévérité des lésions du foie pendant l'hépatite coxsackievirale.

Une étude préalable de liaison génétique, nous avait permis de mettre en évidence le locus *Vms1* (viral myocarditis susceptibility) dans la région distale du chromosome 3. Le

locus *Vms1* est responsable du niveau de la réplication virale, de la nécrose du myocarde et de l'infiltration cellulaire que l'on observe dans le cœur des souris infectées par CVB3. En étudiant des lignées de souris consomiques ainsi qu'en réalisant de nouveaux croisements entre souris sensibles et souris résistantes, nous avons élaboré une cartographie fine de l'intervalle critique contenant le locus *Vms1*. Aussi avons-nous pu constater que le contrôle de la multiplication virale par *Vms1* précède l'infiltration des cellules inflammatoires dans les tissus cardiaques.

Le gène *Tnni3k* code pour une kinase dont l'expression étant spécifique aux cellules cardiaques apparaît comme un gène candidat de choix pour le locus *Vms1*. En comparant avec les souris normales, nous avons trouvé que la surexpression du gène *Tnni3k* dans des souris transgéniques leur confère un phénotype de nécrose et d'inflammation extrêmes du tissu cardiaque suite à l'infection par CVB3. Nous avons également établi que l'infection des cardiomyocytes isolés à partir de ces mêmes souris provoque un accroissement de la réplication du virus CVB3 ainsi qu'un profil d'expression unique des gènes inflammatoires. Les résultats ainsi obtenus ont mis en lumière que la kinase TNNI3K est impliquée dans un circuit de signalisation immunitaire propre au cœur. Ainsi, pris dans leur ensemble, nos travaux apportent des nouvelles voies pour la compréhension du déterminisme génétique de l'hôte dans la sensibilité aux infections par CVB3 ainsi qu'une meilleure connaissance de la pathogénèse de ce virus dévastateur.

PREFACE AND CONTRIBUTIONS OF AUTHORS

This thesis is composed of 5 chapters including a literature review, three original manuscripts, and a general discussion. One of the three manuscripts has been published and the other two are to be submitted shortly. A statement has been included in order to bridge the materials presented in each chapter. I, Sean Wiltshire, under the supervision of Dr. Silvia Vidal, have designed, performed and analyzed the experiments described, unless otherwise indicated. The co-authors listed below contributed as follows:

Chapter 2: Mapping of a quantitative trait locus controlling susceptibility to coxsackievirus b3 induced viral hepatitis.

Sean A. Wiltshire, Jennifer Marton, Gabriel André Leiva-Torres, and Silvia M. Vidal

Jennifer Marton performed many of the plaque assays from the [BcA86xB10]F_2 shown in Figures 3 and 5. Gabriel Leiva-Torres participated in the identification and verification of polymorphic SNPs between C57BL/6 and C57BL/10. Patricia D'Arcy assisted with all infections and necropsies. Jennifer Marie Brecht measured serum ALT at the McGill Diagnostic and Research Support Service. I was responsible for the rational, experimental design and performance, data analysis, as well as the writing of the manuscript.

Before summarizing chapter 3, it is worth mentioning my contributions to the original publication "**Complex genetic control of host susceptibility to coxsackievirus B3-induced myocarditis**", which I co-authored with Mahmoud Aly and forms the base for our subsequent studies. In this 2007 publication I performed: most of the genotyping on chromosomes 1, 3 and 4; all of the data analysis in collaboration with JC Loredo-Osti, and I wrote the manuscript under the supervision of Dr. Silvia Vidal. Mahmoud Aly performed the phenotyping experiments, and the genotyping shown in figure 5.

Chapter 3: Quantitative trait locus analysis, pathway analysis, and consomic mapping show genetic variants of Tnni3k, Fpgt, or H28 control susceptibility to viral myocarditis.

Sean A. Wiltshire, Gabriel André Leiva-Torres, and Silvia M. Vidal

At the time of publication, Gabriel Leiva-Torres was a research assistant in the Vidal laboratory. Gabriel contributed technical support including figure 1, and was an equal participant in creation and infection of the [CSS3xB6]F_2. We also jointly prepared high-molecular weight DNA for the diversity chip. I was responsible for the rational, experimental design and performance, data analysis, as well as the writing of the manuscript.

Chapter 4: TNNI3K modulates cardiomyocyte innate immunity during viral myocarditis

Sean A. Wiltshire, Jennifer Marton, Hao Tang, Douglas Marchuk, and Silvia M. Vidal

At the time of writing, Jennifer Marton was a PhD student in the Vidal lab. Jennifer provided technical assistance, and contributed ideas helping to form the rational for this publication. Douglas Marchuk and Hao Tang provided the TNNI3K^{tg} mice. I was responsible for the rational, experimental design and performance, data analysis, as well as the writing of the manuscript.

I have collaborated in a study led by Yu Xia in the laboratory of Bruce Beutler wherein the authors made use of the C57BL/6 vs. C57BL/10 panel described in chapter 2: *Yu Xia, Sungyong Won, Xin Du, Pei Lin, Charles Ross, Diantha La Vine, Sean Wiltshire, Gabriel Leiva, Silvia M. Vidal, Belinda Whittle, Christopher C. Goodnow, James Koziol, Eva Marie Y. Moresco and Bruce Beutler* **Bulk segregation mapping of mutations in closely related strains of mice**. Genetics, (2010). 186(4), 1139–1146.

I was involved in the same capacity in a study of Jak3 mutation in cerebral malaria led by Dr. Silayuv Bongfen in the laboratory of Dr. Philippe Gros. *Silayuv E. Bongfen, Ian-Gael Rodrigue-Gervais, Joanne Berghout, Sabrina Torre, Pablo Cingolani, Sean A. Wiltshire, Gabriel A. Leiva-Torres, Louis Letourneau, Robert Sladek, Mathieu Blanchette , Mark Lathrop , Marcel A. Behr , Samantha Gruenheid , Silvia M. Vidal , Maya Saleh ,Philippe Gros*. **An N-Ethyl-N-Nitrosourea (ENU)-Induced Dominant Negative Mutation in the JAK3 Kinase Protects against Cerebral Malaria**. (2012) PLoS ONE, 7(2), e31012

I collaborated with Dr. Eduardo Diez in a study on the genetics of HDL cholesterol, where I performed the data analysis, made the figures and wrote the publication. Eduardo Diez under supervison from Anny Fortin conceived of the rational, and experimental design. Qianqian (Dory) Miao under supervision from Momar Ndao, performed ApoA1 western blots. *Sean A. Wiltshire, Eduardo Diez, Qianqian Miao, Marie-Pierre Dube, Mireille Gagne, Olivier Paquette, Ronald G. Lafrenière, Momar Ndao, Lawrence W. Castellani, Emil Skamene, Silvia M. Vidal and Anny Fortin* **Genetic Control of High Density Lipoprotein (HDL)-Cholesterol in AcB/BcA Recombinant Congenic Strains of Mice** Physiol Genomics. 2012 Sep 1;44(17):843-52

I collaborated with Erin Lafferty in a still unpublished study of the susceptibility of Unc93b1$^{-/-}$ mice to CVB3 infection, where I designed and performed all experiments, data analysis, and conceived the rational behind experiments. Erin Lafferty provided Unc93b1$^{-/-}$ mice, was present for experiments, and independently replicated selected experiments: *Sean A. Wiltshire*, Erin Lafferty*, Salman Qureshi and Silvia M. Vidal*. **Effective control of coxsackievirus B3 infection requires Unc93b1 in the heart, but not in the periphery.** Manuscript in preparation.

I contributed to a study of Trypanosoma cruzi infection where I supplied mice, primers and helped design experiments: **Biological validation of T cruzi diagnostic biomarkers in human transgenic mouse model** *Qianqian Miao, Sean Wiltshire, Annie Liang, Brian Ward, Momar Ndao.* Manuscript in preparation.

I contributed to a study of Abcc6 and its role in myocardial calcification led by Jennifer Marton. **Positional identification, functional characterization and therapeutic targeting of a new coxsackievirus susceptibility gene: *Abcc***, *Jennifer Marton, Danica Albert, Sean A. Wiltshire, Robin Park, Arthur Bergen, Salman Qureshi, Danielle Malo, Yan Burelle, and Silvia M. Vidal.* Manuscript in preparation.

I contributed to a study of *Sh2d2a* and its role in immunity to several viruses led by Peter Moussa. **The role of *Sh2d2a* in antiviral immunity**, *Peter Moussa, Greger Abrahamson, Nassima Fodil-Cornu, Gregory Caignard, Sean A. Wiltshire, Gregory Boivin and Silvia M. Vidal.* Manuscript in preparation.

I have also co-written a book chapter on the immunogenetics of viral pathogenesis, which provides a holistic approach to describing the effects of known genetic variations on the immune response to viral infection. *Sean Wiltshire, David I. Watkins, Emil Skamene and Silvia Vidal*. **Immunogenetics of virus pathogenesis** In **The Immune Response to Infection**, ASM Press, American society for Microbiology (2011); edited by Stefan H.E. Kaufman, Barry T. Rouse, and David L. Sacks.

I, Sean Wiltshire, have read, understood and abided by all norms and regulations of academic integrity of McGill University.

CHAPTER 1: GENERAL INTRODUCTION

INTRODUCTION

Viral infections are a near ubiquitous part of life, and the outcome of infection varies widely. Viral infections are sometimes benign, and other times can cause permanent damage or death to the infected host. Though remarkably diverse, viruses are all obligate parasites, which invade a host cell in order to replicate. After entering a host cell, viruses subvert, exploit and appropriate host cellular components in order to replicate. Lytic viruses such as the coxsackieviruses conclude this process by coordinating a necrotic death of the host cell, wherein disruption of the cellular membrane allows the release of newly synthesized infectious coxsackievirus. Viral proteins, and features of the viral life cycle are thus central determinants of the severity of infection. Equally influential on the severity of infection are host determinants. A host response is initiated via direct or indirect sensing of viral infection, and communicated to neighbouring cells and distal tissues. A molecular and cellular response with the aim of limiting, sequestering and eventually sterilizing infection is generated. Other host factors such as cell specific structures, or the presence and accessibility of viral receptor may also determine whether a coxsackievirus infection follows a mild or severe course. Identification and understanding the host determinants of Coxsackievirus B3 infection form the subject of this dissertation.

COXSACKIEVIRUS INFECTION

THE ENTEROVIRIDAE

Coxsackievirus B3 (CVB3) is a subspecies of coxsackievirus, the coxsackieviruses are a species of the genus *Enterovirus*, and the enteroviruses are part of the *Picornaviridae* family. The *Picornaviridae* family of viruses, from *pico* (meaning small) and RNA (for their genome), are defined by their small and single stranded RNA based genome. Picornavirus genomes range between 7 and 8.5kb in length, and are composed entirely of a single coding strand of RNA. Common features within the *Picornaviridae* include a

non-enveloped viral particle with icosahedral capsid. Though viral receptors vary across species and genera, the genes encoded by a picornavirus are relatively conserved. The entire genome is translated as one large polyprotein starting from a non-canonical translation initiation mechanism called an internal ribosomal entry site. The picornaviral polyprotein subsequently processes itself into functional proteins, and genomic RNA replication occurs via a virally encoded RNA dependent RNA polymerase. Picornaviruses are lytic to the infected cell, replicate to high titers and cause a wide range of pathology in their infected hosts.

Notable picornaviruses include the *Rhinovirus* genus. Rhinoviruses replicate preferentially in the upper respiratory tract at lower temperatures (34ºC). Rhinoviruses are thought to be responsible for many if not most cases of the common cold. The *Rhinovirus* genus contains over 100 serotypes; though species are closely related infections across serotypes do not provide serological immunity against other rhinovirus serotypes. This feature, when combined with other genetic attributes of the *Picornaviridae* discussed below help to explain why a vaccine against the common cold is particularly challenging. The *Picornaviridae* also include the *Hepatovirus* genus, which includes the hepatitis A virus. Hepatitis A is a common cause of viral hepatitis transmitted through fecal oral route particularly in contaminated food and water. Hepatitis A is one of the two targets of the popular divalent travel vaccine Twinrix, the other being Hepatitis B virus. Unlike the blood borne Hepatitis B and Hepatitis C viruses, hepatitis A does not generally lead to chronic disease, and is usually self limiting.

The genus *Enteroviridae* within the *Picornaviridae* family represents a diverse subset of pathogens. Common features of enteroviruses include fecal oral transmission and an unusually high tolerance to low pH and harsh conditions. This pH insensitivity allows enteroviruses access to the small intestine where they replicate to high titers. These titers then permit the virus to propagate itself when stool contaminates food or water. The most infamous member of the *Enteroviridae* is the poliovirus. In addition to infecting the small intestine like other enteroviruses, poliovirus can spread to motor neurons. Inflammation and necrosis of the motor neurons occurring as a result of poliovirus infection (poliomyelitis) can lead to paralysis and sometimes death. The quest for a

vaccine to poliovirus in the 1940s and 1950s spurred several advances in virology and cell culture, including the discovery and characterization of coxsackievirus (more below). Vaccination against polio has been a near complete success, following the widespread deployment of an inactive vaccine in the mid 1950s and the live attenuated oral vaccine that was licensed for use in the early 1960s. Perhaps coincidentally, the period immediately following the successful deployment of the polio vaccines coincided with a dramatic uptick in publications mentioning Coxsackievirus [Figure 1].

FIGURE 1: ARTICLES PUBLISHED MENTIONING COXSACKIEVIRUS

Articles indexed by pubmed at the National Center for Biotechnology Information (http://www.ncbi.nlm.nih.gov/pubmed) mentioning coxsackievirus, rhinovirus, hepatovirus, enterovirus, and “polio OR poliovirus”. The number of articles mentioning polio or poliovirus drops from 678 in 1964 down to 419 in 1966, while publications mentioning coxsackievirus or enterovirus increased from 227 and 214 in 1962 up to 515 and 444 in 1964. Following this period, publications level off until recently, when new interest seems to have emerged in the field of all forms of enteroviral research.

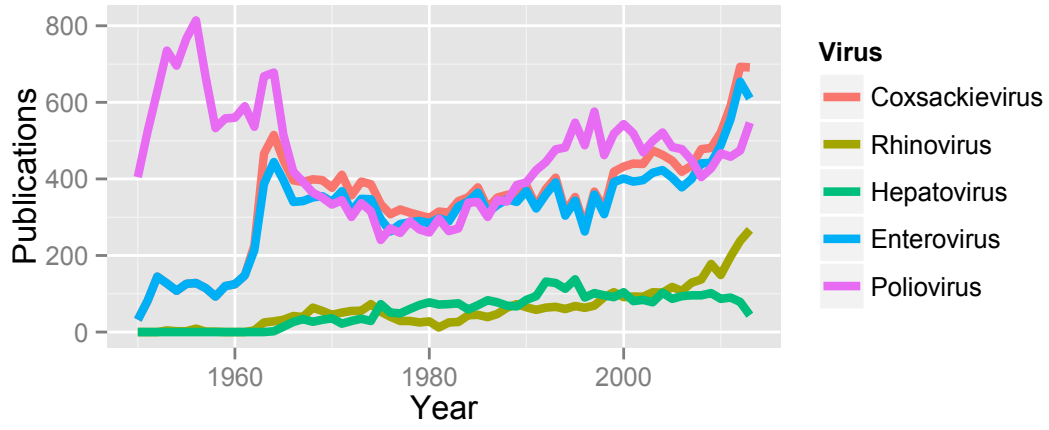

Mostly owing to the complication of assigning distinct species status on the basis of clinical features alone, all newly identified and serologically unique enteroviruses identified following 1970, are assigned a numeric designation starting with 68 (e.g.: human enterovirus 68 or EV68). One such new member is the human enterovirus 71,

which causes severe neurological damage and in some portion of infected individuals infection is lethal (1, 2). The severity of EV71 infection have led some to term it the “new polio”. Though EV71 was originally isolated in California, its notoriety is due to a rapid spread through Asia where it remains a persistent cause of disease (3). Ongoing research is being conducted to identify a safe and effective vaccine to EV71 (4-6).

HISTORICAL PERSPECTIVES ON COXSACKIEVIRUS

Late in the summer of 1947, a 3-year-old, and a 9-year-old boy with flu-like symptoms accompanied by severe muscle pain, were presented to a physician in Coxsackie New York. An infectious agent was identified within the stool of the young boys that could pass through a filter and retain infectivity, could not be grown on an agar plate, but could be cultured by infecting suckling mice or hamsters under 12 days old. Several features distinguished the virus from other known viruses including lack of neutralization by serum from mice infected by other viruses, and an intense necrosis of muscle tissues. This original isolation by Gilbert Dalldorf and Grace M. Sickles(7) would prove to be a seminal discovery and this particular viral isolate would come to be known as Coxsackievirus A. A second notable pioneer in coxsackievirus research was the group of JL Melnick, who isolated and characterized what would come to be called Coxsackievirus B(8).

The Coxsackieviruses were subdivided into A and B types based on pathology induced in suckling mice (9). Coxsackie A types were described as producing a flaccid paralysis and myositis. B types were described as producing spastic paralysis and tremors. Human disease was confirmed via repeated clinical isolation, and occasionally by accidental laboratory acquired infections(10, 11). Indeed, the commonly used laboratory strain of CVB3 (CVB3-Nancy), is an isolate obtained from the stool of JL Melnick’s daughter Nancy after a laboratory acquired CVB3 infection spread through the researcher’s family(12). Though early Coxsackievirus research was focused primarily on similarities with poliovirus and neurological features, Coxsackieviruses were also found to infect the heart, liver, lungs, skeletal muscle, fat pads, and pancreas(13). In hindsight, the focus on neurological symptoms of the viruses isolated may have

reflected the public interest in polioviruses at the time, and inoculation of coxsackievirus for testing in mouse strains was routinely performed via an intracerebral route. As clinical isolates continued to accumulate, subsequent decades saw a convergence of opinion that Coxsackievirus group B frequently led to myocarditis, especially in newborns and young adults(14, 15). Experimental models of Coxsackievirus induced myocarditis were lacking however until JF Woodruff developed a myocarditic strain of CVB3 (CVB3m)(16, 17). Woodruff also learned that the mode of passage of the virus (intraperitoneal vs. intracerebral) had an effect on the tissue specificity of pathology which would develop on subsequent inoculations of the virus(15). Woodruff's CVB3m was originally a CVB3-Nancy strain (18) and the CVB3m strain has since been passaged by several other labs including Charles Gauntt whose passages became the CVB3-CG strain(19, 20). Another CVB3m lineage from the group of Sally Huber was purified from a single plaque(21) and cloned into the also widely used cDNA copy CVB3-H3(22). This lineage means that all subsequent sub-lineages and most work on CVB3 over the preceding 60 years has been performed using virus isolated from one 8-year old girl named Nancy in May of 1950.

Following early hints that virulence was specific to an individual viral isolate or viral passage, Charles Gauntt's group formally demonstrated that virulence could be modulated within a given strain of CVB3 by creating temperature sensitive mutants(23, 24). The role of host genetics would come later in the form of a series of strain surveys comparing mouse genetic background as well as major histocompatibility locus (*H2*)(25-27). Together, these studies provide the theoretical framework on which this thesis is founded: a combination of host and viral genetics determines the pathological outcome of disease. A myocarditic sub-sub-strain of CVB3 Nancy was used in all experiments in order to further interrogate the role of host genetics on CVB3 infection.

COXSACKIEVIRUS WITHIN HUMAN POPULATIONS

Coxsackievirus B3 is a common infection. Estimates place it as being responsible for somewhere between 3 and 9% of identified enteroviral infections. Though, CVB3 is rarely the most commonly identified enterovirus, it is usually one of the top 10 species

identified during enteroviral surveillance(28, 29). Enterovirus infection, and in particular CVB3 infection, follows an epidemic pattern with sudden increases in the number of identified viruses during routine enteroviral surveillance. Infection with CVB3 often follows a late summer pattern, with up to 78% of infections occurring between June and October, though this varies from year to year. The mechanism of this epidemic introduction is unclear, though the enteroviruses primarily fecal oral route of transmission and coincidence with a peak epidemic occurrence during warm summer months might suggest water contamination as a key factor. CVB3 infections are frequently severe. While not every infection is reported, among those that are approximately 5% of positively identified infections are fatal (30, 31).

Severe complications of CVB3 infection are surprisingly diverse and include meningitis, myocarditis, hepatitis, and renal failure(32). In newborns, severe cases of viral hepatitis are periodically reported as a result of group B Coxsackieviruses including CVB3 (33-35). Meningitis remains a frequently reported severe outcome of CVB3 infection in patients under the age of 15 (36). Viral myocarditis is a frequent underlying cause in sudden and unexpected death, where otherwise healthy individuals die suddenly and without an obvious cause (37). Estimates vary, but between 10 and 20% of sudden and unexpected deaths are attributable to viral myocarditis(15, 38). The proposed etiology of death has been suggested to be due to arrhythmia owing to cardiomyocyte necrosis(39). Results vary, but up to 50% of suspected myocarditis may be attributable to enteroviral infection(40). The development of a chronic form of disease, dilated cardiomyopathy will be dealt with in a subsequent section due to the lingering ambiguity regarding causality of coxsackievirus infection in the condition(41).

Due to the dependence of CVB3 severity on both viral genetic and host genetic factors, as well as the epidemic nature of outbreak, it is not surprising that outbreaks of myocarditic strains of CVB3 also occur. One such outbreak occurred in Greece in 2002 where fifty-one cases of myocarditis or pericarditis were diagnosed, following onset of viral infection and three adult women (ages 48, 48 and 50) died of heart failure (42). Subsequent to the cluster of myocarditis and cluster of lethal infection in Greece a broad seropositivity study of 501 individuals determined that 9-21% of the population

had specific antibodies to given CVB strains (43). Another study, based on a cohort in northern England (EPIC-Norfolk), found serological evidence in the range of 50-70% depending on age and viral serotype tested (44). The correct figure for the human population at large likely depends on location, sanitation and other unknown factors. Whether the actual exposure level to CVB3 is closer to 10% of the population or 70%, infections severe enough to be reported must be in the minority, and of those, severe complications appear to occur only in a rare cases.

COXSACKIEVIRUS LIFE CYCLE

ATTACHMENT AND ENTRY

The coxsackievirus gains access to the cell by binding to its specific receptor, the Coxsackievirus and Adenovirus Receptor (CAR, encoded by the *Cxadr* gene). CAR was identified by two groups within months of each other in 1997, first by Bergelson et al. (45) and then shortly after by Tomko et al. (46). CAR was discovered first as a viral receptor, and its role in the normal cell was initially unclear. Subsequently, CAR has been first determined to be a component of the tight junction, those intercellular contact points which turn groups of cells into impermeable barriers (47). CAR deletion resulted in embryonic lethality and altered morphology of embryonic cardiomyocytes (48). This result was confirmed in a heart specific CAR deletion under the control of the myosin heavy chain promoter, where lethality from pericardial edema, and hyperplasia of the cardiomyocytes was observed (49). After embryonic development, CAR expression gradually decreases and shifts to the intercalated disc (50). Inducible deletion of CAR in adult mice also had a severe effect: loss of CAR in the heart led to complete atrioventricular (AV) block, a severe disorder of conduction between the atria and ventricles of the heart. The mechanism proposed for the AV block involves the altering of AV node gap junctions, an intercellular electrical conduction system reliant on connexins (51, 52). Taken together, CAR is a tight junction protein that is essential for cardiac embryonic development, and AV conduction in the adult heart.

Given that the primary site of replication for CVB3 is the polarized epithelium of the intestinal tract, CAR is a curious viral receptor because it is normally inaccessible within

the tight junction. Coxsackievirus is also able to bind decay accelerating factor (DAF, encoded by the *Cd55* gene) as a co-receptor(53). Through its interaction with DAF, CVB3 engages activity of cytosolic GTPases Abl and Rac which reconfigure the actin cytoskeleton and move CVB3 to the tight junction(54, 55). CVB3 also appears to make use of the tight junctional protein occludin (*Ocln*) as virus is internalized with occludin and inhibition of occludin expression also blocks CVB3 entry(56). Following attachment to the CAR receptor, virus is internalized via a caveolin dependent mechanism that resembles macropinocytosis in polarized cells. In non-polarized cells, viral entry occurs via a dynamin and lipid raft dependent mechanism for which DAF is dispensable(57). Other host derived factors required for attachment, entry and replication surely exist. A recent study using RNAi inhibition of host genes found that 46 genes were essential for infection by both poliovirus and CVB3, and that 28 were essential for CVB3 alone (including *CXADR*)(58).

POLYPROTEIN PRODUCTS

Though picornaviruses have specific receptors, their genomic organization post entry are highly similar within and across genera (40). Most of enterovirus virology was originally studied within poliovirus strains, and the highly related coxsackievirus is assumed to be similar (59). Following entry, the viral genome is released into the cell as a single strand of RNA. This RNA strand does not contain the usual 5’ cap that protects cellular mRNA from degradation and promotes translation initiation. Instead a large (750bp) and highly complex 5’ untranslated region (UTR) structure serves as an internal ribosomal entry site (IRES) to initiate translation(60). The origin of IRES sequences appears to be cellular: several growth factors, transcription factors, translation factors, transporters and other genes, all contain IRES sites (61).

The genome of a picornavirus (including enteroviruses such as coxsackievirus) maintains a conserved organizational hierarchy(59, 62). Once the IRES initiates translation of the positive sense genome, the entire coding sequence is translated into one large polyprotein of ~250kDa. This polyprotein is conceptually subdivided into three regions. The P1 region contains the viral structural proteins including capsid proteins VP1, VP2, VP3 and VP4. The P2 and P3 regions contain non-structural proteins. P2

contains the protease 2A, the 2B porin and the vesicle forming protein 2C. P3 contains the 3A protein, which inhibits cellular trafficking, 3B which is integral for priming viral RNA synthesis, a second protease 3C, and the highly conserved RNA dependent RNA polymerase 3D. The polyprotein is cleaved in *cis* by the 2A and 3C genes, the 2A protease cleaves P1 from P2/P3 and 3C cleaves the others into separate functional proteins. Further complicating this compact genome, 2BC (uncleaved 2B and 2C), 3AB (3A and 3B) and 3CD (3C and 3D) all have ancillary functions independent of their cleaved forms. Following proteolytic maturation of the viral polyprotein, a replication complex is formed where the RNA dependent RNA polymerase 3D first synthesizes a negative strand replication intermediate. This anti-sense genome serves as a template for further replication of the positive sense genome.

REPLICATION

Autophagy is an intracellular degradative pathway that plays an essential role in cellular homeostasis. Autophagy is essential for clearing certain forms of infection, is engaged during a stress response and is the cellular process for eliminating damaged organelles and protein aggregates. A specialized organelle is formed consisting of a dual membrane complexed with the light chain 3 protein (LC3 also known as ATG8). This membrane engulfs the material targeted for degradation, and acidifies into an amphisome. The amphisome fuses with lysosome to form the autolysosome where degradation occurs(63-65). Positive strand RNA viruses appear to exploit autophagic machinery for facilitating their replication. CVB3 induces formation of autophagosomes in infected cells *in vitro*, but not autophagolysosomal protein degradation. Blocking of autophagy chemically or through small interfering RNA (siRNA) decreases viral replicative capacity, and inducing autophagy chemically, or through starvation increases viral replication. Blocking fusion of amphisomes with lysosomes also increases viral replication showing that some autophagolysosomal degradation is still occurring(66, 67). These results are confirmed in pancreatic cells in vivo, with the further observation that the autophagic vesicles exhibit a lattice structure which could correspond to the CVB3 3D and replication complex (68, 69). During poliovirus infection it has been

demonstrated that acidification of the autophagic vacuole is required for maturation of virus into an infectious form (70).

The role of specific lipids as scaffolds during viral replication is coming to light in recent years. Replication occurs on a virus specific organelle within the cell where the replication complex is formed. This complex is specifically enriched in phosphatidylinositol 4-phosphate (PI4P), and PI4P is essential for viral replication (71, 72). Viral replication organelles are also enriched with cholesterol. Plasma membrane cholesterol is internalized via clathrin-mediated endocytosis, and directed to replication organelles during infection. Depletion of plasma membrane cholesterol dramatically reduces viral replication efficiency (73).

Replication of genetic information in lytic RNA viruses, such as CVB3 or poliovirus, is also notable in that the error rate of the RNA dependent RNA polymerase is exceptionally high(74-76). Viral RNA dependent RNA polymerases (such as 3D) do not contain proof-reading activity, and make on average one error per replication cycle. As each infected cell produces between 10^4 and 10^5 pfu following infection this amounts to a considerable diversity. In this light the meaning of any single viral species must be placed into context as part of larger quasispecies (77-79). Indeed, quasispecies diversity has been experimentally demonstrated to be an essential feature required for pathogenesis. The key experiments involved a cDNA clone of poliovirus with a single point mutation that was found to lead to greatly reduced error rates during RNA replication (0.31 mutations per genome *vs*. 1.91 in wild type). Infection with this faithful polymerase (mutation G64S) required an initial dose 100-fold higher than wild-type in order to achieve lethality. The high fidelity virus was also unable to replicate in brain or spinal cord tissue to any significant extent. Artificially restoring quasispecies diversity through drug treatment in G64S virus restored virulence. Conversely, an attenuated high-fidelity virus was less likely to revert than wild type, and could form the basis for a vaccine strategy (80, 81). Genomic instability provides clear advantages including the above mentioned tissue adaptability, because mutations required for access to new tissue sites are already contained within the quasispecies population and are fit to replicate immediately. However, there is a threshold of how many mutations can occur

per average replication beyond which genetic information becomes garbled and the quasispecies population collapses in what is called “error catastrophe”. Mutagens have been used to demonstrate that the $3D^{pol}$ mutation rate edges on the border of error catastrophe and pushing them over this limit is an effective antiviral strategy(78, 79, 82).

INTERACTION WITH THE HOST CELL

A variety of viral interactions with host cell proteins and processes have been characterized. Given that viral translation occurs via a cap independent process, the virus is able to target host cell translation machinery without affecting its own replicative capacity. The viral 2A protease has been shown to cleave the elongation initiation factor 4g (eIF4G), a protein that brings 5’capped cellular mRNAs (bound to eIF4E) into contact with the ribosome for translation (83-85). In this way, 2A is sufficient to arrest host cell translation. Host cell translation is further abrogated through the cleavage of the poly(A)-binding proteins (PABP), by protease 3C. PABP proteins associate with the poly(A) tail of cellular mRNAs (86, 87). 3C cleavage of PABP appears to occur most efficiently with PABP associated with ribosomal polysomes compared to other cellular fractions containing PABP. In this way PABP levels in the cell are maintained, while PABP dependent host translation is minimized(87). As viral proteins accumulate within the cell, and PABP is depleted, cap independent viral translation is also inhibited. This is thought to effect a switch in viral replication from early to late and allow accumulation of viral RNA for assembly into virions (88).

Shutoff of transcription of host genes also occurs during enterovirus infection. As transcription is a nuclear phenomenon, and CVB3 spends its life cycle within the cytoplasm this is a particular challenge. The 3CD protein contains a nuclear localization signal within the 3D portion of the protein(89, 90). The nuclear localization signal is absolutely required to traffic 3CD to the nucleus, however it was also shown that in the absence of a concurrent infection 3CD or 3D alone were not able to enter the nucleus. This suggests some other factor’s involvement in arresting host cell transcription (90). Once it is within the nucleus, the 3CD is autocataclytically processed into the 3C protease. The 3C protease in turn inhibits transcription initiation by directly cleaving several transcription factors including TBP, CREB, OCT1, and others (91, 92).

The 2B protein has been shown to act as a viroporin. 2B expression leads to permeabilization of the plasma membrane, which facilitates viral release(93, 94). 2B oligomerizes within its target membrane and creates an aqueous pore capable of disrupting ion gradients(95). 2B and 2A proteins both inhibit the host cell secretory apparatus as well. Counter intuitively, the 2B protein is primarily localized within the ER and Golgi complex rather than the plasma membrane during plasma membrane permeabilization. Furthermore, it was shown that ER localization is dispensable for plasma membrane permeabilization while Golgi complex localization was essential. This also has the effect of inhibiting host protein transit. How a viroporin within the Golgi permeabilizes the plasma membrane is still unclear(96). Expression of 2B was also sufficient to decrease calcium stores in the ER and Golgi. This effect coincided with a suppression of caspase activity and apoptic cell death. Furthermore, mutants defective for calcium release did not block apoptosis, suggesting that 2B plays an anti-apoptotic role during infection(97).

In addition to the above mentioned functions, 2A also cleaves dystrophin, a key structural protein of the heart(98). Dystrophin is the largest gene within the human genome, and anchors the cytoskeleton to the sarcoplasmic membrane. Dystrophin is located near intercellular contacts, and is thought to play a protective role during muscle contraction(99). This is a significant result in mechanistically tying viral myocarditis to dilated cardiomyopathy. Dilated cardiomyopathy is frequently reported in patients with dystrophin deficiency (Duchenne muscular dystrophy), and 2A expression alone is sufficient to cause dilated cardiomyopathy(100).

CELL DEATH: NECROSIS, NECROPTOSIS AND APOPTOSIS

Cell death has been a particularly lively field of research in recent years, as the understanding that the molecular contexts of a dying cell can dramatically alter subsequent immune responses and determine disease(101-103). Broadly, cell death can be categorized as regulated, or unregulated. Unregulated cell death is thought to be passive process wherein the plasma membrane is disrupted. As osmotic differences between intracellular and extracellular milieus are removed, ATP is depleted, necrotic cells become swollen, and their contents leak out. At the other end of the spectrum is

apoptosis, a programmed cell death characterized by shrinkage of the cytoplasm, nuclear condensation and cellular fragmentation. The cytosol is packaged up in bulges (blebs, or apoptotic bodies) from the plasma membrane so that cytosolic components for the most part do not come into contact with the extracellular milieu. Apoptotic bodies are then internalized by other cell types including macrophages, are degraded and generally are not interpreted as an inflammatory signal. Apoptosis can be induced via extrinsic factors (cellular receptors), or by intrinsic factors (no external signal required). The extrinsic pathway involves the activation of death domain containing receptors and triggering of a signaling cascade that converges on the mitochondria. The mitochondria contents become released, and this triggers a second signaling cascade involving caspases, the assembly of an apoptosome from multiple proteins, and ultimately cell death. The intrinsic pathway begins within the cell, and after converging on the mitochondria executes a similar cell death. Somewhere in between apoptosis and necrosis falls necroptosis, a regulated form of necrosis. Necroptosis can be initiated by multiple signals (FAS-L, TNF, various NLR), and involves a RIP1 and RIP3 dependent signaling cascade. The end result of passive necrosis and necroptosis are similar and both processes involve the release of several cellular proteins that elicit an inflammatory response (HMGB1, SAP130, HSPs) (102, 103). Breakdown products from the mitochondria of necrotic cells (such as mtDNA) have been shown to stimulate inflammatory responses resembling a bacterial infection(104).

Cell death following coxsackievirus infection has been variously shown to induce necrosis as well as apoptosis. Caspase 3 (the terminal effector of apoptosis) was activated following CVB3 infection in HeLa cells. Inhibition of Caspase 3 did not block the CVB3 induced cytopathic effect (CPE), suggesting viral CPE is a non-apoptotic death in HeLa cells(85). By closely monitoring cells for necrotic or apoptotic phenotypes over a 42 hour period, it was observed that infection with CVB3 induces an initial wave of necrotic CPE deaths 6 hours post-infection in a monolayer of HeLa cells. This is then subsequently followed by a second wave of cell death with an apoptotic character (coinciding with a surge in Caspase 3 activity) at around the 24 hour mark (105). Direct transfection of 2A or 3Cpro alone were sufficient to induce apoptosis in HeLa cells, by multiple mechanisms including cleavage of Caspase 8 and Caspase 3(106). In

polarized Caco-2 cells, apoptosis is not evident when compared with simultaneously infected non-polarized HeLa cells. Cell death in Caco-2 cells appears to be entirely necrotic, and depends on the calcium dependent Calpain proteins for release into the culture media(107). Finally, a recent systems approach studied the relative impact of necrosis and apoptosis on CVB3 infection by measuring necrosis, caspase cleavage, phosphorylation of various signaling kinases, VP1 production and released viral particles. Blockade of both apoptosis and necrosis led to a slight reduction of released viral particles. When necrosis is blocked, but apoptosis is restored through stimulation via an additional pathway, viral particle release is dramatically reduced. If the ideal outcome for the virus is to maximize the number of viral progeny release from an infected cell, apoptosis is thus an undesirable outcome. Some form of necrotic cell death, whether necrosis or necroptosis seems to be the optimal mechanism for releasing viral progeny *in vitro*(108).

LATENCY AND PERSISTENCE

Coxsackievirus causes necrosis and apoptosis in cells, but in some contexts it may also persist. In a model of CVB1 infection, *in vitro* it was found that through subsequent passages of cells, the virus was able to evolve into a less lytic variant that would accumulate and persist. *In vivo* it was found that CVB1 would persist in the hamstring of infected mice. Using a strand specific RT-PCR assay, it was also shown that roughly equal amounts of coding and anti-sense RNA genomes were present as far as 30 days post-infection. Sequence analysis indicated no significant evolution had occurred *in vivo* (109). CVB3 persistence *in vivo* has also been demonstrated by *in situ* hybridization. Following an acute phase of infection, both positive and negative strand genome were still detectable up to 30 days post infection(110). Through serum starvation and a series of cell-cycle blocking drug treatments, it was discovered that CVB3 replicates to a much lesser extent in quiescent (G0), or in cells stopped in the G2/M phase. Viral replication was greatly increased in cells blocked in the G1 phase, where protein and mRNA synthesis is usually highly active. Moreover, it was found that wounding cells mechanically (a scrape) reactivated persistent virus at the borders of the injury (111). CVB3 persistence in vivo might be in part explained because terminally differentiated

tissues such as the cardiomyocyte are quiescent and do not divide. Persistence of viral RNA has also been shown in intestinal cells(112). CVB3 persistence in the heart is suspected to be a mechanism of long term chronic injury to the myocardium, leading to the condition of dilated cardiomyopathy (DCM). Evidence for enteroviral persistence within DCM patients is significant by meta-analysis of several independent studies (40, 113-115). Though putative mechanisms have been described to account for pathology seen in DCM(100), the proportion of DCM attributable to Coxsackievirus infection, and precise mechanisms of disease remain unclear.

THE HOST, AND HOST RESPONSE TO INFECTION

FORWARD GENETIC MOUSE MODELS IN INFECTION AND IMMUNITY

Natural experiments in a disease as complex and multifactorial as coxsackievirus have proved to be of limited use in understanding the precise mechanisms of disease. For example, during the 2002 Greek outbreak of a myocarditic strain of CVB3, viral myocarditis was recognized in 51 individuals, and was fatal in three people living on the island of Crete(42, 43). Subsequent serological examination revealed approximately 7% of people on the island (population approximately 600,000) had recently been infected by CVB3, and 17% had been exposed at some point. What factors and predispositions distinguished these unlucky three out of up to eighteen-thousand infected (3% of 600,000)? What factors might predict sequelae in the remainder?

One approach to understanding genetic predisposition to severe disease is the use of animal models. The mouse model in particular is used because: 1- Mice are mammals who share significant genetic, developmental, and physiological similarity with humans, and in which several phenotypic features of disease can be modeled successfully. E.g.: mice develop viral myocarditis and DCM following CVB3 infection with myocarditic strains of virus. 2- Mice are commercially available. They reproduce over the course of months, and require little space. And 3- Cost, mice require comparatively little maintenance, especially when compared to other potential animal models such as the killer whale (116). Before discussing the immune response to infection it is worth

considering the various mouse model systems used for studying infectious disease and immunity in a controlled and reproducible environment. Each model brings a unique set of limitations and competencies.

INBRED STRAINS

The earliest form of mouse genetics was the establishment of a series of inbred lines of mice. Over successive generations of inbreeding genomes become fixed, which results in defined allelic combinations and predictable phenotypes. Once mice are inbred, the consequences of either genetic or environmental perturbations can be analyzed individually, sequentially or in combination. The DBA strain of mouse was the first to be inbred, and was developed by Little at Cold Spring Harbor in New York beginning in 1909. Subsequent work by a number of Cold Spring Harbor investigators led to the generation of the C57BL/6, C57BL/10, C3H, CBA, BALB/c and A strains of mouse. These strains were developed close to 100 years ago to study cancer, but remain a mainstay of mouse genetics(117).

Early reports on the capacity of CVB3 to induce pathology in inbred strains of mice tended to focus on one strain at a time, and the subject received little attention(15). A systematic characterization of inbred strains of mice to develop acute and chronic viral myocarditis following CVB3 infection was undertaken by Charles Gauntt in 1984 (20). Gauntt's group identified that sex, background strain and *H2* haplotype all played an important role in determining phenotypic outcome. Myocardial inflammation was relatively uncorrelated (though statistics are not given) to viral replication across different strains. Different strains of virus were used (CVB3m and CVB3-*ts10R*) and remarkably different strain, sex and virus combinations produced surprisingly different results. For example, C57BL/6J males or females were relatively resistant to the CVB3-*ts10R* virus, in terms of viral replication and inflammation, but C57BL/6 males are susceptible to high replication and moderate inflammation when infected by CVB3m virus. In 129/J mice both sexes are highly resistant to viral myocarditis caused by CVB3-*ts10R*, but only male 129/J mice were highly susceptible to CVB3m. Conversely female SWR/J mice were significantly more susceptible than males to either virus strain. *H2* also played a role, as semi-inbred strains carrying differing *H2* alleles displayed

differential susceptibility as well, though this effect was not as large as background strain variability. A subsequent study confirmed this finding by comparing A mice with *H2*^{f}, *H2*^{b}, *H2*^{s} as well as B10.H2^{s}, B10.H2^{u} and C3H mice. Significant differences in viremia, extent of myocarditis, persistence of myocarditis, and development of heart specific auto-antibodies were observed to depend on *H2* genotype. Equally importantly, A.*H2*^{s} mice developed much more severe viremia, inflammation and auto-antibodies than did B10.*H2*^{s}, providing unambiguous proof of *H2*-dependent and *H2*-independent control of viral myocarditis using inbred strains of mice(26). Subsequent studies have gone on to show that inflammatory lesion size, calcification and location within the heart also depend on viral isolate and genetic background strain(118).

TEST CROSSES AND TEST CROSS ANALYSIS

When two inbred strains differ markedly in a phenotypic trait of interest, test crosses such as F_2 intercross or N_2 backcross can be performed in an attempt to identify regions of the genome (or genetic loci) that are inherited in tandem with the trait of interest. Conceptually, these loci can then be further refined into a gene (or genes), and from the gene(s) to underlying sequence level differences(119-121). In practice, several individual components contribute to the possibility of successful cloning of a quantitative trait locus, gene and nucleotide. Magnitude of phenotypic difference between two inbred strains, the amount of trait variance under genetic control, genetic marker spacing as well as the number and effect size of independently assorting QTL all contribute to how likely a QTL will be identified for a given intercross. Equations used to identify the appropriate number of F_2 or N_2 progeny depend on a number of assumptions: phenotypes under control of QTL from one genetic background are assumed to all contribute in the same direction, i.e.: QTL1, QTL2… QTLN from the susceptible strain all increase susceptibility. Experimentally, QTL tend to have effects in opposing directions within the same genetic background (see Chapter 3: *Vms2* and *Vms3*). Moreover, some traits are highly polygenic, and even when large intra-parental differences with modest variance phenotypes exist multiple large crosses continue to uncover new QTL continually (119, 122-125).

The generation of a test statistic for any given locus across the genome depends on both the model used, and which implementation or method is chosen. E.g.: a semi-continuous variable like survival could be modeled directly, or split using a two-part method to analyze survivors and non survivors separately(126), or transformed into binary trait of resistant and susceptible (127). Linear models on continuous, normally distributed variables tend to be preferred with the simplest method being simple regression on the marker(128). Standards for the interpretation and generation of test statistics have been proposed in order to maintain some degree of stringency, but also allow for the identification of small and modest QTL effects(120). Generally, permutation of mouse phenotypes within a given test-cross is performed, the highest genome wide test statistic from each permutation is used to empirically establish a false positive rate and calculate a p-value. Several implementations of marker regression at and between genetic markers have been implemented in the R/Qtl package made freely available by Karl Broman (129). While a testcross approach has the benefit of producing a unique segregation of genotypes in each animal, this is also a drawback in that the results for any given individual cannot be replicated or in most cases subjected to repeated testing.

Testcrosses have been used successfully to study myocardial susceptibility to necrosis and dystrophic calcification (DCC). In mice susceptible to DCC, a variety of mechanisms including freezing, infection, fatty diet and old age, all lead to necrosis, followed by calcification of the dead cardiomyocyte. DCC also occurs in a subset of human patients following myocardial infarction, and cardiomyopathy. This calcium deposition is present in C3H and DBA2/J strains, and absent in most others including C57BL/6, C57BL/10 and A/J. An initial F_2 intercross between C57BL/6 and C3H mice mapped the *Dyscalc* locus to proximal chromosome 7(130). The subsequent identification of the *Abcc6* gene as responsible for the *Dyscalc* locus was achieved using other approaches including recombinant congenic strains (RCS see next section), expression QTL (eQTL) and sequencing (131, 132).

Dilated cardiomyopathy can occur long after viral infection is cleared from the heart, and in many strains of mice is preceded by the development of an autoimmune reaction against heart tissue. Experimental autoimmune myocarditis (EAM) is a model to study

autoimmune aspects of myocarditis without the complicating variability introduced by viral infection. EAM is induced in susceptible strains of mice by injecting cardiac myosin with complete Freund's adjuvant to simulate the release of myocardial antigen and inflammatory response occurring during viral myocarditis. Strains susceptible to viral myocarditis tend also to be susceptible to EAM; A/J strains are susceptible, and C57BL/10 strains are relatively resistant. An F_2 intercross between A.$H2^S$ and B10.$H2^S$ mapped EAM susceptibility to chromosomes 1, 4 and 6 (133). Subsequent studies using a congenic approach confirmed the chromosome 1 locus, and revealed that B10.$Eam1^a$.$H2^S$ lymphocytes were less susceptible to apoptosis than B10.$H2^S$ mice carrying the $Eam1^b$ allele(134).

Our own group has used a model of infection with Coxsackievirus B3 (CVB3) to characterize the contribution of host genetics to viral myocarditis in mice of different genetic backgrounds but with a common *H2* haplotype: A/J and B10.A-$H2^a$. We found evidence of linkage between susceptibility to viral myocarditis and three loci. Loci on chromosomes 1 and 4 were linked to sarcolemmal disruption. A third locus on distal chromosome 3 was linked to myocardial infiltration, sarcolemmal disruption and viral replication (135). Coxsackievirus testcrosses are further described within Chapters 2 and 3.

RIS, RCS AND CSS

Recombinant inbred strains (RIS); recombinant congenic strains (RCS) and consomic substitution strains (CSS) are a similar resource for the study of complex traits that combine features of a testcross and inbred strains. RIS are produced by breeding pairs of F_2 mice from different strains and then inbreeding successive generations of progeny until complete homozygosity is reached (136). Through inbreeding different founder F_2 animals, panel of mice with a mosaic of genomic regions belonging to either parental strain can be created. Recombinant congenic strains are conceptually similar to RIS. Instead of inbreeding F_2 mice to homozygosity, RCS are created from two sequential backcrosses and then inbred(137). E.g.: [[[B x A]xB]xB]. Whereas RIS contain approximately 50% of each background genome, RCS contain approximately 85% of their genome from a background strain, and the remaining 15% from the donor strain.

Consomic substitution strains (CSS) are selectively bred such that each line of mouse is completely homozygous for a donor strain on one chromosome(138). CSS mice can be intercrossed to test epistatic effects, or quickly phenotyped as confirmation of linkage results. Since each line of RIS, RCS, and CSS mice is fully inbred, they can be tested repeatedly, and for multiple phenotypic traits. Each kind of recombinant inbred mouse (RIS, RCS, CSS) sits on a continuum of being able to identify genes on any chromosome, with different power to identify an effect at any given locus. CSS mice do not have any mapping resolution beyond the chromosome, but are definitive in their localization to a given chromosome. RIS mice carry so many donor segments on their genome that mapping anything beyond a simple monogenic trait may not be possible. RCS mice exist somewhere in between, however due to the relatively low amount of donor genome (~15%) per strain, a given locus may not be covered with adequate power. Most screens of RIS, RCS and CSS panels require a subsequent confirmatory test cross for true QTL, and subsequent gene identification(139-142).

As discussed above, A and C57BL/6 strains of mice differ markedly in their susceptibility to CVB3 induced viral myocarditis. Two studies from the group of Kirk Beisel were performed in which suckling mice from the AXB/BXA panel were infected with CVB3-Nancy. In the first study, mice were infected with a lower dose of virus and assessed for myocardial fibrotic lesions and chronic myocarditis(143). The second study examined the same panel infected with a higher dose of the same virus, and measured cardiac anti-myosin antibody titer (144). In both studies the strain distribution patterns following infection were highly similar, and applying a form of linkage to the phenotype genotype combination observed produced one significant result on chromosome 14. This locus corresponded roughly to the T cell receptor gene and the cardiac myosin heavy chain alpha.

A more recent study was undertaken by the group of Marc Horwitz, beginning with CVB3-Nancy infection of CSS mice that were consomic for A/J on a C57BL/6 background. It was found that CSS17 (C57BL/6J-Chr17$^{A/J}$/NaJ) hearts became substantially more inflamed at day 7-post infection, but no differences in viral replication were observed at either day 3 or day 7. Chromosome 17 was pursued using a congenic

approach to map these genetic effects, and differential inflammation was confirmed. Sub-congenics were also created, and used to identify at least three independently acting QTL contributing to viral autoimmune myocarditis (*Vam1*, *Vam2*, and *Vam3*) all on proximal chromosome 17. A role for *Vam3* was partly expected as this locus coincides with the *H2* locus, but the precise nature of this effect still remains to be determined. The exact role for *Vam1* is of particular interest because the interval contains mitogen activated protein kinase 4 (MKK4 or *Map3k4*), a key kinase for activation of p38 signaling (145).

OUTBRED LINES AND THE COLLABORATIVE CROSS

The extent of natural variation within inbred lines of mice is limited due to their relatively small founder populations, compared to wild mice. Wild-type mice can be a rich source of diversity in understanding natural variation in host response to infectious disease. For example the A2G (background A) strain of mouse was the first mouse strain discovered to be relatively resistant to influenza virus (146). The source of resistance in A2G mice was reported as having resulted from an “illegitimate breeding”, possibly from a wild mouse that snuck into the facility. Subsequent studies eventually identified the resistance gene as *Mx*, a protein produced in response to interferon that limits influenza infection(147, 148). In order to capitalize on this diversity, several inbred wild-derived strains are available for purchase, as well as some outbred mouse colonies. Similarly, a large consortium has developed a “Collaborative Cross” (CC) using 8 founder strains of mice (inbred: A/J, C57BL/6J, 129S1/SvImJ, NOD/LtJ, NZO/H1LtJ, wild derived: CAST/EiJ, PWK/PhJ, and WSB/EiJ) in an attempt to maximally represent mouse genetic diversity in inbred lines of mice(149-151). Since each CC strain is fully inbred, and densely genotyped using the diversity array(149-151), this model gains a very high degree of genetic resolution in a given strain survey compared to other techniques. This has led to the re-identification of other alleles of the *Mx* gene(152), and many other QTL(153-155) or eQTL(156) related to infectious phenotypes. Though the model holds much promise it remains to be determined if previously unknown genes will be identified, or if CC derived QTLs will be any simpler to decode than those identified using test crosses, RIS, RCS and CSS mice.

Most of the foundational work in coxsackievirus pathogenesis was performed in the outbred CD-1 mouse stock (see section on history). The NMRI outbred mice(157, 158) have been used to study CVB3 infection in order to study the effect of virus genotype on an outbred population. Principal findings recapitulated the result that persistent viral RNA in the heart was associated with chronic myocarditis, and that this effect was strongly dependent on the viral strain used.

MYOCARDITIS

THE CARDIOMYOCYTE

The cardiomyocyte is a highly specialized cell with three primary functions: continuous conduction of force, intercellular electrical communication, and long-term survival.

While coxsackieviruses can affect many tissues, infection of cardiomyocytes is of particular concern. Cardiomyocyte regeneration is slow, and until recently it was controversial that cardiomyocytes were replenished at all during adult life(159). Taking advantage of the altered atmospheric content of carbon-14 caused by 20th century nuclear weapons testing, Bergmannet al. convincingly demonstrated that adult cardiomyocytes were regenerated during adult life and were much older than surrounding non-cardiomyocytes. This established regeneration was possible but it was still a slow and inefficient process accounting for less than 1% turnover per year in adults (160). Indeed models projected in this study established something on the order of 60% of cardiomyocytes being maintained from birth to the age of 75. Because a functioning heart is essential for unassisted survival, slow or low regenerative capacity presents a particular problem during a lytic infection.

The cardiomyocyte is distinguished by specialized structures including the sarcomere (like all striated muscle), and cell-cell connections known as intercalated discs (161). The sarcomere is the individual unit of force generation within the cardiomyocyte. Sarcomeres consist of a series of modules each consisting of a Z-line which is connected to thin filaments, which associate with thick filaments, a second set of thin filaments and then a final Z-line (i.e.: Z-thin-thick-thin-Z). The active part of force

generation comes from the thick filaments, which are composed mainly of myosin but also some associated modifying proteins. Myosin cross-bridges with the thin filaments (composed mainly of actin), and pulls them towards the center of the sarcomere in an ATP consuming reaction. This process is regulated in a number of ways including by tropomyosin which blocks actin-myosin interaction sites and troponin, which displaces tropomyosin in a calcium ion (Ca^{2+}) dependent manner (162). The thin filaments are joined on either end of the sarcomere to the Z-disc, a multiprotein structure which acts as an anchor for the sarcomere. The Z-disc includes α-actinin as a primary cross-linking protein, as well as many others performing a variety of mechanical and signaling functions. The Z-disc proteins MURF1 and the transcription factor NFAT3 are located in both the nucleus and the Z-disc indicating the Z-disc may be a site involved in transcriptional regulation. The thick filaments and z-discs are both anchored to the sarcolemmal membrane (the cardiomyocyte plasma membrane) via the costameres in which the Z-disc α-actinin is connected to desmin intermediate filaments, gamma actin, vinculin, and importantly dystrophin. These linker molecules then attach to the dystroglycan complex (ß-dystroglycan is the transmembrane component), and the dystroglycans connect with the extracellular matrix. Taken together, calcium flux followed by myosin ATP hydrolysis in the sarcomere pulls actin, which through the Z-disc moves the cytoskeleton and the plasma membrane through intermediate filaments, dystrophin and the dystroglycan complex(161).

Unlike skeletal muscle, cardiomyocytes are joined end to end by structures known as intercalated discs with two functionally distinct sub-units. The first is mechanical integration achieved intercellularly through the fascia adherens, which is composed of homotypic N-cadherin interactions. The cadherins are joined to the actin cytoskeleton via plakoglobin and the catenins. Intracellular desmosomes anchor the intermediate (Desmin) filaments to the intercalated discs through plakoglobin, and desmoplakin. The second key feature of the intercalated disc is electrical coupling through the gap junction. Gap junctions are composed of two interlocking hemi-channels called connexons, each of which is formed by six connexin proteins. Cardiomyocyte gap junctions are composed of connexin 37, connexin 40, connexin 43 and connexin 45 (*Cx37, Cx40, Cx43* and *Cx45*). Gap junctions can be formed by homotypic and heterotypic

interactions though not every variation leads to a functional channel. Gap junctions are permissive for passage of molecules up to 1000 Da, and this is especially important during the conduction of the cardiac action potential (163, 164).

MYOCARDITIS *PER SE*

The first known observation of myocarditis was by Fiedler in 1899, and was translated from German in 1963 (41, 165) as follows:

> *"INTERSTITIAL TISSUE IS DENSELY PERMEATED WITH NESTS OF MONONUCLEAR LEUCOCYTES… THE MUSCLE FIBER SHOWS SWELLING AND DECAY OF THE CROSS BANDS … THE NUCLEI ARE USUALLY CONSERVED BUT AT TIMES ARE SWOLLEN AND STAINED MORE INTENSELY THAN NORMAL… WITHIN THE MUSCULATURE THERE ARE AREAS OF NECROSIS…"*

This encapsulates most of the important features of myocarditis as set down by an expert group of eight pathologists in 1987 as the Dallas Criteria(166). The criteria state that myocarditis is defined within an endomyocardial biopsy (EMB) by cardiomyocyte necrosis, or cardiomyocyte degeneration which is adjacent to inflammatory infiltrate. The criteria require both to be in immediate proximity because either feature taken alone can be artefactual. Necrosis may be observed pathologically as vacuolization, but this alone can be the result of sample preparation and staining. Similarly, fibroblasts, or other cardiac cells can be misinterpreted as a few isolated leukocytes. The criteria further categorize infiltration as mild, moderate or severe; and the distribution of infiltrate as focal, confluent or diffuse. Criticism of the Dallas Criteria is abundant (167, 168) and focused on its limited prognostic value and relative subjectivity. Clinicopathologic descriptions of myocarditis expanded beyond histological features to describe common patient features and classes. In fulminant myocarditis, patients present with flu-like symptoms, deteriorate rapidly, and multifocal or confluent infiltration are observed within myocardial biopsies. Patients developing fulminant myocarditis paradoxically have an excellent prognosis if they are able to survive the initial hemodynamic compromise(168, 169). Acute myocarditis is described as a gradual deterioration preceded by nothing

distinct. Chronic persistent myocarditis is a condition where myocarditis recurrently presents by EMB, with no deterioration and minimal accompanying clinical features(168). Modern diagnosis of myocarditis is a multistage process that integrates serum cardiac biomarkers, cardiac magnetic resonance imaging and electrocardiograms. Endomyocardial biopsies remain the gold standard for definitive diagnosis (170), and immunohistology is recognized to be the most powerful prognostic test in myocarditis (171). Myocarditis can lead to sudden and unexpected death by introducing fatal arrhythmias by direct cardiomyocyte necrosis (39). Myocarditis can also lead to death by cardiogenic shock, where heart function is suppressed to the point that it can no longer supply the body (and itself) with enough blood to survive, as in fulminant myocarditis (168, 169, 172). Dilated cardiomyopathy (DC) is a similar heart condition characterized by decreased force generation of the heart associated with a thinning of the heart muscle, and an enlargement of the heart chambers. DC can result from mutations in key structural proteins within the cardiomyocyte (173). Both viral and inflammatory mechanisms have been implicated in the etiology of DC (174). Enteroviral mRNA persistence is more frequently identified in DC patients than in controls (113), but by the time DC has developed, virus is more usually absent (175). During long term follow-up studies, the incidence of patients diagnosed with acute myocarditis going on to develop DC varies enormously between studies (0% and 52%) (176). DC pathogenesis is certainly heterogeneous, microarray expression studies on EMB samples indicate the disease can be sub-classified as at least two diseases: inflammatory and non-inflammatory (177). Mechanistic understanding of the relationship between viral infection, myocarditis and DC is complicated by heterogeneity in disease presentation, description and likely disease etiology (41).

EXPERIMENTAL PATHOGENESIS

Several experimental models of myocarditis exist including reovirus (178-180), and encephalomyocarditis virus induced myocarditis (181-183), and experimental autoimmune myocarditis (EAM). By far the best studied is coxsackievirus B3 induced viral myocarditis(15, 184-187). The pathogensis of viral myocarditis depends on the strain of virus used (23, 24, 157), as well as host genetic background (25-27, 135, 145,

188), rendering a description of a general scheme complicated. Following infection, most mouse strains will remain asymptomatic for roughly 48 hours, however high titers of virus will be present in most tissues tested including the heart and liver. Serum Interferon-ß is elevated starting at 48 hours in response to virus indicating an innate immune response. By 4 days post infection, resistant strains begin to become distinguishable from susceptible strains. In resistant strains, viral load is either no longer increasing or declining by 4 days post infection, while in susceptible strains viral replication can continue to climb(189-191). Between days 3 and 6, sarcolemmal disruption is clearly evident by evans blue dye staining (EBD is a dye which on injection, binds serum albumin and enters necrotic cells)(192, 193). An inflammatory infiltrate becomes evident between days 6 and 8 and peaks rapidly. The infection can then resolve with sterilizing immunity, persist with lingering viral replication and inflammation, or be acutely fatal.

THE IMMUNE RESPONSE TO COXSACKIEVIRUS INFECTION

The innate immune system is a first line of defense against pathogens and consists of germ-line encoded mechanisms for responding to infection. Innate immunity can broadly be broken down into sensing receptors, signalling pathways, effector mechanisms, and cellular innate immunity. There are four main classes of innate receptor for sensing viral pathogens, the Toll like receptors (TLR), the retinoic acid-inducible gene 1 (RIG-I) like receptors (RLR), the nod like receptors (NLR) and the STING activating cytosolic DNA sensors.

INNATE SENSING: TLRS

Direct pathogen sensing remained elusive until the discovery that the *Toll* gene in drosophila was found to be essential for recognition of fungi, and led to activation of NFκB(194, 195). The existence of at least one mammalian homologue raised the possibility that toll like receptors might play a similar role in mammals (196). Bolstering this hypothesis, insensitivity to bacterial lipopolysacharide (LPS) in C3H/HeJ and C57BL/10ScCr mice, attributed to the *Lps* locus, was found to be due to a defect in TLR4 (197, 198). Therefore, germ line encoded receptors could sense specific

pathogen associated molecular patterns and lead to relevant and immediate immune responses. TLR4 recognizes LPS, but it has also been found to recognize viral, and endogenous ligands during infection or stress(199, 200). Of the 10 human (TLR1-10) and 11 mouse TLR (TLR1-7, 9, 11-13) identified to date, TLR9 receptor was the first identified as recognizing virus. The ligand to TLR9 was originally found to be DNA containing unmethylated CpG motifs, a common feature of bacterial but not mammalian DNA (201, 202). Other TLR recognizing viral nucleic acids include TLR7 (in mice) and TLR8 (in humans), which recognizes single stranded viral RNA and TLR3, which recognizes double stranded RNA (203). The nucleic acid sensing TLR reside within the endoplasmic reticulum and within endosomes, requiring endosomal acidification for proper function. Shared features within the TLR family include an ectodermal leucine rich repeat domain (LRR) as well as an intracellular domain shared between TLR and the interleukin 1 receptor (TIR domain) that mediates signal transduction with the TLR adaptor molecules. Once a pathogen associated molecular pattern has been detected through one of the TLRs this signal is relayed through adaptors in a signaling cascade ultimately reaching transcription factors, which will initiate molecular counter measures. Signal conduction of viral recognition by TLR is so far known to signal through two distinct pathways both of which depend on the intracellular TIR domain (204). TLR7, TLR8 and TLR9 begin signaling by interacting with the Myeloid differentiation primary response 88 (MyD88) adaptor molecule, MyD88 then interacts with IL-1 receptor associated kinase 1 (IRAK1), IRAK4, TRAF6, IKKα, leading to the activation of transcription factors IRF7 and NFκB(203-205). The existence of a MYD88-independent pathway was suggested, as both TLR3 and TLR4 were able to stimulate an IFN response in the absence of MyD88. Investigations based on homology of the TIR domain led to the identification of TIR domain-containing adapter inducing IFN-ß (TRIF)(206, 207). From TRIF the signal leads to NF-κB activation through two pathways, one involving TRAF6 (as in the MyD88-dependant pathway) and another through RIP1. TRIF then relays signal in a pathway dependent on TRAF family member associated NF-κB activator binding kinase 1 (TBK1), and leads to activation of the transcription factor IRF3 and the production of type I IFN.

INNATE SENSING: RLRS

Though TLRs reside within endosomal compartment or plasma membrane and are not cytosolic, many viruses replicate in the cytoplasm. Cytosolic administration of double stranded RNA induced a strong type I IFN response in a TLR3 independent pathway, suggesting another receptor (208). Three such sensors have been discovered, though only two act as positive regulators of the innate immune response. Retinoic acid inducible gene I (RIG-I) and melanoma differentiation associated gene 5 (MDA5) were both found to recognize cytosolic double stranded RNA. RIG-I is critical for recognizing several viruses including SeV, VSV, Influenza, Hepatitis C and JeV (209, 210). Remarkably, RIG-I recognizes single stranded RNA, but only when the RNA strand is capped with a 5' triphosphate group not present in most eukaryotic RNAs. Those which do have 5' triphosphate cap are either obscured within ribosome (5S rRNA), or heavily substituted such as in tRNAs, which decreases RIG-I specificity (211). MDA5 is strongly activated by double stranded RNA, and picornaviruses in particular (212). MDA5 is preferentially activated by long RNA strands, as it stacks into filamentous structures where the signaling caspase activation and recruitment (CARD) domains can oligomerize (213). Following recognition of viral nucleic acid, both RIG-I and MDA5 share a common adapter, the mitochondrial antiviral signaling protein (MAVS), which they interact with via their CARD domains. This leads to a similar signaling cascade as for the TLR, including a TBK1 dependent pathway leading to transcription factor IRF3 activation and a Fas (TNFRSF6)-associated via death domain (FADD) dependent pathway leading to NF-κB activation(214).

INNATE SENSING: CYTOSOLIC DNA SENSORS

Conceptually similar to the RLRs, it has long been known that cytosolic DNA activates TBK1/IRF3 and NF-κB response. It is also known that upstream of this signaling cascade the stimulator of interferon genes (STING) adapter played an essential role (conceptually similar to MAVS, TRIF and MYD88)(215). The actual DNA receptor has remained controversial as several candidates were identified. The first of these to be identified was Z-DNA binding protein (DAI or ZBP1)(216) though DAI deficiency did not recapitulate the effects of STING or TBK1 deficiency in response to vaccines or viral

infection(215). Other putative sensors identified include RNA polymerase III, LRRFIP1, DHX9, DHX36, Ku70 and IFI16. STING is also known to become activated by cyclic di-GMP, a bacterial second messenger (217). James Chen's group recently demonstrated that introduction of DNA into the cytosol led to the production of an endogenous second messenger cyclic GMP-AMP (cGAMP) through the activity of the DNA binding protein cyclic GMP-AMP synthase (cGAS)(218, 219). It remains unclear whether or how the various and putative cytosolic DNA sensors are integrated in the context of infection.

TYPE I INTERFERON AND INTERFERON STIMULATED GENES

Anti-viral type I Interferon was discovered in 1957 as a factor interfering with influenza virus infection (220). Chorio-allantoic membrane cells were rendered resistant to infection after exposure to heat inactivated virus; this interference occurred maximally if the cells had some time to react, and activity was transferrable into the media. Interferon is a primary antiviral mediator in most cell types. Once type I IFN is produced, it is secreted and signals through the type I interferon receptor (IFNAR1 and IFNAR2) in both an autocrine and paracrine manner. Upon ligand binding, the interferon receptor initiates a signaling cascade through the activation Janus kinases (JAK) including JAK1 and TYK2. JAK1 and TYK2 phosphorylate STAT1 and STAT2, which together with IRF9 form a trimer called IFN stimulated gene factor 3 (ISGF3), which translocates to the nucleus. In the nucleus, ISGF3 will bind to IFN stimulus response elements (ISRE), a promoter which activates hundreds of genes to respond to infection (221).

Hundreds of genes are stimulated by IFN, and are known to exert some antiviral activity though the precise mechanisms of many are unknown. Only a small handful of ISGs have characterized non-redundant roles in antiviral immunity, though dozens are known to exert strong antiviral effects on a range of viruses (222). Since the localization of the *Mx* gene (see Outbred lines above), it was been found to be a GTPase involved in either sequestering viral mRNA in the nucleus or in sequestering of viral capsid proteins (223). A total of four families of IFN inducible GTPases have been found, including the p47, p65, Mx and VLIG families, with the exception of Mx their roles *in vivo* remain largely unclear. Other effectors include the OAS1 and RNaseL system(221). OAS was known to produce the oligomerization of ATP by catalyzing 2'-5' phosphodiester bonds

into pppA(2'p-5'A)n. The presence of 2'-5'-oligoadenylates, in turn effects the dimerization and activation of latent RNase L, which degrades single-stranded RNA (224-227). In addition to degradation of viral genome or anti-genomes, RNase L may also produce small dsRNA which re-activate sensor molecule such as RIG-I and MDA-5 enhancing IRF3 signaling(228). RNaseL deficiency leads to increased susceptibility to several RNA viruses in mice. Other interferon-stimulated genes (221) (ISG) include PKR, a latent kinase that is activated upon binding of viral RNA. The activated enzyme phosphorylates eukaryotic translation initiation factor 2A (EIF2α), which blocks GDP recycling thus halting protein translation. PKR has been found to be involved in response to multiple RNA viruses. The highly induced ISG15 protein is an ubiquitin homologue that is bound to a number of substrates and may be a regulator of interferon signaling. ISG15 deficiency in mice results in increased susceptibility to influenza, herpes viruses, Sindbis virus as well as human immunodeficiency virus (HIV) (229). Apolipoprotein B mRNA editing enzyme catalytic polypeptide 3 (APOBEC3G) prevents efficient HIV reverse transcription by first being packaged into progeny virions, and then deaminating cytidine residues to uracil, causing an excess of C->T substitutions(230). A simplified schematic diagram of the key components involved in innate sensing of viral pathogen associated molecular patterns, and the type I interferon response is illustrated in Figure 2.

FIGURE 2: TOLL AND RIGI LIKE RECEPTOR MEDIATED SENSING OF VIRUS AND THE TYPE I INTERFERON RESPONSE

Upon viral infection, virus is initially detected by two classes of receptors. TLR3, 7 and 9 are located in the endosomal compartment and require Unc93b1 for maturation. TLRs 3,7 and 9 bind viral nucleic acid. TLR4 binds an endogenous ligand in the context of viral infection. The cytosolic helicases RIG-I, MDA5 and cGAS perform similar functions in the cytoplasm. Upon binding a PAMP, signal is relayed through an adaptor molecule such as MYD88, TRIF, STING or MAVS to a series of kinases and ultimately to transcription factors such as IRF3, IRF7 or NFκB, which induce the expression of Type I IFN and an inflammatory cytokine response. IFN signals to self and neighbouring cells through the IFN receptor. A signalling cascade involving JAK and TYK2 form the ISGF3

transcription factor from STAT1, STAT2 and IRF9. The transcription factor leads to the production hundreds of genes including anti-viral effector molecules such as MX, PKR and OAS1b.

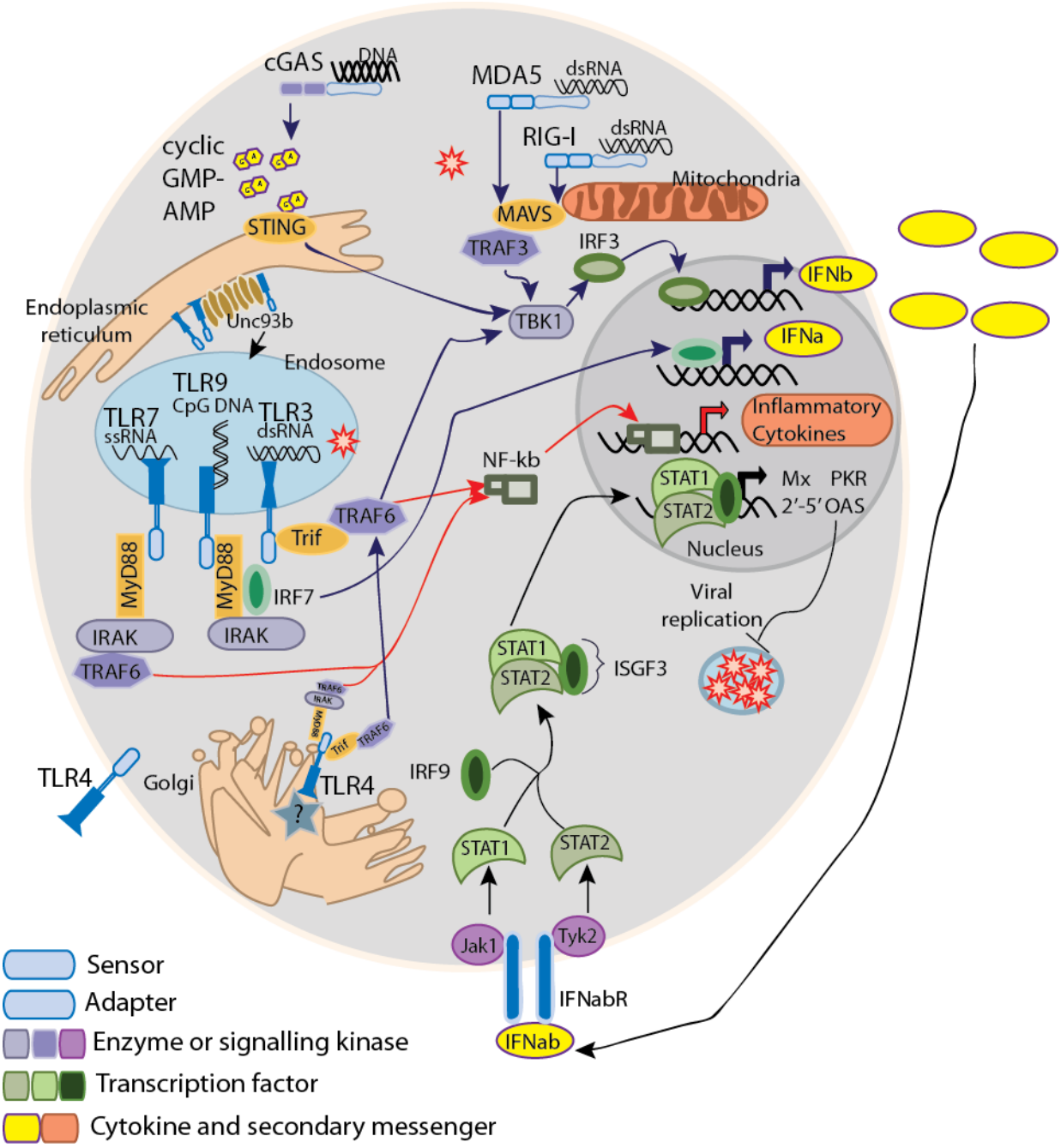

NLRS AND THE INFLAMMASOME

The TLRs and RLRs principally (though not exclusively(231)) recognize pathogen associated molecular patterns (PAMPs). TLRs and RLRs mediate their activity primarily by activating transcription factors and downstream effector genes. This creates a first transcriptional signal for activating of inflammation by transcribing Il-1. The NOD like receptors (NLRs) provide a second protein-activating signal. NLRs recognize both PAMPs as well as damage associated molecular patterns (DAMPs). The NLR proteins share similar domain structure, although these are rearranged across the families. Common features include an interaction domain (PYD, CARD, or BIR), a nucleotide binding domain, and a carboxy terminal leucine rich repeat (LRR) domain. Following LRR binding of their respective ligand, NLRs are brought together through oligomerization domain (NOD) domains. These complexes then recruit pro-caspase-1, either directly through the CARD domains on the NLR and pro-caspase-1, or indirectly via an adapter molecule. Their oligomerization in a large multiprotein complex termed the inflammasome causes the activation of caspase-1. Caspase-1 activity cleaves the pro-form of inflammatory cytokines interleukin-1ß (IL-1ß) and interleukin-18 (IL-18) to induce an inflammatory response(232-234).

INNATE IMMUNITY AND CVB3

The innate immune response to coxsackievirus infection is complex. As a picornavirus, coxsackievirus is expected to be sensed at the cytosolic level by MDA5. Indeed, absence of MDA5 leads to severe liver necrosis and early mortality(235). However, unlike in the C57BL/6 background, in the 129SvJ background MDA5 deficiency has no apparent effect (236), indicating lack of MDA5 is mitigated somehow in the 129SvJ background. Absence of the MDA5 signalling adapter MAVS in the C57BL/6 mice also leads to a similar hepatitis phenotype. Absence of the Type I IFN receptor leads to severe hepatitis and early mortality as well (237). Furthermore, when Interferon-ß is knocked out, the phenotype is recapitulated (190): hepatitis and early lethality with no effect on cardiac viral replication. CVB3 also actively dampens innate RNA-sensing. *In vitro* experiments have shown conclusively that CVB3 $3C^{pro}$ cleaves MAVS, TRIF and RIGI while $2A^{pro}$ targets MAVS and MDA5 to supress Type I IFN production and apoptosis (238, 239)

Absence of TLR3 increased susceptibility to myocarditis, but not hepatitis. In TLR3 deficient hearts, inflammatory cytokines (including IL-1ß, IFN-ɣ, and IL-12) were significantly reduced compared to wild-type. No significant differences in Type I IFN expression was observed. In IFNAR1 knockout mice, TLR3 overexpression was sufficient to rescue the mice from fatal infection(240). However, the TLR3 phenotype may be cardiac independent as transfer of wild-type macrophages into TLR3 deficient mice decreased heart damage, inflammation and increased survival almost to wild-type levels (241). The role for TLR4 in CVB3 infection was established in a knockout model of that gene. Early during infection (day 2) TLR4 knockouts had increased viral replication in the heart relative to wild-type mice. During what is usually the resolving phase (day 12) TLR4 knockouts had less myocardial inflammation and lower levels of virus in the heart and pancreas(242). Somewhat similarly, the absence of one of the TLR4 adapter molecules, MYD88, increased survival of infection dramatically, limited myocarditis, and led to more rapid clearance of virus(243). Unlike MYD88 removal of the TLR3 and TLR4 adapter TRIF led to a cardiomyocyte specific increase in viral replication, inflammation and greatly decreased survival of infection (244, 245). Moreover, whereas TLR3 and TRIF knockout mice both develop increased viral replication and inflammation 10 days post infection, only TRIF knockout mice go on to develop dilated cardiomyopathy (245).

The suppressors of cytokine signalling family of proteins (SOCS1, SOCS2, SOCS3, CISH) are expressed in response to a variety of stimuli and exert a negative feedback effect on cytokine signalling (246). Infection of mice with cardiac specific transgenic overexpression of the suppressors of cytokine signalling 1 and 3 (SOCS1, SOCS3) have demonstrated a clearly cardiomyocyte specific role for innate immunity (247, 248). SOCS1 overexpression greatly enhanced myocarditis, and myocardial necrosis. Gene transfer of a dominant negative form of SOCS1 (dnSOCS1) enhanced neonate rat ventricular myocyte (NRVM) STAT3 and NF-κB responses to CT-1 and TNFα respectively. Mouse hearts subjected to dnSOCS1 gene transfer were protected mice from CVB3 infection and necrosis (248).

A growing picture of multiple innate immune circuits is emerging. Resistance to coxsackievirus infection is determined in the liver by a MDA5, MAVS, IFN-ß, IFNAR1 dependent circuit, though the specific downstream effectors of this resistance remain to be elucidated. In the heart, a TLR3 and TRIF dependent mechanism is required for control of infection. Cardiac specific SOCS1 and SOCS3 proteins also strongly negatively regulate the heart response to CVB3, suggesting the innate response in the heart is at least partly cardiomyocyte driven. Taken together, these studies suggest one or more non-IFN IRF3 transcriptional target is crucial for a balanced *in vivo* cardiac response to CVB3 infection.

CELLULAR IMMUNE RESPONSE

Sensing, signaling and the innate response occurs as a cell-autonomous process within infected tissues, but also in specialized cellular modules of the innate immune system. These serve as a primary defense against infection, but also to provide the cytokine contexts for the generation of an acquired immune response. The cells of the innate immune system can be coarsely subdivided into the myeloid cells, and the innate lymphoid cells. The myeloid compartment contains primarily antibacterial, antiparastic and antifungal granulocytes such as neutrophils, eosinophiles and basophiles; as well as the professional antigen presenting cells (APC) such as the macrophages and dendritic cells. The innate lymphoid cells (ILC) are functionally subdivided based on cytokines they produce. Group 1 ILCs including natural killer cells produce IFN-ɣ, group 2 ILCs produce T-helper 2 (T_H2) cytokines IL5, IL9 and IL13, and group 3 ILCs produce the T_H17 cytokines IL17 and IL-22(249). In the context of viral infection, the natural killer (NK) cells are of particular importance. Originally identified for the ability to spontaneously lyse tumour cell lines, NK cells have also been shown kill virally infected cells as well. NK cell recognition and killing is determined by a balance between absence of normally ubiquitously expressed inhibitory signals on target cells, and the presence of abnormal activation signals. NK effects are mediated by release of cytolytic granules, induction of apoptosis through death receptors, and via cytokine production and secretion (250-253).

Adaptive lymphocytes become activated when they are presented with antigens in the context of major histocompatibility (MHC) class I or MHC class II molecules. Antigens are specific peptides, sugars, glycopeptides, or lipids that can be recognized by a T or B cell receptor; antigens are the functional units of recognition in the acquired immune system. T and B lymphocytes are able to recognize an immense repertoire of non-self antigens due to a process of genomic recombination of the T or B cell receptor during infection within each cell, followed by an affinity maturation during infection. MHC class I molecules are expressed on all nucleated cells, and class I antigens are recognized by the CD8 cytotoxic T lymphocytes (CTL). CTL directly kill target cells, and are an antigen specific cell functionally similar to the NK cells. MHC class II molecules are present only on professional antigen presenting cells such as macrophages or dendritic cells, and B-cells. Antigens presented in a class II context lead to a CD4 “helper” T lymphocyte response, and B lymphocyte antibody response to infection. Much like ILC cytokine production shapes the T cell response, the CD4 T-cells shape the acquired immune response into one favouring cytotoxic cellular immunity (CD4 T_H1), one favouring antibody production (CD4 T_H2), or favouring granulocyte driven inflammation (T_H17) (254). T lymphocytes are subject to a positive (can recognize MHC) and negative (react to self antigens) selection process that minimizes auto-reactivity within the T cell repertoire. During infection antigen specific lymphocytes clonally expand, and following clearance of infection, most of this expanded population is eliminated by apoptosis. The T and B responses are considered acquired immunity in that they both may create a subset of long-lived memory cells. These memory cells are capable of responding to subsequent infection more rapidly and specifically than during the initial infection (214, 255).

The definition of myocarditis includes an inflammatory infiltrate: the composition and relative contribution of different cellular subsets has been extensively characterized. Several cell types have been shown to infiltrate the infected heart at approximately the same time, including neutrophils, macrophages, NK cells and T cells (CD4 and CD8) (256).

Natural killer cells play a role early during infection, this was shown by depopulating NK cells using a similar methodology as in the T cell experiment below. Anti-NK cell anti-serum increased viral replication in the heart by up to 670-fold at day 3 post infection. Though inflammation was similar indicating that NK cells contribute to control of viral replication but not inflammation(19). NK cell activation was found to be specific for infected cells, as uninfected fibroblasts were not lysed(257). ß2-microglobulin (B2M) is a key subunit of MHC class I, and knocking out B2M abrogates surface expression of MHC class I, a key inhibitor of NK cell activity. After knocking out B2M, viral replication was dramatically reduced (2-4 logs) following CVB3 infection(258). The importance of NK cells was more recently demonstrated by the genetic manipulation of CXCL10, a chemokine that attracts a variety of CXCR3 expressing cells including CTL and NK cells. Both knockout and transgenic overexpression of CXCL10 were compared to wild-type. Consistent with previous NK findings, it was found that at day 3 post-infection CXCL10 knockout mice developed increased viral replication, and transgenic overexpression led to decreased viral replication. During the acquired immune phase (days 7 and on) viral replication was equivalent, but biomarkers of heart damage (seum cardiac troponin I) concentrations were elevated in knockouts, and lower in transgenics (259). A key component of the cytolytic granules in CTL and NK cells is perforin, and perforin knockouts have increased survival, and decreased inflammation, while having equivalent levels and tissue distributions of viral replication (260). Interleukin 12 (IL12) is a potent activator of IFN-ɣ by inducing a signal transducer and activator of transcription 4 (STAT4) response in IFN-ɣ producing cells such as ILC1, T_H1 and CD8. In IL12 knockout mice, late myocardial inflammation and viral replication was increased. This effect was replicated by both STAT4 and IFN-ɣ knockouts, and chronic inflammation (day 35) was greatly significantly increased(261). IFN-ɣ has also been demonstrated as essential for survival of CVB4 infection, mice with a global knockout of IFN-ɣ succumb to lethal pancreatitis. Transgenic overexpression of IFN-ɣ in the pancreas decreased viral replication not only in the pancreas but also in all other tissues studied (spleen and kidneys)(262). Together, these results indicate that NK cells are crucial to the control of early viral replication and necrosis in the heart. And that this may be mediated by a perforin independent mechanism, such as cytokine production or apoptosis induction by

death receptors. NK cells do not seem to be central for the generation or control of subsequent cellular infiltration.

The role for T-cells was first identified by Woodruff, who administered an anti-T-cell serum (which lytically depopulates the body of T-cells) prior to CVB3 infection, and found that while viral replication was roughly equivalent, inflammation was greatly decreased(263). This suggested that T cells might be pathogenic during viral myocarditis. Furthering this hypothesis, splenic lymphocytes (a mixed population) from infected mice were found to be lytic for not only CVB3 infected cells, but also for uninfected fibroblasts. Lytic activity of splenocytes was maximal in cells isolated between days 3 and 5, and declined to background levels by day 7 (264). Woodruff also demonstrated that administration of cortisone, an immunosuppressive led to greatly increased viral replication, extensive necrosis, but also to an equivalent level of antibody production and less infiltration of the myocardium(18). The existence of autoreactivity was confirmed by Rose (one of the first to describe autoimmunity(265)), who went on to show that heart specific autoantibodies were produced following CVB3 infection(266). The interplay between CD4 and CD8 T cells is complex. CD4 knockouts develop severe myocarditis, but less viral replication, suggesting some functional compensation by cytotoxic CD8 T cells. Indeed, depletion of CD8 cells within CD4 knockouts decreases myocarditis, but increases heart viral titres (258). More directly, knockouts of CD4, CD8, CD4 and CD8, and the T cell receptor (TCR) were compared with each other. Deletion of either CD4 or CD8 alone had little effect, and CD8 deletion alone decreased survival. The double knockout, or TCR knockout were significantly more resistant to myocardial inflammation, while antibody production, viral replication and necrosis remained relatively unchanged across groups or tissues studied (267). Therefore, T-cells appear to be redundant in resolving CVB3 infection, and can also be pathogenic for myocardial inflammation. However, broad suppression of the immune system leads to uncontrolled viral replication and sarcolemmal damage.

TREATMENTS AND POSSIBLE TREATMENT OPPORUNITIES

Current treatment options for coxsackievirus infection, myocarditis are limited and in many cases still experimental. Only two compounds have been demonstrated to be effective clinically: Pleconaril and IFN-ß. Pleconaril is an antiviral compound specific to picornaviruses, which blocks the uncoating of the virus by binding to and stabilizing the VP1 capsid protein (268, 269). Pleconaril has been shown effective in the treatment of disseminated infant coxsackieviral infection (270). However, it has also been demonstrated that escape mutants exist, and that only one amino acid substitution is required to achieve resistance (271). In mice the deletion of the IFN-ß gene or its receptor, has no clear effect on CVB3 replication in the heart (190, 237). However, the administration of type I IFN (272) or IFN stimulating compounds such as TLR3 agonists (273), prior to infection greatly ameliorates viral myocarditis. This contradiction may be accounted for in a number of ways: administration of IFN before infection renders other tissues refractory to viral infection (274), alternatively IFN is also known to significantly boost NK cell killing activity(250). In a small and uncontrolled trial in patients with chronic viral myocarditis, it was shown that treatment with IFN-ß significantly ameliorated patient heart function, and cleared enterovirus from the heart. A controlled clinical trial is currently underway (NCT00185250) to assess if IFN-ß treatment performs significantly better than placebo.

Other treatments that seem promising include ribavirin, which was able to protect mice from early mortality, cardiac inflammation and necrosis, but only if treatment was started early (275). Nitric oxide (NO) donors such as glycerol trinitrate (GTN, nitroglycerin) have been shown to inhibit proteases 2A and 3C *in vitro*, and in mice reduce CVB3 induced inflammation. Despite anti-protease activity *in vitro* no effect on viral replication or survival was observed in treated mice(276). Targeting viral 2A protease directly by RNA interference was moderately protective when administered in the context of highly susceptible IFNAR1 knockout mice (277). Inhibition of the p38 MAP kinase *in vitro* appears to inhibit necrosis and decrease the amount of released viral particles following infection(108). *In vivo* p38 inhibition has also been reported to decrease inflammation and the percent area of myocardium with replicating virus (278).

The Myocarditis Treatment Trial was less successful. During the trial, 64 patients were given the immunosuppressives cyclosporine and prednisone, and 47 controls were given the standard of care to treat heart failure with no immunosuppressives. No effect was observed (P=0.96). One possible confounder could have been that patient inclusion was based on Dallas criteria, but did not require EMBs to be negative for viral replication. Immunosuppression has long been reported to be deleterious in response to CVB.

Lacking clinical trial evidence for specific treatments for viral myocarditis, the current standard of care is largely supportive. Current treatments address the heart failure resultant from myocarditis rather than the myocarditis *per se* (170). These include decreasing cardiac work and stress through avoiding exercise, as exercise significantly exacerbates myocarditis(279, 280). Pharmacological interventions such as diuretics to prevent fluid overload, or angiotensin converting enzyme (ACE) inhibitors to decrease cardiac load and limit progression to dilated cardiomyopathy(170).

RATIONALE, HYPOTHESIS AND OBJECTIVES

RATIONALE

Coxsackievirus B3 (CVB3) infection is a common cause of myocarditis, a potentially fatal inflammation of the heart. In newborns, severe cases of viral hepatitis are also reported. At present, treatments and prognostics are scarce and non-specific for these devastating conditions. This effort is markedly hindered by the diverse nature of the pathogenesis of coxsackievirus infection, which can be fulminant, acute, resolving, persistent and all things in between.

Since their discovery in 1947, our understanding of coxsackieviral infection has been advanced through the use of mouse models. Some aspects of infection include: 1) viral ability to attach, enter and replicate within target cells; 2) a cell autonomous innate immune response to the virus; 3) an inflammatory cellular response to the virus and 4) the ability of the host to resolve infection completely. However several unanswered questions persist. Which factors govern why severe disease outcomes affect only a

subset of individuals during an outbreak? Which factors determine why some individuals are highly susceptible to coxsackieviral hepatitis, whereas others are more susceptible to coxsackieviral myocarditis? Finally, there is a persistent sub-textual debate within the literature on whether inability to control coxsackievirus replication causes severe myocarditis, or if it is a differential inflammatory response to an equivalently controlled coxsackievirus infection, or both?

HYPOTHESIS

Natural variation between genetically inbred strains of mice in response to susceptibility to CVB3 infection exists, and is poorly understood. We hypothesize that differences in susceptibility between genetically inbred strains of mice during CVB3 infection is under genetic control. We also hypothesize that through interrogation of genetically determined resistance or susceptibility to CVB3 infection we may identify genes whose involvement in coxsackievirus infection has not previously been reported.

OBJECTIVES

AIM 1: PHENOTYPE THE AcB/BcA PANEL, IDENTIFY AND CHARACTERIZE DEVIANT STRAINS.

Inbred mouse strains respond differently to CVB3 infection including susceptible strains with A/J background and resistant strains with C57BL background. Forward genetic analysis using mouse models constitutes a powerful tool to study natural variation in human complex traits and disease. We have previously made use of such a forward genetic approach on susceptibility to CVB3-induced myocarditis, and significant linkage was identified with at least 3 separate loci. In order to identify additional loci controlling susceptibility to CVB3 infection the recombinant congenic AcB/BcA panel was screened. Recombinant congenic strains are generated by two sequential backcrosses of one inbred donor strain (12.5% of the genome) to a background recipient strain (87.5% of the genome) and have been developed as a tool for complex trait mapping. We will then use the strain distribution pattern (SDP) of the RCS to identify interesting and highly discordant strains. Following this, we will characterize discordant strains with a

phenotyping panel of serum biomarkers for tissue damage, and measure viral replication within selected tissues. After identifying a discordant strain with discordant phenotype, an outcross will be performed with a closely related strain of mouse to identify genetic linkage to the trait of interest. Identification of linkage within a deviant strain will provide a new genetic model of susceptibility to CVB3 infection.

AIM 2: CONFIRM, CHARACTERIZE AND REFINE LINKAGE OF VMS1 ON MOUSE DISTAL CHROMOSOME 3

We have previously used a forward genetic approach to identify significant linkage between myocardial inflammation and necrosis with mouse distal chromosome 3 at the *Vms1* locus. In order to replicate linkage to *Vms1*, we will phenotype and characterize consomic mice containing a donor chromosome 3 from the susceptible strain in a resistant background i.e.: C57BL/6J-Chr3$^{A/J}$/NaJ (CSS3). We will then perform an F_2 test cross between CSS3 and C57BL/6 mice with the aim of providing confirmation that myocarditis is linked to distal chromosome 3. Subsequently, CSS3 and C57BL/6 mice will be characterized earlier during infection at 1, 2 or 4 days to determine if differences in viral replication levels or Type I IFN production precede inflammatory infiltration of the myocardium. Subsequent to identifying a day on which differences in viral replication are evident, but Type I IFN and inflammation are equivalent, we will employ microarray analyses on cardiac tissue to generate further insights into the expression profiles of resistant and susceptible hearts. Finally, integration of data from [B10.AxA/J]F_2 and [B6xCSS3]F_2 will be performed to boost our power to refine the interval and identify candidate genes. Confirmation and refinement of linkage to distal chromosome 3 will provide new insight into how natural variation in susceptibility to CVB3 infection is determined between A/J and C57BL mice.

AIM 3: CHARACTERIZE THE CONTRIBUTIONS OF TNNI3K TO THE HOST RESPONSE TO CVB3

Our third aim seeks to asses the effect of overexpression of the cardiac specific kinase TNNI3K on host susceptibility to viral myocarditis. DBA2/J mice carrying a cardiac specific transgene for the TNNI3K gene (TNNI3K^{tg}) will be compared to wild-type

littermates (DBA2/J) following infection. Viral replication will be measured at 2, 4, 6 and 8 days post infection to determine whether TNNI3K has any effect on viral RNA replication or released viral particles. Sarcolemmal necrosis and myocardial inflammation will be measured on days 4, 6 and 8 post infection to determine whether TNNI3K overexpression has an impact on the development of cardiac pathology following CVB3 infection. Microarray analysis will again be employed at a time preceding outright inflammatory infiltration to identify differences characterizing resistant and susceptible hearts. Expression of genes selected to represent functional modules from this analysis will be measured at days 2, 4, 6 and 8 following infection to create temporal associations with our phenotypes of interest. Selected candidate response genes will also be pursued *ex vivo* in adult primary cardiomyocytes infected with CVB3. Little is known about the natural function of TNNI3K, and nothing in the context of CVB3 infection. These experiments will allow us to identify a possible pathway that can be modulated to control the pathogenesis of viral myocarditis.

CHAPTER 2: MAPPING OF A QUANTITATIVE TRAIT LOCUS CONTROLLING SUSCEPTIBILITY TO COXSACKIEVIRUS B3 INDUCED VIRAL HEPATITIS.

Sean A. Wiltshire, Jennifer Marton, Gabriel André Leiva-Torres, and Silvia M. Vidal

Department of Human Genetics, McGill University, Montreal, Quebec, H3A 1B1, Canada;

BRIDGING STATEMENT FROM CHAPTER 1 TO CHAPTER 2

A/J and C57BL/ strains have previously been demonstrated to differ in their susceptibility to CVB3 infection. A/J strains develop more severe inflammation and necrosis following infection with the CVB3-CG strain of virus, whereas C57BL/6 and C57BL/10 strains are relatively resistant and survive the infection. Previous screens of inbred and recombinant inbred lines have identified the *H2* locus, and a locus on central chromosome 14 close to the myosin heavy chain alpha (*Myhc6*) gene. We had also identified linkage to a locus on distal chromosome 3 (*Vms1*) controlling myocarditis, as well as loci on chromosomes 1, and 4 controlling sarcolemmal disruption. Nevertheless, it remained unclear whether other genes or combinations of genes might determine susceptibility in the A/J and C57BL/ backgrounds.

ABSTRACT

The pathogenesis of coxsackieviral infection is a multifactorial process involving host genetics, viral genetics and the environment in which they interact. We have used a model of infection with Coxsackievirus B3 (CVB3) to characterize the contribution of host genetics to survival of infection and viral hepatitis in mice. We screened 25 AcB/BcA RC mouse strains by CVB3 infection in order to map genes controlling coxsackieviral infection. As compared to its relatively resistant C57BL/6 background, the BcA86 strain was found to be particularly susceptible to early mortality and hepatitis necrosis as measured by serum ALT levels. Linkage analysis in the BcA86 strain revealed a new locus on chromosome 13, which controls ALT levels as early as 48 hours following infection, and lead to elevated expression of type I Interferon. These results provide new evidence for the presence of a locus contributing to the susceptibility of mice to viral hepatitis.

INTRODUCTION:

Coxsackievirus B3 (CVB3) is frequently studied in the context of myocarditis and its long-term sequela dilated cardiomyopathy. However, coxsackievirus infection is systemic: early accounts detail that CVB3 is capable of inducing myositis, meningitis, pancreatitis, hepatitis as well as myocarditis (281). A recent study in diabetic individuals estimates that up to 75% of people are seropositive to any single strain of coxsackievirus (CVB3=66%)(44). In contrast, severe symptoms are comparatively rare. In newborns, severe cases of viral hepatitis are periodically reported as a result of group B Coxsackieviruses (CVB), including CVB3(33-35). Clinically observed heterogeneity is recapitulated in the mouse model, where disease progression and presentation depend on both host and viral factors(20, 26, 184, 185).

The central role of the host immune response to determining the outcome of CVB3 infection has been clearly demonstrated in a number of reverse genetic (knock-out) studies. The type I Interferon (IFN) axis seems to be central in controlling viral replication within the liver, but may be redundant in controlling viral replication in the heart. IFN receptor (*Ifnar1*) knockout mice succumbed early to lethal infection, with greatly increased viral replication in the liver, and ten-fold higher liver damage as measured by serum alanine aminotransferase (ALT) compared to wild type. However no significant changes in viral replication or inflammation were observed in *Ifnar1*$^{-/-}$ hearts (282). These results are consistent when the Interferon ß gene (*Ifnb1*) is knocked out instead of *Ifnar1*(190). Whereas abrogation of type I IFN had a great effect on the liver, and no apparent effect on the heart, abrogation of all JAK/STAT signalling by transgenic overexpression of the suppressor of cytokine signalling 1 (*Socs1*), greatly enhanced myocarditis and no effect was observed in the liver(248). Deficiency for toll-like receptor 3 (*Tlr3*), a viral pattern recognition receptor sensitive to lumenal double stranded RNA, increases susceptibility to myocarditis, but not hepatitis (241). Absence of the cytoplasmic dsRNA sensor Melanoma Differentiation-Associated protein 5 (*Ifih1* or MDA5*)* leads to greatly increased mortality, accompanied by severe hepatic necrosis(235), and greatly elevated ALT levels. Absence of the MDA-5 transducing

mitochondrial antiviral signalling protein (*Mavs)* also leads to early mortality (day 2-3) accompanied by severe hepatic necrosis.

Further complicating matters, genetic background effects contribute to pathogenesis and tissue tropism, presumably through as yet unmapped genes. For example, in the C57BL/6 genetic background MDA5 is essential for survival of CVB3 infection and protection from hepatic necrosis, however MDA5 deficiency in the 129SvJ background has no apparent effect (236).

Forward genetic analysis using mouse models constitutes a powerful tool to study natural variation and background variation in complex traits and disease. It is known that the A/J and C57BL/6 strains are respectively susceptible and resistant to CVB3 infection(27). We have previously made use of a forward genetic approach to scan the mouse genome for loci linked to susceptibility to CVB3-induced myocarditis between the A/J and C57BL/6 strains(135, 188). In order to identify additional loci controlling susceptibility to CVB3 infection the recombinant congenic AcB/BcA panel derived from A/J and C57BL/6 progenitors was screened (283). Recombinant congenic strains are generated by two sequential backcrosses of one inbred donor strain (12.5% of the genome) to a background recipient strain (87.5% of the genome) and have been developed as a tool for complex trait mapping. Following a screen of the AcB/BcA panel, one strain (BcA86) with a dramatically discordant phenotype was singled out for further analysis. Viral replication and common serum biochemical markers were tested to characterize pathogenesis in BcA86 mice. Serum ALT in the BcA86 mice was found to be elevated compared to other strains, and was pursued using an informative F_2 cross approach. Linkage analysis revealed a single significant locus on distal chromosome 13 that controls ALT levels.

MATERIALS AND METHODS

MICE, CELLS AND VIRUS

Inbred C57BL/6J (B6), C57BL/10, and A/J mice were purchased from the Jackson Laboratory (Bar Harbor, ME). The set of 36 AcB/BcA recombinant congenic strains (RCS), derived from A/J and B6 parents, were generated according to a previously described breeding scheme and genotyping protocol (283). (BcA86 X C57BL/10) and (C57BL/10 X BcA86) F_1 crosses were generated; F_2 crosses were then performed by standard (F_1brother X F_1sister) mating. The mice were maintained in the McGill University animal facility in compliance with the Canada Council on Animal Care as approved by the McGill University Animal Care Committee. Coxsackievirus B3 used for all experiments was the CVB3-CG strain as previously described (284). HeLa cells (ATCC: CCL-2) were grown and maintained in Dulbecco's Modified Eagle Medium (DMEM) supplemented with 10% FBS, 100 µg/mL Penicillin/Streptomycin (1X media). Homogenized organs were serially diluted 10-fold in non-supplemented DMEM and the dilutions were used to infect HeLa cells in triplicate for 60 minutes. After initial infection by homogenate, HeLa cells are covered in a layer of 2%FBS DMEM media with 0.25% agarose and incubated for three days. Cells were fixed in formaldehyde and stained with crystal violet to count plaques as previously described (188).

MOUSE INFECTION AND PHENOTYPE DETERMINATION

For each experiment, a vial of viral stock was thawed and diluted in cold PBS at $5x10^4$ plaque forming units (PFU) per ml. Inbred, F_1 and F_2 mice were inoculated intraperitoneally with 400 PFU of CVB3-CG per gram of body weight at seven to nine weeks of age. Animals were weighed daily and observed for changes in fur characteristics, level of activity and appearance of respiratory distress. During the recombinant congenic strain survival screen, moribund mice were humanely euthanized at an acceptable clinical endpoint. A total of 70 BcA mice and 30 AcB mice, and 210 [BcA86xC67BL/10]F_2 mice were phenotyped. Following the survival screen, mice were euthanized at day 2 post-infection, and exsanguinated by cardiac puncture to serum. Heart and Liver tissues were removed aseptically snap frozen and stored at -80°C in

two separate aliquots. One portion was subsequently homogenized and submitted to three freeze-thaw cycles to release infectious virus for determination of viral titre by plaque assay. RNA was extracted from the other portion by TRIzol (Invitrogen), and reverse transcribed by MMLV (New England Biolabs) according to the manufacturers' instructions. Serum levels of creatine kinase (CK) and alanine aminotransferase (ALT) were measured by the McGill Comparative Medicine Animal Resources Centre's Diagnostic and Research Support Service using a colorimetric method. Quantitative PCR primers for were designed to span exon junctions with the help of Primer3plus(285). Cytokine gene expression and relative CVB3 quantification were determined relative to the house keeping gene *Gapdh* by 2^-∂∂Ct calculations(286).

LIST OF PRIMERS USED:

CVB3-H3 forward: ATGGCAGAAAACCTCACCAG, CVB3-H3 reverse: ATGTTCTGCCCAAACAGTCC; Gapdh forward: AAGGGCTCATGACCACAGTCC, Gapdh reverse: GATGCAGGGATGTTCTGG; Tnfa forward: CATCTTCTCAAAATTCGAGTGACAA, Tnfa reverse: TGGGAGTAGACAAGGTACAACCC, Ifnb1 forward: TGACGGAGAAGATGCAGAAG, Ifnb1 reverse: ACCCAGTGCTGGAGAAATTG

GENOTYPE ANALYSIS

The C57BL/10 strain is not a Mouse Phenome Project priority strain (http://phenome.jax.org/), and so existing publically available genotype information is limited. Most SNPs polymorphic between C57BL/10 and C57BL/6 for use in the generation of a panel capable of distinguishing between C57BL/10 and BcA86 were identified using the JAX Diversity Array (287). In this panel, 7499 SNPs were polymorphic between C57BL/6 and C57BL/10, though these tended to be clustered and gaps remained [Supplemental Figure 2]. These gaps in the genetic map were filled in by comparing the genotype of C57BL/6 against all other C57BL strains available in all datasets contained within the Mouse Phenome Database. When the C57BL/6 genotype was divergent, C57BL/6 and C57BL/10 were genotyped by Sanger sequencing to confirm the private C57BL/6 SNP. Finally, the map was completed with microsatellites

identified by us as previously(135), and in collaboration with others(288) for a total of 107 markers that are informative between BcA86 and C57BL/10 [Supplemental Table 1]. All SNP genotyping was performed by Sequenom iPlex Gold technology. Genotyping of the F_2 was performed at the McGill University and Genome Quebec Innovation Centre). Microsatellite PCR Reactions performed manually used a 10 µl total reaction volume, 200 µM dNTPs, 1.5 mM $MgCl_2$, 2 pmol of each primer and 0.5 U of *Taq* polymerase (Invitrogen, Burlinton, ON). Reactions were performed as follows: 96˚ for two minutes; 30 cycles of 94˚ for 45 seconds, 56˚ for 45 seconds, 72˚ for 60 seconds; and a final extension step 72˚ seven minutes. PCR products were then separated on 2-4% high-resolution agarose (USB, Cleveland, OH) gels containing Ethidium bromide and visualized under UV light.

STATISTICAL ANALYSIS

Statistical analyses were conducted with the freely available program R; linkage was performed with the package 'R/qtl' version 3.02. Survival analysis was performed using the 'Survival' package version 2.37. Skewness was detected using the D'Agostino test from the 'moments' package version 0.13. ALT, Liver and Heart Viral titre F_2 phenotypes were normalized using the Box-Cox(289) method as implemented in the 'Caret' package version 5.17. Viral replication is also reported as Log_{10}[PFU/mg] in figures for the sake of interpretability. The scanone function of the 'R/qtl' package version 1.28-19, was used to perform Haley-Knott regression (HK) of the phenotype on genetic markers. Significance values were evaluated with 10 000 permutations. The LOD support interval of QTL peaks was calculated using a 1.5-LOD drop by 'R/qtl' on the interval map. P-values shown in the figures are a result of two-tailed t-Tests with *$P < 0.05$, **$P < 0.01$, and ***$P < 0.001$ unless otherwise indicated.

RESULTS

MICE OF THE BCA86 RECOMBINANT CONGENIC STRAIN SUCCUMB TO LETHAL CVB3 INFECTION

The course of infection with Coxsackievirus B3 is highly variable and depends on both host and viral background(20, 26). It is known that the A/J and C57BL/6 strains are respectively susceptible and resistant to CVB3 infection(27), though little is known about the genetic determinants underlying this trait. It was therefore of interest to challenge the recombinant congenic strain (RCS) panel of AcB/BcA mice with CVB3 infection. The screen was undertaken using an infectious dose which had previously been used to study myocarditic potential of CVB3 in A/J and B10.A-*H2*^{a} mice(135). It was observed early into screening the RCS panel that the majority of AcB (A/J background, C57BL/6 donor) and BcA (C57BL/6 background, A/J donor) mice did not survive the infection until the previously established experimental endpoint on day 8. Therefore survival of infection was used as a phenotype. In total, 109 male RC mice were screened, with between 2 and 6 per strain (median 4) [Figure 1]. Consistent with previous reports of the involvement of *H2* in susceptibility to CVB3 infection(25-27), the two *H2*^{a} carrying BcA strains (BcA69 and BcA74) were relatively resistant, and survived infection. Most other strains were comparatively susceptible to lethal infection. In particular, the BcA86 strain succumbed to early mortality between days two and five post infection (N=6, P=0.0012 compared to C57BL/6).

Further phenotyping was conducted in a panel of A/J, BcA86, C57BL/6 and the closely related C57BL/10. C57BL/10 mice were included knowing that the genetic architecture underlying the phenotype of BcA86 might include not only A/J loci, but also de novo mutations on the C57BL/6 background. Two *de novo* mutations have been mapped so far within the AcB/BcA panel on the background strain(290, 291). Reports of early mortality within CVB3 infection have implicated metabolic failure secondary to hepatic necrosis (118, 235, 237), so viral replication in the heart and liver, as well as serum biomarkers for heart and liver damage were assessed at the early time point of 48 hours post infection [Figure 2]. It was found that viral replication in BcA86 was slightly higher

in the heart than in C57BL/6 (one-way ANOVA with Tukeys multiple comparison test, P=0.03), while being comparable in the spleen and liver. No significant differences in the heart damage biomarker creatine kinase (CK) were observed at this time point. BcA86 mice showed a marked increase in serum levels of the liver damage biomarker alanine aminotransferase (ALT) as compared to A/J, C57BL/6 and C57BL/10 mice (one-way ANOVA with Tukeys multiple comparison test P=0.0005, 0.0055, 0.0007). The BcA86 phenotype of elevated ALT relative to C57BL/10 mice was reproduced in independent experiments (Supplemental Figure 1)

SEGREGATION ANALYSIS OF SERUM ALANINE AMINOTRANSFERASE LEVELS, AND VIRAL REPLICATION REVEALS COMPLEX INHERITANCE

In order to identify genetic determinants conferring susceptibility to BcA86 mice, we undertook a [C57BL/10x BcA86]F_2 cross (N=210). Segregation analysis indicated that serum ALT levels, liver and heart viral replication were all highly skewed distributions (skewness=2.45, 2.90, 6.61 respectively, all p<1e-9). To facilitate genetic mapping, these phenotypes were normalized using the Box-Cox method and the transformed data was compatible with a mixture of random normal variables [Figure 3]. Liver viral replication was significantly correlated with serum ALT (R^2=0.44), and also with heart viral replication but to a lesser degree (R^2=0.30). Heart and Liver viral replication were also correlated to each other (R^2=0.36). These results are consistent with common and distinct genetic determinants of susceptibility within the [BcA86x B10]F_2 mice.

LINKAGE ANALYSIS REVEALS TWO LOCI CONTROLLING SUSCEPTIBILITY TO CVB3 INFECTION IN [BCA86X B10]F_2 MICE

In order to perform linkage analysis, a panel of genetic markers was created to distinguish between BcA86 and C57BL/10 backgrounds (described further in methods). The full panel of polymorphic markers between C57BL/6 and C57BL/10 has been successfully used and described elsewhere(288, 292). Linkage to serum ALT was identified with a single significant peak on distal chromosome 13 with LOD=4.50, P=0.003 and 9.4% variance explained, peak marker rs3702296 [Figure 4 and Figure

5A]. Chromosome 13 in the BcA86 strain does not contain any A/J donor genome segments. No significant linkage was found to viral replication in the liver, however a suggestive QTL with maximum LOD score (2.81) and P value (0.14) was also detected at marker rs3702296. Linkage to viral replication in the heart revealed one peak on chromosome 17 of LOD=3.4 and with borderline significant P=0.046. The 1.5-LOD support interval on chromosome 13 extends between 80.3 Mb 110.3 Mb, with a peak of linkage at 102Mb. On chromosome 17, the 1.5-LOD support interval extends between 49.7 Mb and 69.7 Mb. The BcA86 strain carries an A/J haplotype block beginning at 47.7Mb and extending to 58.6Mb, is present within the chromosome 17 interval (127). Allele effect plots indicated that in both cases, the BcA86 genotype conferred susceptibility at the two loci. Mice inheriting homozygous BcA86 genotype on chromosome 13 had an median serum ALT level of 8820IU/L and mice homozygous for C57BL/10 had a median serum ALT level of 1986IU/L [Figure 5B and 5C]. These same mice homozygous for chromosome 13 had median liver viral replication of 4.84 Log[Pfu/mg] and 4.48 Log[PFU/mg] respectively. Mice inheriting homozygous BcA86 genotype on chromosome 17 had median heart viral titre of 4.35 Log[PFU/mg] and mice homozygous for C57BL/10 had median heart viral titre of 3.78 Log[PFU/mg] [Figure 5E and 5F].

DIFFERENTIAL CONTROL OF TYPE I INTERFERON IN BCA86 AND B10 MICE AND IN F2 MICE

Given the known role of the Type I Interferon circuit in hepatic control of CVB3(190, 241, 248, 282), quantitative RT-PCR was performed to ascertain differences in gene expression between C57BL/10, and BcA86 for coxsackieviral mRNA, and selected cytokines [Figure 6]. In addition to the parental strains, [BcA86xC57BL/10]F_2 mice homozygous at the peak marker (rs3702296) for each genotype were included in the analysis. Unlike viral titre by plaque forming assay [Figure 2B], differential control of viral replication between BcA86 and B10 was observed using the more sensitive technique of RT-PCR (P=0.008, Mann-Whitney). Differential control of viral replication was not recapitulated in the F_2 mice consistent with no significant linkage between rs3702296 and control of viral replication [Figure 6A]. Type I Interferon measured by *Ifnb* was

elevated in BcA86 mice as compared to C57BL/10 (P=0.01) as well as in F2 mice carrying BcA86 genotype (P=0.026 one-tailed T-test). Other cytokines (*Il6*, *Il1b*, *Tnfa*) were similarly tested, but none achieved statistical significance within the F_2 mice (not shown).

These results identify the presence of a locus controlling susceptibility to CVB3 infection, which results in elevated serum ALT, and increased hepatic expression of interferon ß following infection.

DISCUSSION

Most individuals appear to become infected with Coxsackievirus B3 or closely related species at some point in their lives(44, 293, 294), and systemic infection can be severe(33-35). The contrast raised between comparatively rare reports of severe symptoms with a common infection suggests a non-uniform response to the virus. There remains a need to account for divergent clinical presentation between otherwise normal and immunocompetent individuals. Mouse models represent a simplified system where aspects of pathogenesis can be modulated and interrogated one at a time. Natural variation in response to Coxsackievirus in the mouse model is diverse, and depends on host genetic factors (25, 26, 135, 143, 188), viral genetic factors(22, 295, 296) and also environmental factors such as age(297), sex(298, 299) or diet (17, 191).

To study host genetic factors which determine ability to control infection within relatively resistant C57BL/6 and relatively susceptible A/J mice, we have made use of a recombinant congenic strain panel (RCS)(283). In a typical RCS study(290, 300), strains are compared against their respective genetic background (e.g.: BcA *vs*. C57BL/6 and AcB *vs*. A/J) to identify discordant strains. In this manner, donor segments conferring susceptibility (or resistance) can then be mapped either directly or in a subsequent test cross. In the present study, it was determined that most BcA strains were more susceptible to CVB3 infection than C57BL/6 mice. This suggests that the resistance of C57BL/6 mice is either relatively easily overcome by a polygenic A/J donated susceptibility, or that susceptibility conferring mutations had occurred during or before the creation of this panel. Three out of seventeen strains challenged completely survived CVB3 infection, of these were the only two that carried the A/J allele of the major histocompatibility complex ($H2^a$). Previous reports have indicated a role for *H2* in controlling CVB3 infection, but also that non-*H2* loci seem to control the majority of phenotypic variance between strains(25, 26, 143). This is in agreement with our findings, and so the specific role of $H2^a$ in enhancing or maintaining C57BL/6 resistance was not pursued further. Of the BcA strains, the most discordant studied was strain BcA86, which succumbed to infection rapidly (2-4 days), and presented greatly elevated serum ALT (a marker of necrotic hepatocyte death) 48 hours post-infection.

Using an informative F_2 mapping cross between BcA86 and C57BL/10 revealed one locus on chromosome 13 that controlled serum ALT. The locus increased median ALT levels by 6834 IU/L in mice homozygous for BcA86 at this locus (median 8820IU/L) over mice homozygous for C57BL/10 (median 1986IU/L). Further phenotyping of F_2 mice with a homozygous BcA86 genotype at this locus revealed approximately double the levels of *Ifnb1* expression as compared to mice homozygous for C57BL/10. Lack of significant linkage of viral replication and chromosome 13, with no observed difference in viral RNA levels in these same F_2 mice suggests a novel phenotype unlike MDA-5, IFNAR1 or IFN-ß knockouts (190, 235, 282), where high viral replication in the liver is usually accompanied by hepatic necrosis and early mortality.

The 1.5-LOD interval was calculated using interval mapping as being between 80.3Mb 110.3Mb. This region contains over 148 known protein coding genes, several of which would make interesting candidates for further study. The RAS P21 Protein Activator (GTPase Activating Protein) 1 (*Rasa1*) gene located towards the proximal end of the interval (85.2Mb) was recently identified to be strongly antiviral in the context of CVB3 infection of polarized human brain microvascular endothelial cells(301). Coagulation factor II (thrombin) receptor (*F2r* or PAR1) located at 95.6Mb has been shown to control CVB3 infection in the heart and liver at late (but not early) time points, and may be involved in cooperative signaling with TLR3(302). 3-hydroxy-3-methylglutaryl-Coenzyme A reductase (*Hmgcr* 96.6Mb), the enzymatic target of statin class of pharmaceuticals, performs a rate limiting step in cholesterol biosynthesis. The link between CVB3 replication and cellular cholesterol availability was recently established in a study that demonstrated CVB3 causes cholesterol to be trafficked from the plasma membrane and specialized organelles for viral production (73). Phosphatidylinositol 3-kinase, regulatory subunit, polypeptide 1 (p85 alpha) (*Pi3kr1*) located at 101Mb is a regulatory subunit of PI3K. It has been shown in HeLa cells that PI3K signaling is beneficial for CVB3 replication, presumably by providing a survival signal (possibly via NFkB) to counter apoptotic signals(303, 304). A gene cluster of NLR family, apoptosis inhibitory proteins (*Naip1-Naip7*, 100Mb) have been reported to bind bacterial components and lead to cellular pyroptosis(305, 306). Distally, the IL-6 receptor signal transducer (*Il6st*, or gp130) is located at 112Mb. Gp130 signalling does not appear to be directly antiviral,

but provides a strong cytoprotective effect in the context of CVB3 infection. Furthermore, cardiac specific ablation of gp130 signaling by SOCS3 overexpression leads to greatly increase cardiac necrosis, and lethality between 4 and 6 days after infection(307). Chromosome 13 comes from an originally C57BL/6 segment in the BcA86 strain of mice. Genotyping results from the diversity chip [Supplemental Figure 1] strongly suggest that distal chromosome 13 is shared ancestrally between C57BL/6 and C57BL/10. This suggests a possible *de novo* mutation in BcA86 mice at this locus. Mutations in one or more of the discussed genes, or others with no known role in CVB3 infection are possible, and further studies will include exome sequencing and candidate gene analysis.

ACKNOWLEDGEMENTS:

This work was supported by grants from the Canadian Institutes of Health Research (CIHR MOP-86592) S.A.W., G.A.L. and J.M. were supported by FRSQ Scholarships, and S.M.V. by the Canada Research Chair program.

FIGURE AND LEGENDS TO FIGURES:

FIGURE 1: SURVIVAL OF CVB3 INFECTION IN ACB/BCA RECOMBINANT CONGENIC STRAINS OF MICE

(a) Strain distribution plot of mean± standard deviation of survival time for recombinant congenic strains of mice. Between 2 and 8 male mice per strain (median 4) were tested for a total of 109 mice. Both *H2*^{a} carrying BcA strains (BcA69 and BcA74) survived infection.

(b)The BcA86 strain succumbed to early mortality between days two and five post infection (N=6, P=0.0012 compared to C57BL/6).

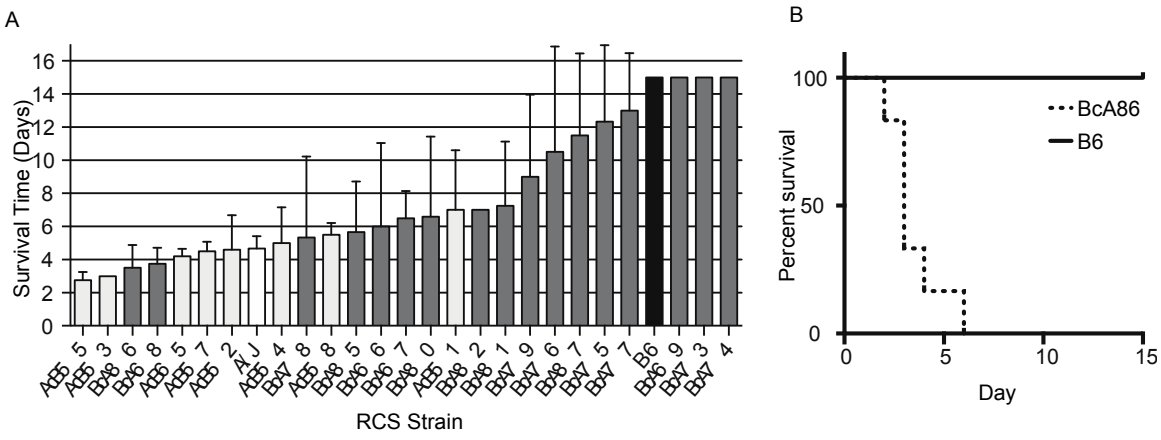
A
Survival Time (Days)
0
2
4
6
8
10
12
14
16
AcB5 5
AcB5 3
BcA8 6
BcA6 8
AcB5 5
AcB5 7
AcB5 2
A J
AcB5 4
BcA7 8
AcB5 8
BcA8 5
BcA6 6
BcA6 7
BcA8 0
AcB5 1
BcA8 2
BcA8 1
BcA7 9
BcA7 6
BcA8 7
BcA7 5
BcA7 7
B6
BcA6 9
BcA7 3
BcA7 4
RCS Strain
B
Percent survival
0
50
100
BcA86
B6
0
5
10
15
Day

FIGURE 2: ELEVATED SERUM ALT IN BCA86 MICE COMPARED TO GENETIC BACKGROUND AND DONOR STRAINS

Mean ± standard deviation for viral replication measured in the heart (a), liver (b) and spleen (c) were measured in A/J, BcA86, C57BL/6 C57BL/10 mice. Only viral replication in the heart was statistically significantly different between the four strains of mice (one-way ANOVA with Tukeys multiple comparison test, $P<0.05$). Levels of the serum biomarker for necrotic heart damage (c) creatine kinase (CK), and liver damage (d) alanine aminotransferase (ALT) showing hepatic damage specifically in BcA86 (one-way ANOVA with Tukeys multiple comparison test $P=0.005$).

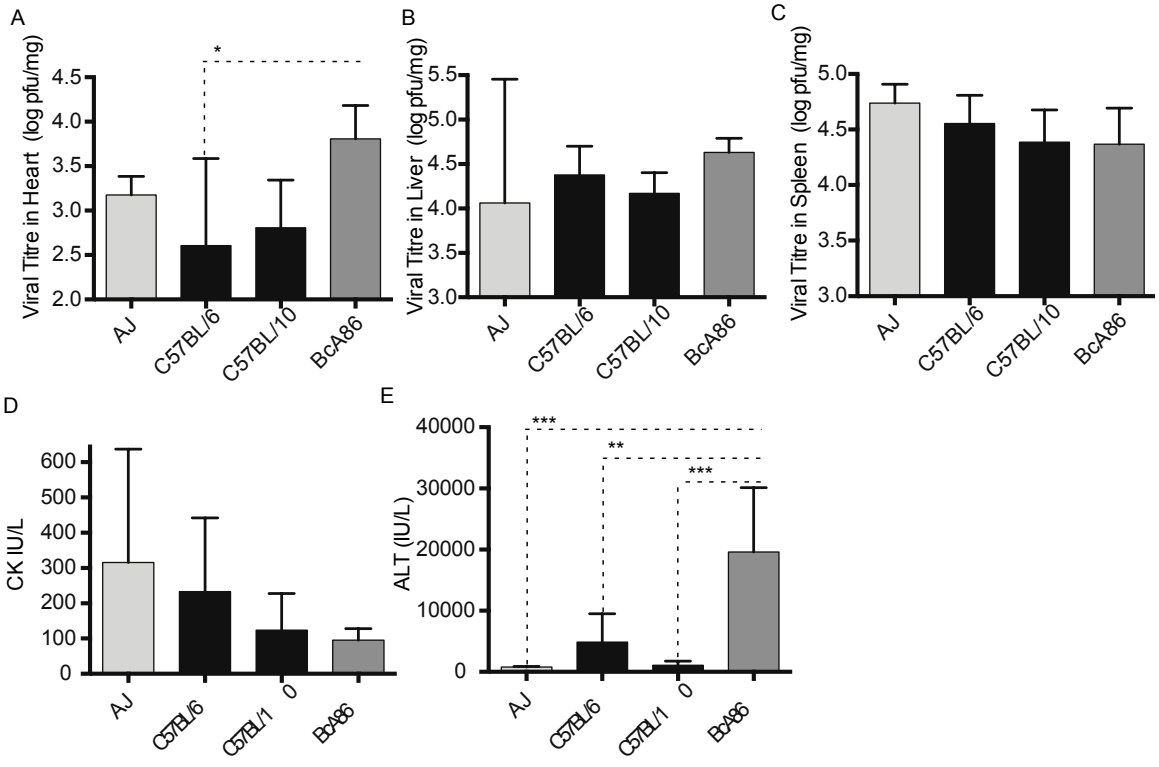
A
Viral Titre in Heart (log pfu/mg)
4.5
4.0
3.5
3.0
2.5
2.0
*
AJ
C57BL/6
C57BL/10
BcA86
B
Viral Titre in Liver (log pfu/mg)
5.5
5.0
4.5
4.0
3.5
3.0
AJ
C57BL/6
C57BL/10
BcA86
C
Viral Titre in Spleen (log pfu/mg)
5.0
4.5
4.0
3.5
3.0
AJ
C57BL/6
C57BL/10
BcA86
D
CK IU/L
600
500
400
300
200
100
0
AJ
C57BL/6
C57BL/10
BcA86
E
ALT (IU/L)
40000
30000
20000
10000
0
***
**
***
AJ
C57BL/6
C57BL/10
BcA86

FIGURE 3: DISTRIBUTIONS OF VIRAL REPLICATION AND ALT WITHIN F_2 MICE

Histograms of distribution of serum ALT (a), viral replication in the liver (c) and heart (e) in [BcA86xC57BL/10]F_2 mice. Strong skewness was detected in the three phenotypic distributions, and so phenotypes were normalized by Box-Cox (b, d, f) for further analysis.

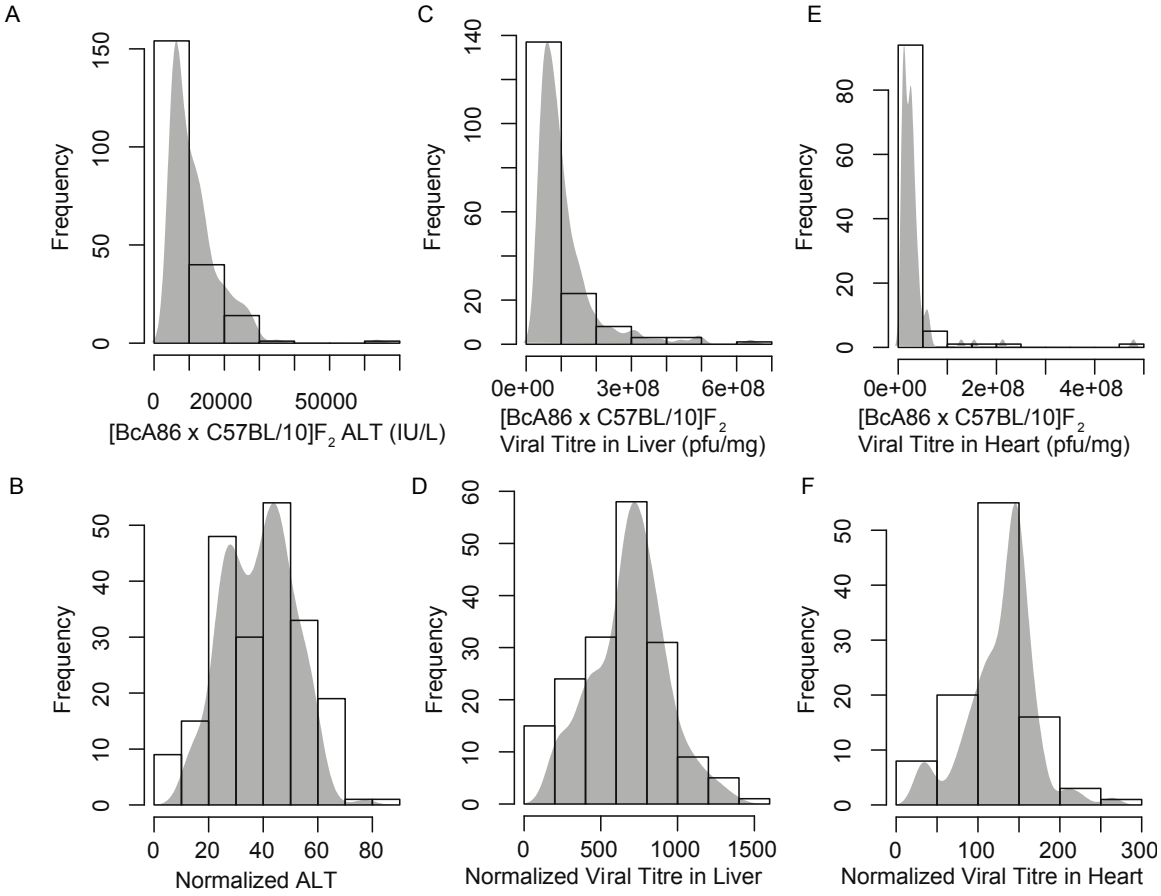
A
Frequency
0
50
100
150
0
20000
50000
[BcA86 x C57BL/10]F2 ALT (IU/L)
C
Frequency
0
20
60
100
140
0e+00
3e+08
6e+08
[BcA86 x C57BL/10]F2
Viral Titre in Liver (pfu/mg)
E
Frequency
0
20
40
60
80
0e+00
2e+08
4e+08
[BcA86 x C57BL/10]F2
Viral Titre in Heart (pfu/mg)
B
Frequency
0
10
20
30
40
50
0
20
40
60
80
Normalized ALT
D
Frequency
0
10
20
30
40
50
60
0
500
1000
1500
Normalized Viral Titre in Liver
F
Frequency
0
10
20
30
40
50
0
100
200
300
Normalized Viral Titre in Heart

FIGURE 4: GENOME WIDE LINKAGE ANALYSIS IN [BCA86XC67BL/10]F2 MICE REVEALS TWO LOCI SIGNIFICANTLY

Genome wide linkage scans for ALT (black line), viral replication in the liver (blue line) and in the heart (red). Linkage analysis was performed on normalized phenotypes, and genome wide significance was determined by 10 000 permutations, with alpha = 0.05 shown as a dashed horizontal line). A single locus on distal chromosome 13 was significantly linked to ALT levels (LOD=4.50, P=0.003). An additional locus on chromosome 17 was linked to viral replication levels in the heart (LOD=3.4, P=0.046).

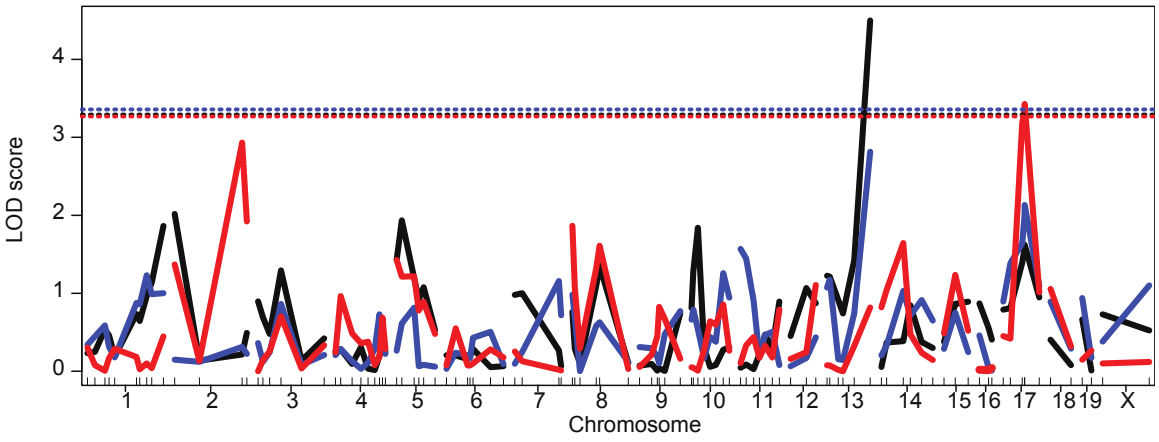
LOD score
0
1
2
3
4
1
2
3
4
5
6
7
8
9
10
11
12
13
14
15
16
17
18
19
X
Chromosome

FIGURE 5: LINKAGE OF CHROMOSOME 13 AND 17 TO CVB3 VIRAL REPLICATION AND SERUM ALT LEVELS

(a): LOD score plot for ALT (black line), viral replication in the liver (blue line) and in the heart (red) calculated using interval mapping. Peak linkage to ALT on distal chromosome 13 occurs at rs3702296 with LOD 4.50 and p=0.003.

(b): Phenotypes by genotype plot of 210 F_2 mice for normalized serum ALT levels at rs3702296. Where 86/86 represents animals homozygous for BcA86 alleles, B10/B10 represents animals homozygous for C57BL/10 alleles, and 86/10 represents animals heterozygous for the two allele types. F_2 mice homozygous for the BcA86 allele at this locus showed increased susceptibility to CVB3-induced viral hepatitis. (c): Phenotypes by genotype plot of for raw serum ALT levels at rs3702296.

(d) LOD score plot for ALT (black line), viral replication in the liver (blue line) and in the heart (red)on chromosome 17 calculated using interval mapping; peak occurs at D17Mit88 with LOD 3.4 and p=0.046

(e): Phenotypes by genotype plot of 102 F_2 mice for viral replication in the heart at D17Mit88. F_2 mice homozygous for the BcA86 allele at this locus showed increased susceptibility to CVB3-induced viral hepatitis. (F): Phenotypes by genotype plot of for viral replication in the heart in Log_{10} pFU/mg units at D17Mit88.

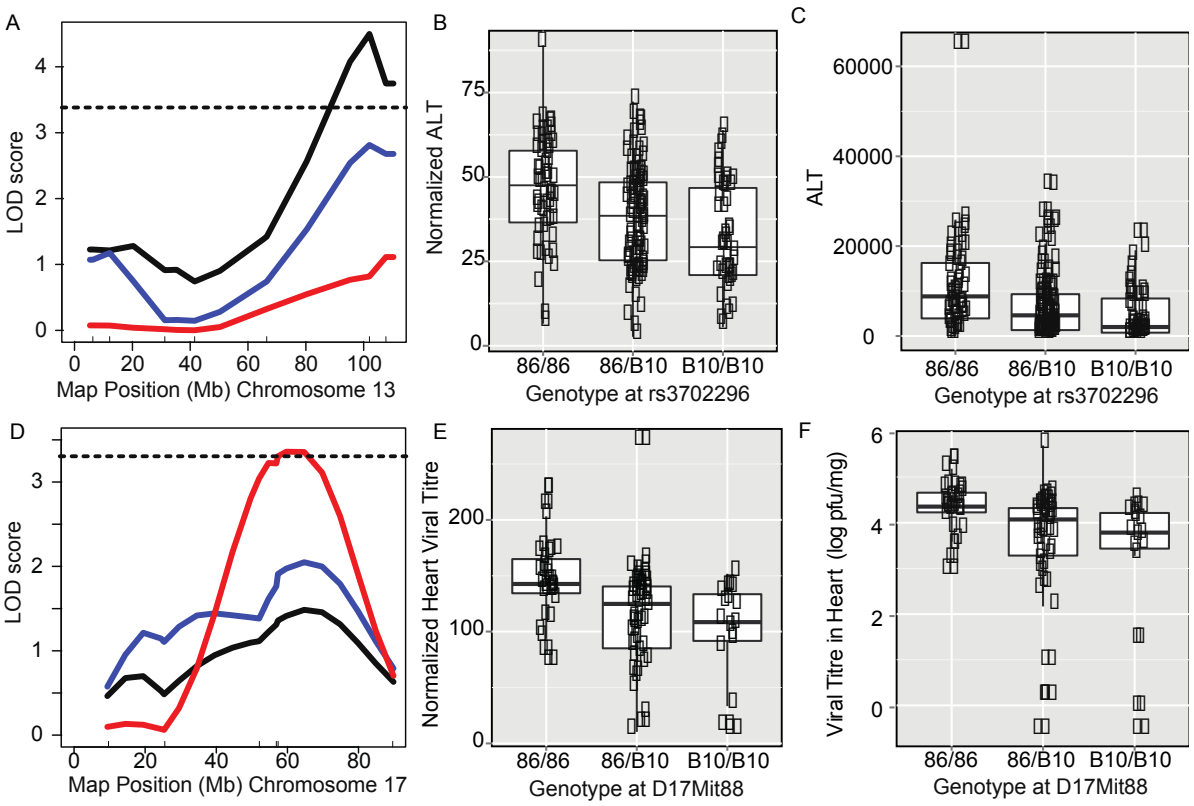
A
LOD score
Map Position (Mb) Chromosome 13
B
Normalized ALT
86/86
86/B10
B10/B10
Genotype at rs3702296
C
ALT
86/86
86/B10
B10/B10
Genotype at rs3702296
D
LOD score
Map Position (Mb) Chromosome 17
E
Normalized Heart Viral Titre
86/86
86/B10
B10/B10
Genotype at D17Mit88
F
Viral Titre in Heart (log pfu/mg)
86/86
86/B10
B10/B10
Genotype at D17Mit88

FIGURE 6: DIFFERENTIAL EXPRESSION OF TYPE I INTERFERON BASED ON GENOTYPE AT DISTAL CHROMOSOME 13.

(a) Quantitative RT-PCR (qPCR) in liver tissue comparing CVB3 mRNA levels in C57BL/10 and BcA86 mice 48 hours post infection. As well as [BcA86xC67BL/10]F_2 mice homozygous for BcA86 at rs3702296: F2-chr13@102(BcA86) compared to F_2 mice homozygous for the C57BL/10 genotype: F2-chr13@102(B10). Significantly higher viral replication was detected in BcA86 mice (P=0.008, Mann-Whitney), but CVB3 mRNA was equivalent between the selected [BcA86xC67BL/10]F_2 mice (P=0.6, one-tail Mann-whitney).

(b) Quantitative RT-PCR (qPCR) in liver tissue comparing Interferon ß mRNA levels in C57BL/10 and BcA86 mice 48 hours post infection. As well as [BcA86xC67BL/10]F_2 mice homozygous for BcA86 and B10 at rs3702296. Significantly higher *Ifnb1* RNA was detected in BcA86 mice (P=0.010, T-test), and also in F2-chr13@102(BcA86) mice as compared to F2-chr13@102(B10) mice (P=0.263, one-tail T-test). Data shown as mean ± standard deviation for both panels.

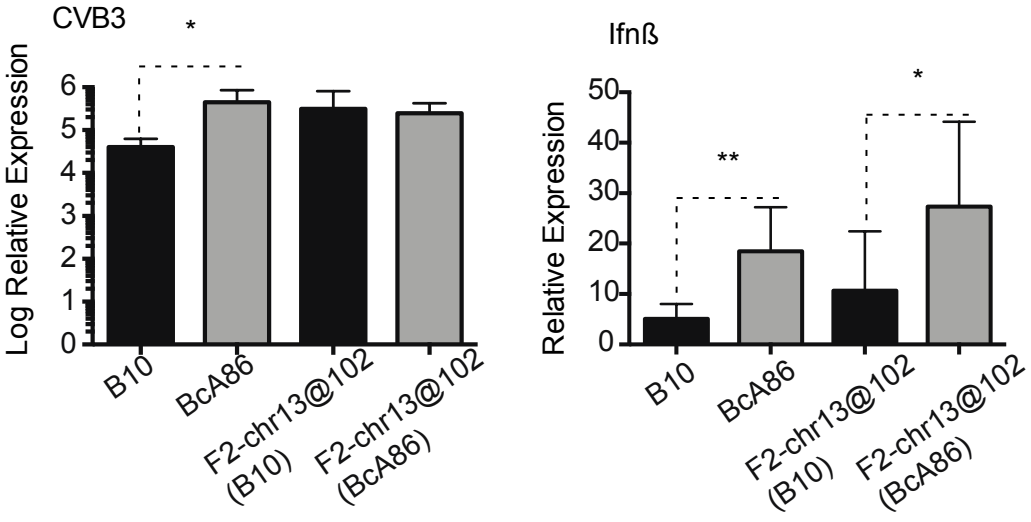
CVB3
*
Log Relative Expression
0
1
2
3
4
5
6
B10
BcA86
F2-chr13@102 (B10)
F2-chr13@102 (BcA86)
Ifnß
**
*
Relative Expression
0
10
20
30
40
50
B10
BcA86
F2-chr13@102 (B10)
F2-chr13@102 (BcA86)

SUPPLEMENTAL FIGURE 1: BCA86 ALT ELEVATED RELATIVE TO C57BL/10

(a) Serum ALT levels in mice used as controls during infections of [BcA86xC57BL/10]F_2 mice. Each bar represents 10 mice and represents data pooled from multiple experiments.

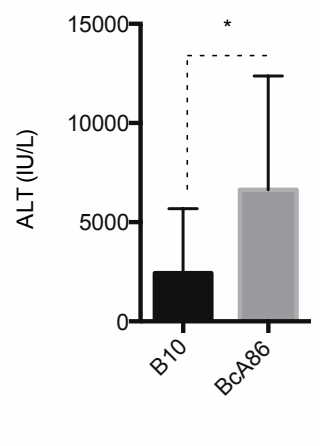

SUPPLEMENTAL FIGURE 2: DIVERSITY CHIP SNPS POLYMORPHIC BETWEEN C57BL/6 AND C57BL/10

(a) Each vertical line corresponds to a mouse chromosome and each horizontal line corresponds to one SNP polymorphic between the C57BL/6 and C57BL/10 strains. Blocks of dense polymorphism suggest different origins for the two strains in these genomic regions. Only polymorphic SNPs are shown, and each chromosome actually begins at 1bp.

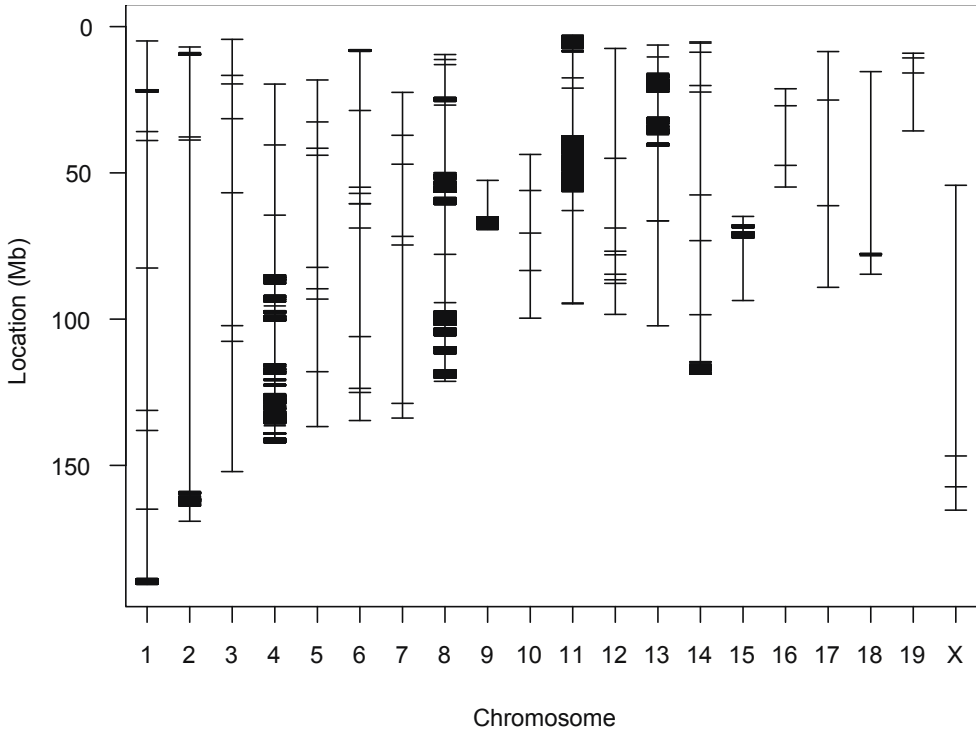

SUPPLEMENTAL TABLE 1: BCA86 AND C57BL/10 MAPPING PANEL

SNPs and microsatellites polymorphic between BcA86 and C57BL/10 used for mapping in [C57BL/10 x BcA86]F_2. Microsatellite genotypes are given as PCR amplicon size.

SNP ID	Chromosome	Position (Mb)	DSO (BCA86)	C57BL/10	BcA86	C57BL/6	A/J
Mod4c2_64_1	2	64.506226	C57BL/6	112	112	120	-
D8mit30	8	67.95025	A/J	164	176	164	176
D8Mit156	8	131.419404	A/J	140	154	140	154
D9mit137	9	116.167899	A/J	145	131	145	131
D12mit112	12	47.855788	A/J	154	136	154	136
D12MIT214	12	82.743296	A/J	146	170	146	170
D12mit101	12	103.73305	A/J	170	118	170	118
D15mit85	15	40.145172	A/J	195	179	195	179
D15mit63	15	65.076746	A/J	146	138	146	138
D17mit57	17	9.705768	A/J	300	320	300	320
D17mit139	17	52.659266	A/J	136	164	136	164
D17mit20	17	57.227447	A/J	180	170	180	170
D17mit88	17	57.368714	A/J	242	186	242	186
D18mit68	18	21.578635	A/J	113	95	113	95
D18mit184	18	66.944612	A/J	172	147	172	147
rs3708897	1	22.348543	C57BL/6	GG	AA	AA	AA
rs32737961	1	39.032305	C57BL/6	TT	CC	CC	TT
rs13475886	1	61.228463	C57BL/6	CC	TT	TT	CC
rs13475913	1	70.127169	C57BL/6	CC	TT	TT	CC
rs31767016	1	82.636707	C57BL/6	CC	TT	TT	CC
rs6327099	1	131.282938	C57BL/6	GG	AA	AA	GG
rs31375526	1	138.180275	C57BL/6	CC	TT	TT	CC
rs13476182	1	153.950459	C57BL/6	GG	TT	TT	GG
rs6341208	1	165.06283	C57BL/6	AA	TT	TT	AA
rs3680295	1	190.724768	C57BL/6	GG	AA	AA	AA
rs13476344	2	9.314267	C57BL/6	GG	TT	TT	GG
rs13476872	2	159.118061	C57BL/6	GG	AA	AA	GG
rs27312411	2	169.27213	C57BL/6	GG	AA	AA	GG
rs13476956	3	5.370727	C57BL/6	AA	GG	GG	AA
rs31500060	3	16.369915	C57BL/6	CC	TT	TT	CC

rs30354938	3	31.16887	C57BL/6	GG	AA	AA	GG
rs31596392	3	56.511763	C57BL/6	GG	AA	AA	GG
rs30661719	3	101.914952	C57BL/6	GG	AA	AA	GG
rs31594267	3	151.88254	C57BL/6	CC	AA	AA	CC
rs13477622	4	28.24936	C57BL/6	GG	AA	AA	GG
rs32786595	4	40.225498	C57BL/6	CC	TT	TT	CC
rs13477746	4	65.605269	C57BL/6	CC	TT	TT	CC
rs28325196	4	85.06993	C57BL/6	TT	CC	CC	TT
rs28234425	4	100.667454	C57BL/6	GG	CC	CC	GG
rs6381371	4	115.708649	C57BL/6	TT	CC	CC	TT
rs4224765	4	125.991071	C57BL/6	TT	CC	CC	CC
rs32203940	4	132.774342	C57BL/6	CC	TT	TT	CC
rs3661982	4	139.269393	C57BL/6	AA	TT	TT	TT
rs29779004	5	32.62917	C57BL/6	CC	TT	TT	CC
rs46835784	5	44.059873	C57BL/6	CC	TT	TT	CC
rs13478320	5	71.1333	C57BL/6	TT	GG	GG	TT
rs33067522	5	81.685659	C57BL/6	CC	TT	TT	CC
rs33249065	5	92.510104	C57BL/6	CC	TT	TT	CC
rs3662161	5	117.909356	C57BL/6	CC	TT	TT	CC
rs3710142	6	8.012701	C57BL/6	CC	TT	TT	CC
rs30764547	6	28.66591	C57BL/6	AA	TT	TT	AA
rs33852049	6	54.89985	C57BL/6	GG	AA	AA	GG
rs30915467	6	60.541414	C57BL/6	AA	GG	GG	AA
rs6157367	6	67.237174	C57BL/6	AA	TT	TT	-
rs30421807	6	105.962107	C57BL/6	AA	TT	TT	AA
rs6334723	6	134.651968	C57BL/6	GG	AA	AA	GG
rs31221380	7	38.216957	C57BL/6	GG	TT	TT	GG
rs32285588	7	54.410823	C57BL/6	AA	GG	GG	AA
rs13479522	7	136.179208	C57BL/6	CC	TT	TT	CC
rs13479540	7	141.188625	C57BL/6	GG	AA	AA	GG
rs33166255	8	7.701082	C57BL/6	GG	CC	CC	GG
rs33157972	8	12.958088	C57BL/6	GG	AA	AA	GG
rs3661760	8	24.557766	C57BL/6	TT	GG	GG	TT
rs33080067	8	60.422745	C57BL/6	GG	AA	AA	GG
rs13480109	9	25.697427	C57BL/6	GG	AA	AA	GG
rs29644859	9	52.593224	C57BL/6	CC	AA	AA	CC
rs29640230	9	65.282831	C57BL/6	GG	AA	AA	GG

rs6396602	9	69.29458	C57BL/6	AA	CC	CC	CC
rs3673457	9	81.753447	C57BL/6	TT	CC	CC	TT
rs29336522	10	29.57704	C57BL/6	TT	CC	CC	TT
rs13480575	10	33.372829	C57BL/6	CC	TT	TT	CC
rs29356879	10	43.717117	C57BL/6	TT	CC	CC	TT
rs13480619	10	57.472268	C57BL/6	GG	AA	AA	GG
rs29320152	10	70.678993	C57BL/6	TT	GG	GG	TT
rs29344872	10	83.411614	C57BL/6	AA	GG	GG	AA
rs13480728	10	99.701075	C57BL/6	CC	TT	TT	CC
rs13480770	10	113.178567	C57BL/6	AA	TT	TT	AA
rs26895374	11	8.476784	C57BL/6	TT	GG	GG	TT
rs29413390	11	21.040136	C57BL/6	GG	AA	AA	GG
rs6406223	11	37.583571	C57BL/6	GG	TT	TT	TT
rs26979995	11	50.271114	C57BL/6	TT	CC	CC	CC
rs6268547	11	62.886983	C57BL/6	CC	TT	TT	CC
rs13481117	11	79.065732	C57BL/6	TT	GG	GG	TT
rs29436909	11	94.49965	C57BL/6	AA	CC	CC	AA
rs13481676	13	6.303301	C57BL/6	CC	TT	TT	CC
rs13459139	13	12.155224	C57BL/6	TT	CC	CC	TT
rs13481741	13	31.195478	C57BL/6	TT	CC	CC	TT
rs3722313	13	41.538155	C57BL/6	CC	TT	TT	CC
rs51679066	13	66.467951	C57BL/6	AA	GG	GG	GG
rs3702296	13	101.979187	C57BL/6	CC	TT	TT	CC
B10SNPS0198	13	107.699046	C57BL/6	AA	GG	GG	--
rs31187642	14	10.769899	C57BL/6	AA	GG	GG	GG
rs31151615	14	22.151051	C57BL/6	GG	AA	AA	GG
rs30650651	14	59.200668	C57BL/6	CC	TT	TT	CC
rs30264676	14	74.815528	C57BL/6	TT	AA	AA	TT
rs31059846	14	100.024215	C57BL/6	CC	TT	TT	CC
rs31233932	14	124.508019	C57BL/6	AA	GG	GG	AA
rs3700812	15	93.667136	C57BL/6	CC	TT	TT	CC
rs4165506	16	27.156167	C57BL/6	AA	GG	GG	AA
rs3687811	16	47.489432	C57BL/6	AA	GG	GG	AA
rs4187220	16	54.901204	C57BL/6	TT	CC	CC	TT
rs29512740	17	25.523395	C57BL/6	TT	GG	GG	TT
rs33353857	17	89.633195	C57BL/6	CC	GG	GG	CC
rs31112038	19	15.408257	C57BL/6	CC	GG	GG	CC

rs31241164	19	35.648431	C57BL/6	GG	AA	AA	GG
rs6368704	X	55.120804	C57BL/6	CC	TT	TT	CC
rs13459160	X	158.414344	C57BL/6	TT	GG	GG	TT

CHAPTER 3: QTL ANALYSIS, PATHWAY ANALYSIS AND CONSOMIC MAPPING SHOW GENETIC VARIANTS OF *TNNI3K, FPGT* OR *H28* CONTROL SUSCEPTIBILITY TO VIRAL MYOCARDITIS

Sean A. Wiltshire, Gabriel André Leiva-Torres, and Silvia M. Vidal

Department of Human Genetics, McGill University, Montreal, Quebec, H3A 1B1, Canada

Correspondence should be addressed to S. M. V. (McGill Life Sciences Complex, Room 367, 3649 Promenade Sir William Osler, Montreal, QC, H3G 0B1; Fax: 514-398-2603; e-mail: silvia.vidal@mcgill.ca).

Published in: *Journal of Immunology (Baltimore, Md : 1950)*, (2011)*186*(11), 6398–6405. doi:10.4049/jimmunol.1100159

BRIDGING STATEMENT FROM CHAPTER 2 TO CHAPTER 3

Our studies in the RCS mice, and in [A/Jx B10.*H2*^{A}]F_2 mice provided compelling evidence for multiple loci controlling distinct aspects of the host response to coxsackieviral infection. Distal chromosome 13 was linked to the amount of hepatic necrosis as measured by serum alanine aminotransferase and potentially represents a novel mutation within the BcA86 strain. In other previous work, loci on chromosomes 1 and 4 (*Vms2* and *Vms3*) were linked to control of sarcolemmal necrosis, and a locus on distal chromosome 3 (*Vms1*) was linked to control of both myocarditis and sarcolemmal necrosis. *Vms1* was an attractive QTL for further study because the effect of chromosome 3 on more than one phenotype suggested it might be a central regulator of myocarditis. Linkage to distal chromosome 3 was highly significant and the *Vms1*^{A} allele promoted susceptibility to myocarditis instead of resistance. The effect size and significance of *Vms1* were identified in a segregating [A/Jx B10.*H2*^{A}]F_2 intercross, and it was therefore unknown what if any effect would be observed upon isolation in a fixed genetic background. Isolation of *Vms1*^{A} on the B6 background rather than in the B10.*H2*^{A} background would also mean fixing 3 susceptibility donating QTL: *Vms2*^{B}, *Vms3*^{B} and *H2*^{B}.

ABSTRACT:

Coxsackievirus B3 (CVB3) infection is the most common cause of viral myocarditis. The pathogenesis of viral myocarditis is strongly controlled by host genetic factors. While certain indispensible components of immunity have been identified, the genes and pathways underlying natural variation between individuals remain unclear. Previously, we isolated the Viral Myocarditis Susceptibility 1 (*Vms1*) locus on chromosome 3, which influences pathogenesis. We hypothesized that confirmation and further study of *Vms1* controlling CVB3-mediated pathology, combined with pathway analysis and consomic mapping approaches, would elucidate both pathological and protective mechanisms accounting for natural variation in response to CVB3 infection. *Vms1* was originally mapped to chromosome 3 using a segregating cross between susceptible A/J and resistant B10.A mice. To validate *Vms1*, C57BL/6J-Chr 3^{A}/NaJ (CSS3) were used to replicate susceptibility compared to resistant C57BL/6J (B6). A second segregating F2 cross was generated between these confirming both the localization and effects of *Vms1*. Microarray analysis of the four strains (A/J, B10.A, B6 and CSS3) illuminated a core program of response to CVB3 in all strains that is comprised mainly of interferon stimulated genes. Microarray analysis also revealed strain specific differential expression programs and genes that may be prognostic or diagnostic of susceptibility to CVB3 infection. A combination of analyses revealed very strong evidence for the existence and location of *Vms1*. Differentially expressed pathways were identified by microarray and candidate gene analysis revealed *Fpgt*, *H28* and *Tnni3k* as likely candidates for *Vms1*.

INTRODUCTION:

Viral myocarditis and its long-term sequela, dilated cardiomyopathy (DC), are a common cause of morbidity and mortality(308). Adenoviruses, influenza, herpesviruses have been implicated; however, enteroviruses particularly coxsackie B3 (CVB3) strains are the most prominent etiology(184). In mice, experimental infection with CVB3 has served to elucidate three distinct clinical aspects of human disease progression 1) an initial phase of viral replication and cytolytic damage of cardiomyocytes; 2) a phase of intense myocardial infiltration by immune effectors, which may resolve infection or persist indefinitely in susceptible animals(309); 3) a delayed phase in which initial infiltration and response may transition into autoimmune or inflammatory cardiomyopathy(310). Furthermore, different individuals or inbred mouse strains display variable degrees of cardiomyopathy, likely influenced by their genetic background. Myocarditis and DC can also be induced experimentally in the absence of virus by administration of cardiac myosin with adjuvant. As with viral myocarditis, inbred strains of mice also differ in their inherent susceptibility to experimental autoimmune myocarditis (EAM), implicating genetic controls of myocardial inflammation(311). Therefore, two outstanding questions in the field are: 1) does uncontrolled viral replication drive inflammation during myocarditis, or is virus merely an equivalent trigger to unequal inflammation; 2) which host genetic variants are associated with the outcome of virus-induced disease.

Phenotype characterization of CVB3 infection in mutant mouse stocks has so far delimited three major systems essential in predicting disease severity: integrity of myocardial structure, protection by innate immunity, as well as the balance between curative immunity and chronic inflammation or autoimmunity. The cytoskeletal protein dystrophin is cleaved by CVB3 protease 2A, a protein essential for viral life cycle; this cleavage affects cardiac function and morphology(312). Type I interferon (IFN) is produced by immune and non-immune cells in response to pathogen sensing through innate receptors. High levels of type I IFN activate antiviral response systems(313), and enhance early cytotoxic effectors such as natural killer (NK) cells(314). Thus, mice deficient in toll-like receptor 3 (TLR3) suffer from severe myocarditis and a high viral

load in the heart and liver(315). Similarly, type I IFN receptor-(282) and IFN-β-knockout mice(316) show increased viral burden in the liver and heart respectively. These data strongly suggest a protective role for type I IFN, particularly IFN-ß, during coxsackieviral infection. Recently, the constitutive expression of CXCL10 in the heart has been shown to attract NK cells to the heart reducing overall viral replication(317). Though much progress has been made, there is still a need to account for differential susceptibility to viral myocarditis among otherwise normal individuals due to natural variation.

The major histocompatibility complex (MHC) genes have been linked to susceptibility to myocarditis in both humans and experimental mouse models(145, 318). Non-MHC genes may also have an important impact on disease susceptibility. Recently, functional TLR3 variants (homozygous 412F and heterozygous P554S) were found in excess among patients presenting enteroviral myocarditis or DC(319). To identify novel genetic factors associated with disease, we have applied quantitative trait locus (QTL) mapping in an experimental mouse model. Previously, using an F_2 cross between susceptible A/J and resistant B10.A-*H2*^{a} (B10.A) mice, we identified three quantitative trait loci (QTL) on chromosomes 1 (*Vms2)*, 3 (*Vms1)* and 4 (*Vms3)*. Only *Vms1* was linked to the three phenotypes under study, i.e. myocarditis score (P=0.005), extent of sarcolemmal damage (P=0.001)(284), and heart viral load (P=0.010). This suggested that *Vms1* is a central determinant of disease severity; in the present study we seek to determine the precise contribution of *Vms1* in viral myocarditis. To achieve this, we validated the existence of *Vms1* through phenotyping of a chromosome substitution strain (CSS) that carries a diploid A/J chromosome 3 (CSS3) on a C57BL/6 (B6) background(320). We then used a second F_2 cross, this time between B6 and CSS3 mice, to refine the *Vms1* genetic interval. Investigation of the mechanistic basis of *Vms1* function using genome-wide expression and pathway analysis in the four parental strains (susceptible A/J and CSS3 mice, as well as resistant B10.A and B6 mice) indicated that *Vms1* susceptibility alleles impair antiviral mechanisms downstream of viral sensing or type I IFN pathways. This combined effort demonstrated that viral load and myocarditis severity are likely controlled by a more resolved locus, *Vms1.1*, whose critical interval contains three candidate genes: *Fpgt*, *H28*, and *Tnni3k*.

MATERIALS AND METHODS:

MICE AND VIRUS:

Inbred A/J (000469), B10.A-H2a H2-T18a/SgSnJ (B10.A, 000646), C57BL/6J-Chr 3A/J/NaJ (CSS3, 004381) and C57BL/6J (B6, 000664) mice were purchased from Jackson Laboratories. The mice were maintained in the McGill University animal facility in compliance with the Canada Council on Animal Care as approved by the McGill University Animal Care Committee. Coxsackievirus B3 used for time course and microarray experiments was CVB3-CG strain as previously(284). All other experiments including CSS3/B6/F1 as well as [CSS3 x B6]F2, were infected with the plaque purified CVB3-H3(321) generously provided as a plasmid by the lab of Dr. Kirk Knowlton (University of California, San Diego). Like CVB3-CG, CVB3-H3 was also derived from the highly myocarditis CVB3 Woodruff lineage(321). In this model it behaves comparably to CVB3-CG and has the added benefit of being a known and widely used genotype allowing for more direct comparisons by other researchers.

MOUSE INFECTION AND PHENOTYPE DETERMINATION:

Mice were inoculated intraperitoneally with 400 PFU of CVB3-CG per gram of body weight (or 10PFU/g of CVB3-H3) diluted in sterile PBS at seven to eight weeks of age. Experiments shown in Figure 1 were replicated with both viruses with equivalent results. Uninfected controls in microarray experiments were mock infected with PBS in parallel. Survival, weight, and signs of infection were evaluated on a daily basis and the mice were humanely sacrificed one, two, four or eight days post-infection. Moribund mice were humanely euthanized at an acceptable clinical endpoint. At necropsy, mouse hearts were removed aseptically, cut in half sagitally and fixed in buffered formaline, the remainder was stored at -80°C. The apex of hearts were subsequently homogenized and submitted to three freeze-thaw cycles to release infectious virus. After centrifugation at 1,000 g for five minutes to remove debris, the supernatant was isolated for quantification by plaque assay. Samples to be used for microarray were taken from a transverse section above the apex of approximately 30mg.

PLAQUE ASSAY:

HeLa cells (ATCC: CCL-2) were grown and maintained in Dulbecco's Modified Eagle Medium (DMEM) supplemented with 10% FBS, 100 µg/mL Penicillin/Streptomycin (1X media). One day prior to infection, the cells were harvested at 70-80% confluence and plated on 12-well plates, at 3.1 x 10^5 cells per well. Homogenized organs were serially diluted 10-fold in non-supplemented DMEM and the dilutions were used to infect HeLa cells in triplicate for 60 minutes. After initial infection by homogenate, HeLa cells are covered in a layer of media with 0.25% agarose and incubated for three days. Cells were fixed in formaldehyde and stained with crystal violet to count plaques.

GENOTYPE ANALYSIS:

Genomic DNA was prepared from tail biopsies of individual F_2 mice by overnight incubation at 55ºC in 700 µl of a buffer (100 mM Tris-HCl, pH 8.0, .0.5 mM EDTA, 200 mM NaCl, 0.2% SDS) containing 0.5 mg/ml Proteinase K, and followed by RNAse treatment (0.3 mg/ml; 2 h at 37ºC). DNA was purified by serial phenol-chloroform extractions and ethanol precipitation. In this genome scan, 9 MIT markers spaced approximately 15cM apart from each other, with increased density towards distal chromosome 3 to distinguish between A/J and B6 alleles (*D3Mit164*, *D3Mit224*, *D3Mit346*, *D3Mit291*, *D3Mit147*, *D3Mit128*, *D3Mit116*, *D3Mit19*, *D3Mcg1*). Markers in the peak of *Vms1* were chosen to match those previously used to facilitate direct comparison between the two datasets. Reactions performed manually used a 10 µl total reaction volume, 200 µM dNTPs, 1.5 mM $MgCl_2$, 2 pmol of each primer and 0.5 U of *Taq* polymerase (Invitrogen, Burlinton, ON). Reactions were performed as follows: 96º for two minutes; 30 cycles of 94º for 45 seconds, 56º for 45 seconds, 72º for 60 seconds; and a final extension step 72º seven minutes. PCR prodcts were then separated on 2-3% high-resolution agarose (USB, Cleveland, OH) gels containing Ethidium bromide and visualized under UV light. Identification of likely genotyping errors was performed using R/qtl; all genotypes with error LOD scores greater than 3 were repeated and verified(322).

STATISTICAL AND BIOINFORMATICS ANALYSIS:

Statistical analyses were conducted with the freely available program R and linkage was performed with package ‘R/qtl’. The scanone function of the ‘R/qtl’ library was used to perform maximum likelihood interval mapping (EM) of phenotype on genetic markers. Significance values were evaluated with 10 000 permutations. In joint analysis between [A/J x B10.A]F_2 and [CSS3 x B6]F_2, combined cross analysis was performed with experimental cross used as a covariate term in all calculations as previously described(192). LOD support interval was calculated using a 1.5 LOD drop by ‘R/qtl’. SNPs were identified using the mouse phenome database (http://phenome.jax.org/SNP) and were also provided by the mouse genome project group at the Wellcome Trust Sanger Institute and can be obtained from (http://www.sanger.ac.uk/resources/mouse/genomes/). SNPs were analyzed using the SIFT algorithm(323) for potentially deleterious effects. Interferon stimulated genes were annotated using the ISG and Interferome databases(324, 325), DAVID(326) and by Ingenuity Pathways Analysis (Ingenuity® Systems, ingenuity.com). Pathways identified through Ingenuity are characterized with a ‘Network Score’, which is defined as the negative exponent of the right-tailed Fishers exact test. P-Values shown in figures are a result of two-tailed T-Test with *P<0.05, **P<0.01 and ***P<0.001.

MICROARRAY AND QPCR

Hearts used for microarrays were first perfused with cold sterile buffer (110mM NaCl, 10mM NaHCO3, 16mM KCl, 16mM MgCl2, 1.2mM CaCl2, 5U/L Heparin, pH 7.9) and tissues were preserved in RNA-later stabilization reagent (ambion) before being frozen at -80C. Total RNA was extracted from ~30mg of heart tissue from a transverse section using Qiagen RNeasy extracton kit. Quality control by agilent bioanalyzer, cDNA synthesis and microarray hybridization was performed at the McGill University and Genome Quebec Innovation Centre. Three infected and three uninfected female mice of each genotype were independently prepared and analyzed on an Illumina Mouse-WG6 version 2.0 array (one genotype and 6 mice per array, 4 arrays total). A/J vs. B10.A and CSS3 vs. B6 experiments were performed and analysed separately. Raw data is available through NCBI GEO with accession number GSE19496. Normalization, and analysis was performed using FlexArray(327), expression values were normalized using

the log2, RMA and configuration of Lumi. Principal component analysis figures (Supplemental Figure 3) were also generated within FlexArray. Genes were filtered for consideration as follows: the 40th percentile was determined across all normalized probes as an arbitrary cutoff value. If no probes from any experimental group were greater than the 40th percentile, the gene was considered absent in all samples and not considered further. A starting list was use where at least one genotype either infected or uninfected met this criterion for 20261 targets. Paired experimental groups (*e.g.:* A/J infected vs. uninfected) were compared by CyberT(328) with default parameters and considered to be differentially expressed if the fold change (FC) was less than 0.5 or greater than 2 and unadjusted P-value was less than 0.05. Interaction between strain and genotype was defined as: at least one strain is differentially expressed ($0.5 \geq FC \geq 2$, $P<0.05$), ANOVA [strain:infection] significant ($P<0.05$); as well as the absolute difference of difference between strain means $[|((\mu_{AJ}-\mu_{AJ\ infected}) - (\mu_{B10.A}-\mu_{B10.A\ infected}))| > 1.25]$. This final step was determined as an effective filter in removing parallel changes between genotypes following infection. This much-abbreviated list was then annotated to identify which strain was significantly different (*e.g.:* AJ responds to infection by increasing expression of a gene, B10.A does not; this is an AJ specific gene). See Supplemental Figure 1 for example and distribution of this parameter. Highly differentially expressed genes were chosen identified with an arbitrary cutoff of ($0.2 \geq FC \geq 5$, $P<0.05$). Quantitative PCR primers were designed to span exon junctions with the help of primer3plus(285).

LIST OF PRIMERS USED:

CVB3-H3 forward: ATGGCAGAAAACCTCACCAG, CVB3-H3 reverse: ATGTTCTGCCCAAACAGTCC, Gbp1 forward: ACTGAGAAGATGGAGCAGGAAC, Gbp1 reverse: GTTGCAAGCTCTCATTCTGG, H28 forward: ACAGGACTGGATTTGCCTTG, H28 reverse: GCATGCTTTCAACCAGAGAC, Ifnb1 forward: TGACGGAGAAGATGCAGAAG, Ifnb1 reverse: ACCCAGTGCTGGAGAAATTG, Tnni3k (as described in (329))forward: AGATTTCTGCAGTCCCTGGAT, Tnni3k reverse: AAGACATCAGCCTTGATGGTG, Eif4e forward: TACCACTAATCCCCCACCTG, Eif4e reverse:

GGTTTGCTTGCCAAGTTTTG, Lrrc40 forward: CCACAAAAACGACCCTCATC, Lrrc40 reverse: CCAACACCATTTCCTTCAGC, Gapdh forward: AAGGGCTCATGACCACAGTCC, Gapdh reverse: GATGCAGGGATGTTCTGG, Adh1 forward: TGTGGCTGACTTCATGGCTA, Adh1 reverse: TGGTGCTTGAATCAGTCTGG, D3Mcg1 forward: GGAGTTCTGAGGAGGTCGAG, D3Mcg1 reverse: CATGGCGTAACGAAACAAAA.

CYTOKINE MEASUREMENT:

Interferon ß concentration was measured using an ELISA kit from PBL interferon source.

RESULTS

CHROMOSOME 3 CONTROLS VIRAL MYOCARDITIS SEVERITY

In mice, severity of viral myocarditis is controlled by genetic background(27). Strong linkage of chromosome 3 to myocarditis, sarcolemmal disruption(284), and viral titer [Supplemental Figure 2] encouraged us to isolate the role of chromosome 3 in viral myocarditis. The CSS3 mice are ideally suited to assess the contribution of chromosome 3, as CSS3 mice carry the susceptible A/J allele of *Vms1* (*Vms1*^{s}), while controlling for background compared to B6. Differential control of viral replication was observed at Day 8, with CSS3 mice being significantly more susceptible than B6 mice (2.61 ± 0.13 *Vs.* 4.04 ± 0.08 Log[PFU/mg], P<0.001) [Figure 1A]. Furthermore, CSS3 mice have significantly higher levels of inflammation in the heart than B6 mice (2.85 ± 0.26 *Vs.* 1.4 ± 0.23, P<0.001) [Figure 1B]. No significant differences were observed between the sexes and [CSS3 X B6]F_1 mice were not significantly different from B6 mice in terms of viral replication or inflammation. These results replicate *Vms1*^{s} susceptibility to viral replication and intensity of peak inflammation; they also suggest *Vms1*^{s} is recessive to *Vms1*^{r}.

GENOME WIDE LINKAGE REPLICATES VMS1

To characterize the inheritance of susceptibility to CVB3, we determined heart viral titer and myocarditis in 126 [CSS3 X B6]F_2 mice. The mean of F_2 viral titers (3.22 ±0.09) and myocarditis scores (1.73 ±0.11) were similar to that of the B6 parental strain, which is consistent with a major gene effect and recessive *Vms1*^{s} susceptibility [Figure 2A, 2B]. As shown in Figure 2c, correlation was noted between viral load and myocarditis severity (Spearman, ρ=0.54, P<0.0001). Unlike the previous [A/J x B10.A]F_2, sex differences in susceptibility within the F_2 mice were not evident in either myocarditis or viral replication (P=0.470, 0.305).

Linkage analysis revealed a locus on distal chromosome 3, overlapping the previously described *Vms1* locus, controlling heart viral titer (LOD= 3.74; P=0.018)

[Figure 3a]. *Vms1*^{r} mice were protected from high viral load in the heart (2.87 ± 0.29 Log [PFU/mg]) when compared to *Vms1*^{s} (3.75 ± 0.13 Log [PFU/mg]) [Figure 3b]. *Vms1* linkage to inflammation was also significant (LOD= 3.57; P=0.0032); *Vms1*^{r} (1.07 ± 0.23) mice were protected compared to *Vms1*^{s} mice (2.28 ± 0.24). In a single QTL model, *Vms1* accounted for 11.89% of the variance observed in viral titer and for 11.02% in myocarditis score, a notable increase from respectively 5.87% and 3.25% in the [A/J x B10.A]F_2 cross. The *Vms1* interval in both crosses is defined between D3Mit291 and D3Mcg1, spanning 16cM and 16Mb.

DIFFERENTIAL CONTROL OF VIRAL REPLICATION OCCURS BETWEEN TWO AND FOUR DAYS POST INFECTION.

Differential gene expression in response to infection may be causally related to the observed phenotypes, or may be a reaction secondary to the primary causal locus. Understanding differential gene expression globally and within *Vms1* will aid in identifying potential candidates for *Vms1*. Presumably, the gene mediating *Vms1*^{r} resistance or *Vms1*^{s} susceptibility to viral myocarditis exerts some effect before the peak of myocarditis at day 8. As a prerequisite to transcriptional profiling by cDNA microarray, we first ascertained at which time point expressed genes might play a role. We assessed viral titer at multiple time points in A/J and B10.A mice [Figure 4A], as well as in CSS3 and B6 mice [Figure 4b], prior to the development of inflammation. After 96 hours PI, A/J and CSS3 mice have significantly higher levels of viral replication than B10.A or B6 mice. Higher type I IFN levels have been reported in the B6 strain(330), suggesting a possible mechanism for resistance. We observed that susceptible A/J mice produce significantly more IFN-ß than resistant B10.A mice during infection [Figure 4c]. CSS3 and B6 mice did not produce significantly different amounts of IFN-ß at the times measured. These observations are consistent with a genetically determined lack of ability to control viral replication by 96 hours after infection, which is not accounted for by higher IFN-ß in resistant mice.

MICROARRAY ANALYSIS OF RESISTANT AND SUSCEPTIBLE HEARTS REVEALS A CORE PROGRAM OF RESPONSE TO VIRAL MYOCARDITIS

Global gene expression 96 hours PI was compared by microarray in A/J, B10.A, CSS3 and B6 hearts. Although it has not yet been demonstrated that *Vms1* is a heart specific effect, the lack of difference in viral control at 48 hours PI suggests an equal seeding of the myocardium followed by an unequal response to infection towards 96 hours PI [Figure 4b]. Therefore, the heart seemed the most likely tissue to interrogate in order to identify mechanisms or cells identifiable by gene expression. Principal component analysis (PCA) indicates that infection accounted for the majority of variation, as expected [Supplemental Figure 3]; followed by variation due to genotype in A/J vs. B10.A and CSS3 vs. B6 mice.

Genes highly expressed or repressed after infection (at least a 5 fold change in all strains) were considered to be part of a common pathway. This set of 129 genes was strongly indicative of an interferon response: 46 of the 129 (35%) genes were annotated as being interferon induced(325). The interferome database used for comparison contains 1925 mouse genes annotated as being interferon induced in various cell types, corresponding to 6.3% of the arrays used in this study. Of the 46 genes identified, 14 suggested a type I IFN response, 1 a type II IFN response, and the remaining 31 were inducible by either. Functional clustering of these by DAVID revealed that the strongest enrichment terms were ‘response to virus’ and ‘RIG-I-like receptor signalling’ ($P<0.00005$). Highly expressed genes included effector interferon-stimulated genes (ISG) (*Oas1g, Mx1*), transcription factors (*Irf7*), and class one MHC (*H2-d1, H2-k1*). These results are summarized in Figure 5 and detailed in Supplemental Table 1. The observation that ISG pathways themselves are strongly upregulated in resistant (B6, B10.A) and susceptible (CSS3, A/J) strains is consistent with the hypothesis that though IFN is required to survive systemic CVB3 infection (282, 316), IFN may not be sufficient to control cardiac viral replication(331, 332).

DIFFERENTIAL MICROARRAY ANALYSIS REVEALS MYOCARDITIS SUSCEPTIBILITY EXPRESSION PROGRAMS

As a robust IFN response seems approximately equal between strains, differential expression of sets of genes within a pathway may represent unequal mechanisms of

adaptation to infection or pathological processes. In order to determine expression programs differentially activated by infection, sets of genes were created which identify qualitatively different expression patterns (*e.g.*: A/J increase expression of *H28* after infection, but B10.A do not). Using these priority ranked lists [Supplemental Table 1], pathway analysis and functional grouping was performed.

A/J specific programs [Figure 6a] were involved in metabolism, cell structure, and cardiovascular development pathways. B10.A differed in that cell mediated immunity markers, antigen presentation, and immune cell trafficking were identified as primary pathways for this strain [Figure 6b]. The CSS3 specific pathway [Figure 6c] shared several component genes with A/J, most of which are not located on chromosome 3. CSS3 specific pathways were identified to be tissue and organ development related. Notably, cell-mediated immune response pathways not present in A/J were expressed in B6 and CSS3 hearts. No B6 specific pathways were identified and only five genes are particular to a B6 response (*Chad, Dkk3, Mybphl, Prss35* and *Sln*); of these, only *Mybphl* is expressed on chromosome 3, over 30cM away from *Vms1*.

Differentially expressed genes following infection within *Vms1* (*Adh1*, *Gbp1*, and *H28*) were identified between A/J and B10.A, and confirmed in CSS3 and B6; no genes were found within Vms1 that were differentially expressed between CSS3 and B6 but not between A/J and B10.A [Figure 7].

Similarly, genes not differentially expressed following infection, but with basal expression differences (*e.g.*: B10.A express *Tnni3k* before and after infection at equivalent levels while A/J do not) represent possible candidate genes, as presence or absence of one or more key genes may provide a mechanism of resistance (or susceptibility) whose activity does not require induction. Between CSS3 and B6, a total of 28 genes with basal expression differences were identified. Of these, 14 were located on chromosome 3 and four of those were located within *Vms1*: *Gbp1*, *Eif4e*, *Tnni3k*, and *Lrrc40*.

REFINED QTL AND CANDIDATE GENE PRIORITIZATION

A common set of genetic markers, as well as the high degree of similarity between B10.A and B6 on chromosome 3, permitted a joint analysis with the aim of increasing linkage resolution using both the previous [A/J x B10.A]F_2 and the present [CSS3 x B6]F_2 crosses. An increased number of meioses in the combined cross has considerably shortened the interval under consideration. The interval controlling viral replication was narrowed between D3Mit116 and D3Mcg1 (78.7cM to 83.29cM), which we will refer to as *Vms1.1a*. Using the same technique, a region between D3Mit128 and D3Mcg1 (76.7cM to 84cM) was found to control inflammation, which we refer to as *Vms1.1b.* The *Vms1* interval is thus reduced from 16cM or 16Mbp as defined previously(284) to 6.3cM or 9Mb containing *Vms1.1a* and *Vms1.1b*. The region containing both *Vms1.1a* and *Vms1.1b* will be referred to as *Vms1.1* for the sake of simplicity [Figure 7A, 7B].

Candidate gene analysis for *Vms1* (as defined by either F_2 cross) identified seven candidate genes for *Vms1* on the basis of allele specific expression, differential response to infection or coding sequence variation. Of these, only *Tnni3k*, *Lrrc40*, *H28*, and *Fpgt* are contained within *Vms1.1.* Confirmation of significantly higher basal expression levels were found in *Tnni3k* by qPCR (Figure 7d), but not in *Lrrc40* (data not shown). *Tnni3k* was found to be 2.7 fold less expressed in $Vms1^s$ than $Vms1^r$ mice. Increased expression of *H28* following infection in $Vms1^s$ and not $Vms1^r$ mice was also confirmed by qPCR (Figure 7c). Finally, 5 coding non-synonymous SNPs (cnSNP) within 5 genes (*Tyw3*, *Tnni3k*, *Fpgt*, *Sfrs11*, and *Rpe65*) have been identified within *Vms1.1*, but only two are predicted to be non-conservative and damaging to function: $Fpgt^{rs30203847\text{-}C}$ (C517R) and $Tnni3k^{rs30712233\text{-}T}$ (T659I). After alignment, $Fpgt^{rs30203847\text{-}C}$ allele possessed by B6, AKR, and 129S1 mice is predicted to be damaging (score 0.03) since the $Fpgt^{rs30203847\text{-}R}$ allele (A/J, BALB/c, C3H) is shared with most vertebrates. In fact, the cnSNP in *Tnni3k* predicted as damaging is secondary to a more recently identified SNP rs49812611, which accounts for the lack of basal expression of *Tnni3k* in A/J or CSS3 mice due to aberrant splicing(329). This interval shortens the list of likely candidate genes for *Vms1.1* to *H28*, *Tnni3k* or *Fpgt*.

DISCUSSION

The myocarditic potential of the coxsackieviruses was recognized shortly after their discovery(333). Despite considerable progress in the understanding of CVB3 pathogenesis, coxsackieviral infection is a persistent cause of human disease(30, 334). There remains, however, a need to account for variation of clinical presentation between any two otherwise healthy, normal, and immunocompetent individuals. Surveys of inbred mouse strains have long indicated a genetic component in susceptibility to CVB3-induced disease(27, 318). Our previous analysis identified a locus on chromosome 3, *Vms1*, which controlled several aspects of disease. This led us to isolate the role of chromosome 3 from other potentially segregating or confounding loci.

Chromosome substitutions strains (CSS) represent a valuable model in which to study complex traits. As a prelude to further refinement and positional cloning of *Vms1*, it was necessary for us to at least replicate our initially observed phenotypes in the CSS3 mice. CSS3 mice control for other previously identified loci respective to B6 (*Vms2*, *Vms3* and *H2*); however, it was not obvious that $Vms1^s$ susceptibility would be recaptured. Unlike our initial [B10.A x A/J]F_2 cross (all $H2^a$), CSS3 and B6 mice are $H2^b$; *H2* is already known to be a strong modifier of disease(27, 318). CSS3 are also on a C57BL/6 and not C57BL/10 background; though B6 and B10 are closely related, we have found at least 7500 SNPs (unpublished and previous data (335)), some of which may cause inter-strain differences in response to infection. Nevertheless, phenotypes of both myocardial inflammation and viral replication were recapitulated. Variability in mean viral titer was similar in [CSS3 x B6]F_2 (3.22 ±0.09 Log[PFU/mg]) compared to the larger [A/J x B10.A]F_2 cross (3.01 ± 0.06 Log[PFU/mg]); however, *Vms1* explained more variance in the present cross (11-12% vs. 3-6%). Even in this genetically simplified context, a considerable amount of variation exists between mice, even of identical genotype (see Figure 1). As an enterovirus CVB3 exists as a quasispecies with a high mutation rate (~1 amino acid substitution/genome)(336, 337), providing ample opportunity for every possible mutation within an infection where of infected tissue can contain as many as 10^5 pfu/mg. This provides an example of increased resolution and power by isolating

genetic variation to a single chromosome in spite of considerable environmental variation. Replication of linkage between distal chromosome 3 and both inflammation and viral titer phenotypes strongly supports the strong role of *Vms1* in infection.

Previous studies have successfully used gene expression to better understand myocarditis and dilated cardiomyopathy(311, 338-340). In addition to identifying likely candidate genes, global expression analyses give us key mechanistic insights that aid in the identification of *Vms1*. Since viral replication in the heart is controlled in *Vms1*^{r} mice as early as four days post infection, this time point was chosen for expression analysis. It has previously been reported that A/J and B6 mice differ substantially in their production of Type I IFN following infection(330, 341). Another QTL that has never been cloned, but influences peak interferon levels called *If1* colocalizes with *Vms1*(342). These together suggested an initial hypothesis that a sensing or signalling defect in IFN might be present in susceptible mice. However, in this study IFN response between susceptible and resistant mice was roughly equivalent or in the case of A/J and B10.A mice, higher viral load was accompanied by higher IFN. Susceptible *Vms1*^{s} mice sense virus and produce antiviral IFN-ß with similar kinetics and magnitude as compared to *Vms1*^{r} mice. This makes it so that a defect in viral sensing, signalling or response to IFN is unlikely to underlie *Vms1*^{s}.

Strain specific expression analysis revealed similarities to previous work and several novel results. Comparison between A/J and B10.A mice showed A/J preferentially express genes and pathways involved in cardiovascular development and metabolism. This was consistent with previous findings (also A/J mice), which postulated that these changes reflect undamaged cardiomyocytes compensating for damaged neighbors(340). A notable addition to the A/J specific response was *Amica1* (also known as JAML), which was highly induced (19.6 fold) in A/J compared to B6, B10.A or CSS3 mice (1.3-3 fold). *Amica1* is a co-stimulatory molecule that becomes strongly induced on γ∂ T-cells upon ligation to the CVB3 receptor (*Cxadr*) on injured cells(343). γ∂ T-cells are known to play a pathogenic role during viral myocarditis(344). Conversely, all mice of the B6/B10 background, including susceptible CSS3 mice, expressed several markers (*Cd8b1, Nkg7, Cd244/2B4, Klra7*) of antiviral CD8/NK immune responses. Lack of CD8/NK cells

and overabundance of inflammatory γ∂ T-cells in A/J mice suggests that this is another possible (non-*Vms1*^{s}) mechanism accounting for A/J specific susceptibility to CVB3 infection. In contrast to A/J vs. B10.A mice, expression profiling did not reveal any *Vms1*^{s} or *Vms1*^{r} specific cell type suggesting that *Vms1* does not control the recruitment of a cellular immune response.

Three candidate genes were identified within the refined *Vms1.1* locus via expression and publically available SNP data (150-159.6Mb on Chromosome 3): *H28*, *Tnni3k*, and *Fpgt*. This method of identifying candidate genes via associative data is limited in that if a modest (less than twofold) change in expression underlies our phenotype, it would be missed. An alteration of protein function, but not expression level in genes containing non-synonymous SNPs (*Tyw3*, *Sfrs11* or *Rpe65*) is also possible even in the absence of predicted negative impact. We have also treated *Vms1.1a* and *Vms1.1b* controlling viral replication and myocarditis score respectively as a single entity *Vms1.1*, which controls both. In the absence of congenic and sub-congenic mice that parse individual gene contributions, it is impossible at this stage to identify whether changes in expression are causal or consequential and of which phenptype. However, differential control of viral replication before myocarditis suggests protective mechanisms acting at day four or earlier in *Vms1*^{r} mice at which time *H28*, *Tnni3k* and *Fpgt* remain the most attractive candidates.

H28 is expressed in the *Vms1*^{s} genotype following infection but not in *Vms1*^{r}. *H28* has no known function and has only been previously described as being presented during allograft rejection between BALB.B (*H2*^{b}) and B6 mice. Of the 5 coding non-synonymous SNPs (cnSNPs) in *Vms*1.1 (*Tyw3*, *Tnni3k*, *Fpgt*, *Sfrs11*, and *Rpe65*), only *Tnni3k* and *Fpgt* were both expressed in the heart and predicted to be deleterious. *Fpgt* catalyzes the formation of the fucosyl donor GDP-ß-fucose, as part of the fucose salvage pathway (345). L-fucose is a sugar present in glycoproteins involved in inflammation and immunity, e.g. sialyl-lewis X, the inflammatory ligand of selectins, contains L-fucose. A possible link between the ability of infected cells to effect immediate inflammatory signals and *Fpgt* may make this gene an attractive candidate.

Tnni3k was identified as having a basal expression difference: *Vms1*^{r} mice express significantly higher basal levels of the gene than *Vms1*^{s} mice. Indeed, the SNP rs49812611 was recently identified as leading to nonsense mediated decay of *Tnni3k* transcripts(329). *Tnni3k* was identified as a cardiac specific tropinin interacting kinase in 2003(346). Although the normal function of *Tnni3k* is still obscure, some recent results have somewhat clarified the situation. Transgenic overexpression of *Tnni3k* in differentiated P19cl6 cells led to increased contractile force and frequency, as well as to increased adrenergic response and protection from ischemic injury (347). *Tnni3k* has also been implicated in dilated cardiomyopathy (338) and heart failure. Mice not-expressing *Tnni3k* were resistant to CSQ heart failure (DBA/2, BALB and C3H) whereas 'normal' expressers (B6, 129/X1 and AKR) or mice transgenic for the human allele were highly susceptible to heart failure (329). This raises the possibility that *Tnni3k* may prevent myocardial injury during acute injury (347), but also become pathogenic and increasingly disregulated during chronic disease (329, 338).

This work was begun with the understanding that the outcome of CVB3 infection is largely influenced by three factors: integrity of the myocardium, interferon response, and progression to adaptive immunity. Here, we present evidence that differential viral replication and myocardial inflammation at early time points may be controlled by *Tnni3k* (implicating myocardial integrity), *Fpgt* (implicating cellular immune response) or *H28* (by unknown mechanisms). Future work will include the generation of congenic and sub-congenic mice, as well as reverse genetic approaches, in order to assess the contribution of individual genes before progressing further.

ACKNOWLEDGEMENTS:

We are grateful: to Francois Pepin for his continuing support with R; to Tony Kwan for his advice on expression analysis; to Mahmoud Aly, Emeric Bojarski, and Han Yao for [A/J x B10.A]F_2 data acquisition; and to Eve-Marie Gendron-Pontbriand for her editing services.

FIGURE AND LEGENDS TO FIGURES:

FIGURE 1: REPLICATION OF *VMS1* PHENOTYPES IN *C57BL/6J-CHR3^{A}/NAJ*

A: Viral titer in CSS3, B6 and [CSS3 X B6]F_1 mice 8 days post infection, as measured by plaque assay. CSS3 mice of both sexes have significantly more virus in the heart than B6 or [CSS3 X B6]F_1 ($P<0.001$).*

B: Myocarditis is scored with 4 being most severe and 0 being no inflammation evident. CSS3 mice were more susceptible than B6 or [CSS3 X B6]F_1 ($P<0.05$). N≥11 per group).*

*Both A and B represent a composite of multiple CVB3-H3 infections ([CSS3 X B6]F_2 controls) and were replicated with CVB3-CG.

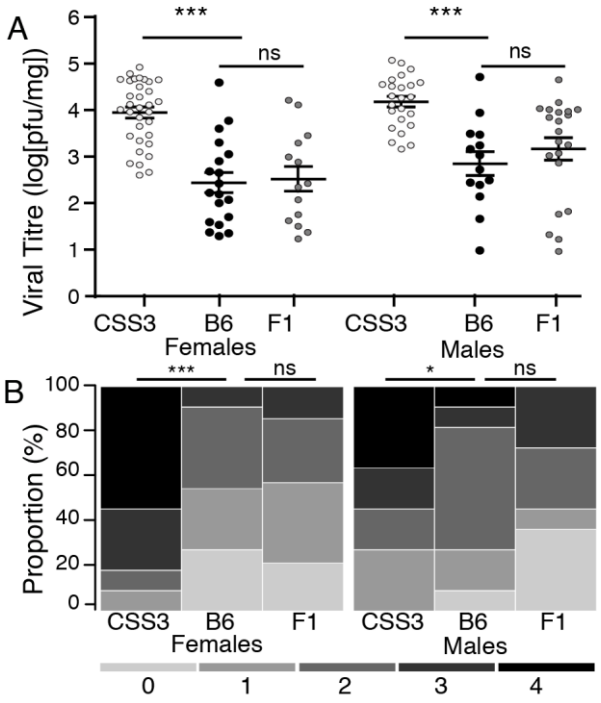
A
Viral Titre (log[pfu/mg])
***
ns
***
ns
CSS3
B6
F1
CSS3
B6
F1
Females
Males
B
Proportion (%)
***
ns
*
ns
CSS3
B6
F1
CSS3
B6
F1
Females
Males
0
1
2
3
4

FIGURE 2: PHENOTYPE DISTRIBUTIONS WITHIN THE [CSS3 X B6]F_2 POPULATION.

A: Histogram of the distribution of viral titers in [CSS3 x B6]F_2 mice, with a mean of 3.22 ±0.09.

B: Histogram of the distribution of myocarditis scores in [CSS3 x B6]F_2 mice, with a mean of 1.73 ±0.11.

C: The distribution of [CSS3 x B6]F_2 mice, showing significant correlation ($R^2=0.29$, $P<0.0001$) between myocarditis score and viral titer. This reveals a trend where higher myocarditis score is correlated to higher viral titer.

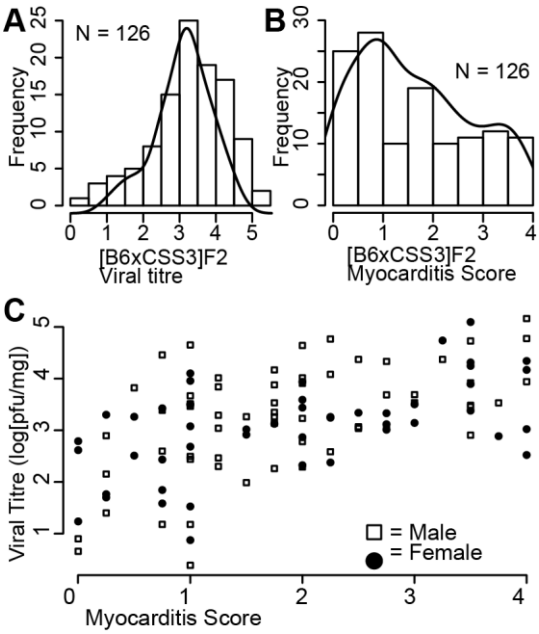
A
N = 126
Frequency
[B6xCSS3]F2
Viral titre
B
N = 126
Frequency
[B6xCSS3]F2
Myocarditis Score
C
Viral Titre (log[pfu/mg])
Myocarditis Score
= Male
= Female

FIGURE 3: LINKAGE OF CHROMOSOMES 3 TO CVB3 REPLICATION IN THE HEART AND TO MYOCARDITIS.

A, C: Overlapping LOD plots of [A/J x B10.A]F_2 (black) and [CSS3 x B6]F_2 (grey) mice shows significant linkage on distal chromosome 3 to viral replication in the heart (A) and to myocarditis (C). Threshold values corresponding to α=0.05 are represented as horizontal lines of corresponding shade. Peak linkage to viral replication and to myocarditis in [A/J x B10.A]F_2 occurred at *D3Mit19*(284). Peak linkage to viral replication and to myocarditis in [CSS3 x B6]F_2 occurs at *D3Mit19* (LOD= 3.74; P=0.018) and *D3Mit116* (LOD= 3.57; P=0.0032).

B: Viral titer vs. genotype at D3Mit19 shows that the AA genotype leads to a higher viral titer than BB in both crosses: 3.5±0.11 vs. 2.84±0.12 Log [PFU/mg] in [A/J x B10.A]F_2 and 3.75 ± 0.13 vs. 2.87 ± 0.29 Log [PFU/mg] in [CSS3 x B6]F_2.

D: *D3Mit19* genotype of AA leads to higher myocarditis scores than BB in both crosses: 2.83±0.11 vs. 2.06±0.12 in [A/J x B10.A]F_2 and 2.28 ± 0.24 vs. 1.07 ± 0.23 in [CSS3 x B6]F_2.

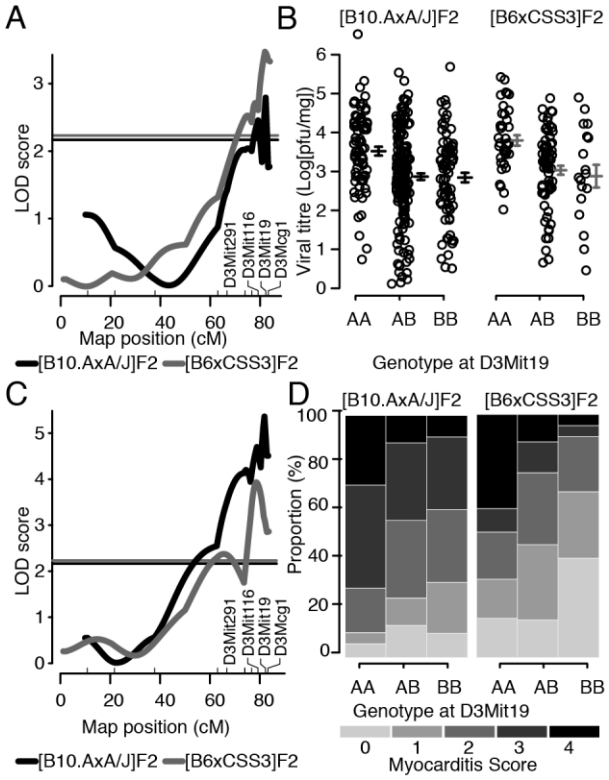
A
LOD score
Map position (cM)
D3Mit291
D3Mit116
D3Mit19
D3Mcg1
[B10.AxA/J]F2
[B6xCSS3]F2
B
[B10.AxA/J]F2
[B6xCSS3]F2
Viral titre (Log[pfu/mg])
AA
AB
BB
Genotype at D3Mit19
C
LOD score
Map position (cM)
[B10.AxA/J]F2
[B6xCSS3]F2
D
[B10.AxA/J]F2
[B6xCSS3]F2
Proportion (%)
Genotype at D3Mit19
Myocarditis Score

FIGURE 4: VIRAL REPLICATION IS HIGHER IN A/J AND CSS3 THAN IN B10.A AND B6 96 HOURS AFTER INFECTION.

A, B: Level of infectious CVB3 within the heart measured by plaque assay at 24, 48 and 96 hours in A and B. Differential control is significant at 96 hours post infection in both comparisons ($P<0.05$).

C, D: Concentrations of interferon beta (IFN-ß) in the serum were measured by ELISA in the same animals as in A,B. Significantly higher amounts of IFN-ß were detected in A/J mice compared to B10.A at 48 and 96hrs PI ($P<0.05$). No significant differences were observed between CSS3 and B6 mice.

(A, C: N=4 per time point, B, D: N=6 per time point, replicated with N=8 per strain at 48 hours).

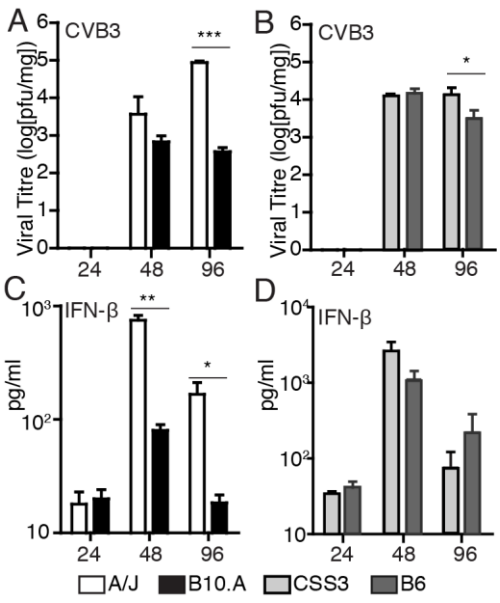
A
CVB3
Viral Titre (log[pfu/mg])
***
B
CVB3
Viral Titre (log[pfu/mg])
*
C
IFN-β
pg/ml
**
*
D
IFN-β
pg/ml
24
48
96
A/J
B10.A
CSS3
B6

FIGURE 5: CORE PROGRAM OF HIGHLY AND NOT DIFFERENTIALLY EXPRESSED GENES RESPONDING TO CVB3 INFECTION.

Microarray analysis of A/J, B10.A, CSS3, and B6 hearts at 4 days PI. Genes highly expressed or repressed after infection (at least 5 fold change in all strains) were considered to be part of a common pathway. Mice strains (A/J, B10.A, CSS3, and B6) are represented in rows stratified by infection status where + indicates infected tissue and – indicates mock-infected control tissue. This set of 129 genes constitutes a shared program of response to infection and damage in both susceptible and resistant mice. Pathway analysis of these genes identifies inflammation and response to infection. Functional clustering suggested RIG-I like signaling was involved and Interferome annotation identified 46/129 genes as known interferon-stimulated genes. Network score represents a statistical likelihood that the pathway identified is involved in the tissue analyzed given the genes involved.

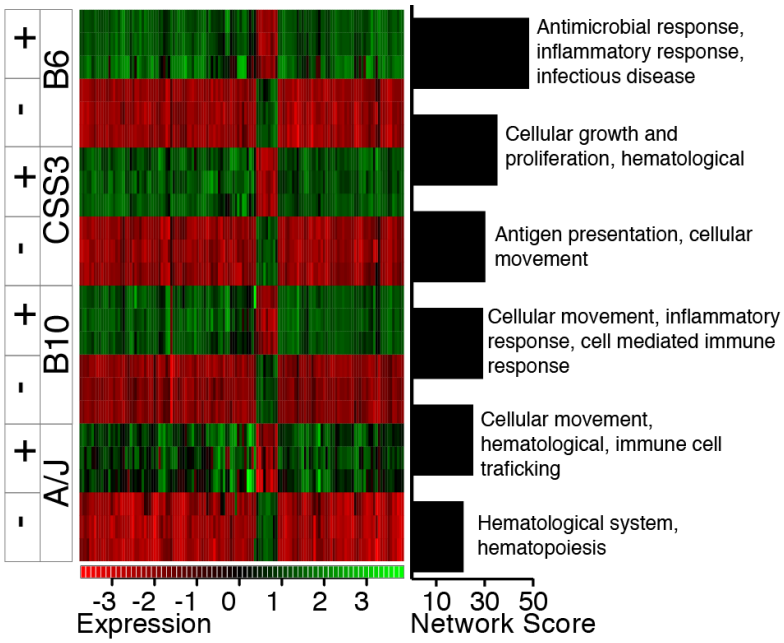
+
-
B6
+
-
CSS3
+
-
B10
+
-
A/J
-3 -2 -1 0 1 2 3
Expression
10 30 50
Network Score
Antimicrobial response, inflammatory response, infectious disease
Cellular growth and proliferation, hematological
Antigen presentation, cellular movement
Cellular movement, inflammatory response, cell mediated immune response
Cellular movement, hematological, immune cell traficking
Hematological system, hematopoiesis

FIGURE 6: DIFFERENTIALLY EXPRESSED GENES IN A/J, B10.A, CSS3, AND B6 MICE IDENTIFY COMMON AND DISTINCT PATHWAYS.

Mice strains (A/J, B10.A, CSS3, and B6) are represented in columns stratified by infection status where + indicates infected tissue and – indicates mock-infected control tissue.

A: A/J specific genes (increased or decreased expression in A/J mice after infection, but not in B10.A) cluster into pathways involving cardiovascular development, survival, inflammatory disease, and metabolism.

B: B10.A specific genes differentially expressed compared to A/J were primarily involved in cell mediated immunity and strongly indicative of a cytotoxic response.

C: CSS3 specific genes (increased or decreased expression in CSS3 mice after infection, but not in B6) were less numerous than A/J, but fell into similar functional categories of development. There were no B6 specific pathways identified.

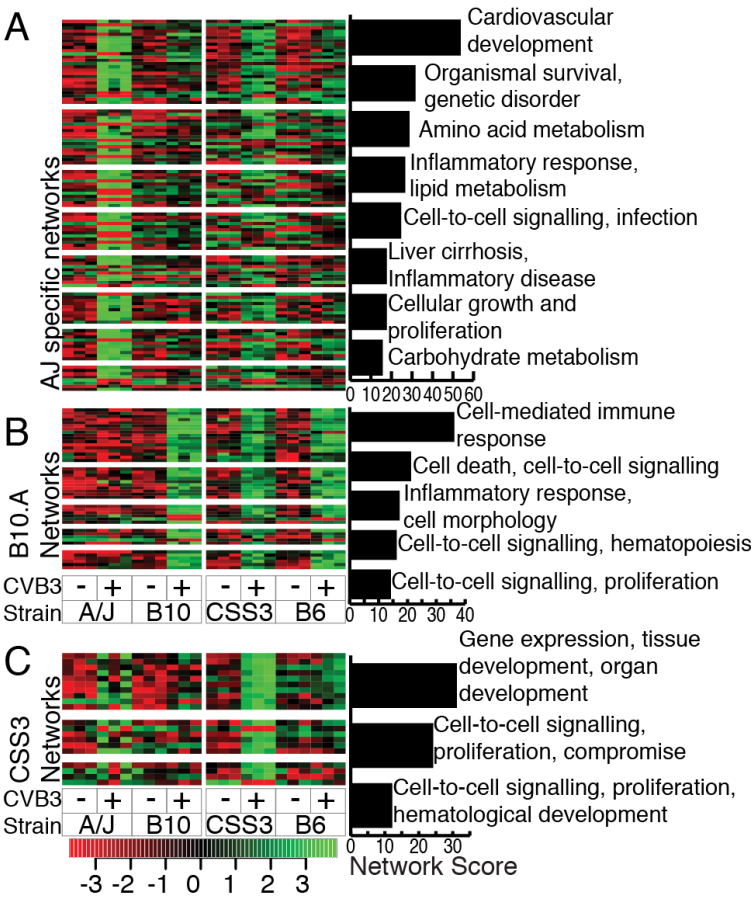
A
AJ specific networks
Cardiovascular development
Organismal survival, genetic disorder
Amino acid metabolism
Inflammatory response, lipid metabolism
Cell-to-cell signalling, infection
Liver cirrhosis, Inflammatory disease
Cellular growth and proliferation
Carbohydrate metabolism
0 10 20 30 40 50 60
B
B10.A Networks
Cell-mediated immune response
Cell death, cell-to-cell signalling
Inflammatory response, cell morphology
Cell-to-cell signalling, hematopoiesis
Cell-to-cell signalling, proliferation
CVB3 - + - + - + - +
Strain A/J B10 CSS3 B6
0 10 20 30 40
C
CSS3 Networks
Gene expression, tissue development, organ development
Cell-to-cell signalling, proliferation, compromise
Cell-to-cell signalling, proliferation, hematological development
CVB3 - + - + - + - +
Strain A/J B10 CSS3 B6
0 10 20 30
Network Score
-3 -2 -1 0 1 2 3

FIGURE 7: ENHANCED RESOLUTION OF LINKAGE OF VMS1 TO CHROMOSOME 3 BY COMBINED ANALYSIS AND INTEGRATION OF CANDIDATE GENE ANALYSIS.

A: Linkage of viral replication to distal chromosome 3 is shown as LOD profiles of A/J x B10.A]F_2 and [CSS3 x B6]F_2 (grey and black lines) for the 16 cM support interval of *Vms1*. Combining both analyses leads to significantly improved resolution (dashed line), with a new support interval of 4.5 cM linked to viral titer referred to as *Vms1.1a*.

B: Linkage of myocarditis score to distal chromosome 3 shown as in (A) with a new support interval of 7.5 cM myocarditis score referred to as *Vms1.1b*.

The overlapping region of *Vms1.1a* and *Vms1.1b* is *Vms1.1*. Candidate genes identified by differential expression (*Adh1*, *Gbp1*, *H28*), by basal expression difference (*Tnni3k*), and containing non-synonymous mutations (*Fpgt*) are shown in approximate position.

B: Boxplots of microarray data for candidate genes with expression differences. Horizontal lines represent the 40^{th} and 60^{th} percentile of expression of all genes. *Adh1*, *Gbp1*, and *H28* are expressed at significantly higher levels in A/J and CSS3 mice following infection, but not in B10.A and B6 mice. *Gbp1*, *Eif4e*, and *Tnni3k* were expressed at different levels even in the absence of infection.

C, D: Quantitative RT-PCR (qPCR) confirmation that *H28* is induced preferentially in $Vms1^s$ following infection and that *Tnni3k* transcript is less present in $Vms1^s$ at basal levels.

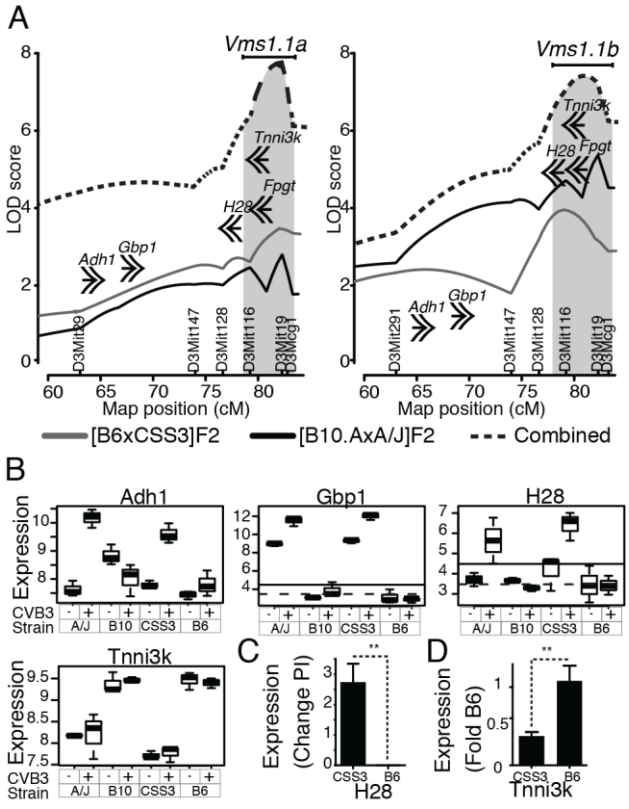
A
Vms1.1a
Vms1.1b
LOD score
Map position (cM)
Tnni3k
Fpgt
H28
Adh1
Gbp1
D3Mit9
D3Mit147
D3Mit128
D3Mit116
D3Mit19
D3Mit291
[B6xCSS3]F2
[B10.AxA/J]F2
Combined
B
Adh1
Gbp1
H28
Tnni3k
Expression
CVB3
Strain
A/J
B10
CSS3
B6
C
Expression (Change PI)
H28
D
Expression (Fold B6)
Tnni3k

CHAPTER 4: TNNI3K MODULATES CARDIOMYOCYTE INNATE IMMUNITY DURING VIRAL MYOCARDITIS

SEAN A. WILTSHIRE, JENNIFER MARTON AND SILVIA M. VIDAL

Department of Human Genetics, McGill University, Montreal, Quebec, H3A 1B1, Canada;

Correspondence should be addressed to S. M. V. (McGill Life Sciences Complex, Room 367, 3649 Promenade Sir William Osler, Montreal, QC, H3G 0B1; Fax: 514-398-2603; e-mail: silvia.vidal@mcgill.ca).

BRIDGING STATEMENT FROM CHAPTER 3 TO CHAPTER 4

In the previous chapter, we provided confirmation of the existence of *Vms1* in an independent test cross, refined the *Vms1* interval, and identified a small handful of candidate genes that might play a role in conferring the *Vms1* phenotype. One candidate gene *Tnni3k* was located near the peak of linkage in our interval. *Tnni3k* is a heart specific kinase that has been described as being activated following stress. Moreover, differential RNA and protein level expression had already been characterized in between strains, so *Tnni3k* seemed like an excellent candidate gene for further study in the context of viral myocarditis.

ABSTRACT

The pathogenesis of viral myocarditis is a complex process. We previously made use of a genetic model to identify candidate genes controlling the pathogenesis of Coxsackievirus B3 (CVB3) induced viral myocarditis. Here we report on the role of one such candidate: the cardiac specific Tnni3 kinase (*Tnni3k*). The contribution of a human TNNI3K transgene was compared to mice expressing very low levels of *Tnni3k* in the DBA2/J background. We show that viral replication is modulated by TNNI3K, and that myocardial necrosis and inflammation are greatly enhanced across the course of infection. We show that TNNI3K transgenic hearts are distinguished by a unique gene signature involving IFNγ TNFα and NFκB/IKKß regulated genes. We also show that isolated cardiomyocytes from transgenic mice allow enhanced CVB3 RNA replication and chemokine transcription compared to those from wild-type littermates. These results indicate that TNNI3K function manifests early during the course of CVB3 infection, originates from the cardiomyocyte itself and it can be exploited by the virus for its own replication.

INTRODUCTION:

Coxackievirus infection is a known cause of viral myocarditis, a disease characterized by inflammation and necrosis of the heart (184, 308). Control of viral myocarditis is highly complex, and experimental models have identified at least three key phases in determining pathogenesis. The initial phase of primary replication within the cardiomyocyte depends on a number of host factors including sarcolemmal integrity(98, 348) and the innate immune response within the cardiomyocyte(185, 240, 245, 247, 248, 259). This is followed by a phase of myocardial infiltration by immune effector cells, which may aid in clearing infection (309). Finally, infiltration of the myocardium may trigger autoimmunity, or fail to clear the virus leading to cardiomyopathy or death (310).

Infection of mice with CVB3 results in a wide spectrum of clinical symptoms that varies among inbred mouse strains, suggesting a contribution of the genetic background in the control of the infection. Previously using segregating crosses involving mice of either susceptible A/J or resistant C57BL (B10 and B6) genetic backgrounds, the viral myocarditis susceptibility 1 (*Vms1*) locus was identified in [B10.A x A/J]F2 mice(135), and confirmed in [B6x B6.chr3^{AA}]F_2 mice (188). We showed that the *Vms1* locus was linked to virus replication, cardiomyocyte injury and myocarditis whereas the target *Vms1* interval contained a small handful of promising candidate genes. In particular the Tnni3 interacting kinase (*Tnni3k)* was of great interest. *Tnni3k* is expressed differently in resistant and susceptible strains; *Tnni3k* is extremely cardiac specific in its expression (349-351). *Tnni3k* also modulates hypertrophy and heart failure in the mouse (350, 352-354). A recent report has described that *Tnni3k* is responsible for an activation of the p38 signaling cascade, generation of increased reactive oxygen species in cardiomyocytes, and enhanced necrosis, all following reperfusion injury (349).

It was of interest to test directly whether *Tnni3k* would play a role in CVB3 pathogenesis. To this end, a DBA2/J mouse over-expressing a human cDNA transgene of TNNI3K (DBA2/J.TNNI3K^{tg}) was compared to wild-type DBA2/J littermates, across 4

time points from early infection, and leading up to the peak of inflammation (day 2, 4, 6 and 8). For the purpose of comparison to previous *Vms1* results, DBA2/J is resistant to infection and requires fifty times more CVB3 inoculum to show symptoms of infection as compared to C57BL/6 or C57BL/10. It has long been known that different combinations of strain, sex and virus (including C57BL/6 and DBA2) can produce markedly different pathogenesis in infected mice (26, 118). It was found that TNNI3K^{tg} mice produce more viral RNA from early time points, then go on develop increased cardiac necrosis, and inflammation compared to littermates. Microarray analysis earlier in infection indicated the presence of heightened inflammatory gene expression before cellular infiltration of the heart was observed. This result was supported using primary ventricular cardiomyocytes in which TNNI3K overexpression led to an increase in cardiomyocyte viral replication, and inflammation. This work has demonstrated that TNNI3K overexpression leads to increased inflammation at the cellular and tissue level through a cell-intrinsic CVB3-mediated mechanism that also promotes virus replication.

MATERIALS AND METHODS

MICE, CELLS AND VIRUS

Inbred DBA2/J mice were purchased from the Jackson Laboratory (Bar Harbor, ME), and DBA.TNNI3K^{tg} mice (line 23) were generously provided by Douglas Marchuk and described previously (350, 353). DBA.TNNI3K^{tg} mice were maintained and bred on the DBA2/J background which expresses almost no endogenous *Tnni3k*(350). The mice were maintained in the McGill University animal facility in compliance with the Canada Council on Animal Care as approved by the McGill University Animal Care Committee. Coxsackievirus B3 used for time course and microarray experiments was CVB3-H3(321) generously provided as a plasmid by the lab of Dr. Kirk Knowlton (University of California, San Diego). Mice were inoculated intraperitoneally with 500PFU/g of CVB3-H3 diluted in sterile PBS at seven to eight weeks of age. Uninfected controls in microarray experiments were mock infected with PBS in parallel. Survival, weight, and signs of infection were evaluated on a daily basis and the mice were humanely sacrificed two, four, six or eight days post-infection. Evans blue dye was injected in a 1% solution 24 hours prior to necropsy as previously described(135, 355). At necropsy, hearts used for microarrays and EBD were first perfused with cold sterile buffer (110mM NaCl, 10mM NaHCO3, 16mM KCl, 16mM MgCl2, 1.2mM CaCl2, 5U/L Heparin, pH 7.9). Hearts were then cut in half sagitally and fixed in buffered formaline or frozen in OCT medium. Tissues for RNA extraction were preserved in RNA-later stabilization reagent (ambion) before being frozen at -80C. The apex of hearts were stored at -80ºC, homogenized and submitted to three freeze-thaw cycles to release infectious virus. After centrifugation at 1,000 g for five minutes to remove debris, the supernatant was isolated for quantification by plaque assay as previously(135, 188). All experiments comparing DBA2/J and TNNI3K^{tg} were performed on littermates. Each day in the time series experiments was performed as a separate experiment, and results are shown together for simplicity.

STATISTICAL AND BIOINFORMATICS ANALYSIS

Statistical analyses were conducted with the freely available program R and Graphpad Prism version 6. Time course data was analyzed by two way ANOVA. P-values within time course figures represent Šidák corrected row means comparisons with p-values generated *P<0.05, **P<0.01 and ***P<0.001, ****P<0.0001. Evans Blue image analysis was performed using ImageJ software(356) and is expressed as the percent of EBD positive surface, area relative to total myocardial surface area. Microarray analysis was performed as previously described to identify differentially expressed genes and those highly expressed in both strains(188). Interferon stimulated genes were annotated using the ISG and Interferome databases(324, 325, 357), DAVID(326) and by Ingenuity Pathways Analysis (Ingenuity® Systems, ingenuity.com) upstream analysis tool.

ISOLATION ,CULTURE AND INFECTION OF ADULT VENTRICULAR CARDIOMYOCYTES

Isolation of mouse adult ventricular cardiomyocytes was performed according to previously described methods(247). Briefly, mice were heparinized with 50U heparin in PBS before being anaesthetized with sodium pentabarbital. Hearts were removed aseptically and mounted on a canula and perfused retrogradely for 2-3 minutes in heart solution in containing in (mmol/L) 120 NaCl, 5.4 KCl, 1.2 $MgSO_4$, 1.2 NaH_2PO_4, 20 NaHCO3, 5.6 D-glucose, 20 of 2,3-butanedione monoxime (Sigma-Aldrich, St Louis, Mo), 5 taurine, and 1 pyruvate. This was followed by enzymatic digestion for 10-20 minutes with 1.5mg/ml of type 2 collagenase (Worthington Biochemical, Lakewood) in heart solution. Gravity sedimentation in heart solution containing 5mg/mL BSA (A1470, sigma) was followed by two was steps in increasing calcium concentration (0.2mM, 0.4mM, 0.6mM). Cardiomyocytes were plated in heart medium (M1018 Sigma) containing (in mmol/L) 4.16 $NaHCO_3$ and 9.89 2,3-butanedione monoxime on 6-well plates coated with 1-2µg/cm^2 laminin (L2020, sigma). Cardiomyocytes were cultured overnight prior to infection. Infection was performed using CVB3-H3 virus purified by pelleting at 189,000 x *g*(20), quantified by plaque assay and resuspended in heart medium. Infections were carried out at an MOI of approximately 10X for 1 hour. After 1 hour, heart medium was changed, and 1 well was immediately extracted as baseline t=1hr RNA; collections also occurred 24, and 48 hours later. RNA was prepared using

RNeasy spin columns as per the manufacturer's instructions. Gene expression and relative CVB3 quantification was calculated relative to t=1hr by 2^-∂∂Ct calculations(286).

MICROARRAY AND QPCR

Total RNA was extracted from ~30mg of heart tissue 4 days post-infection from a transverse section using Qiagen RNeasy extracton kit. Quality control by agilent bioanalyzer, cDNA synthesis and microarray hybridization was performed at the McGill University and Genome Quebec Innovation Centre. Three infected and three uninfected female mice of each genotype were independently prepared and analyzed on an Illumina Mouse-WG6 version 2.0 array. Normalization, and analysis was performed using FlexArray(327), expression values were normalized using the RMA, VST and Robust Spline options of lumi. Quantitative PCR primers were designed to span exon junctions with the help of primer3plus(285), experiments were performed in duplicate.

LIST OF PRIMERS USED:

CVB3-H3 forward: ATGGCAGAAAACCTCACCAG, CVB3-H3 reverse: ATGTTCTGCCCAAACAGTCC, Cxcl1 forward: CACCTCAAGAACATCCAGAGC, Cxcl1 reverse: CTTGAGTGTGGCTATGACTTC, Gapdh forward: AAGGGCTCATGACCACAGTCC, Gapdh reverse: GATGCAGGGATGTTCTGG, Sele forward: CCATGTGCCTTCTTACAACG, Sele reverse: TTAAGCAGGCAAGAGGAACC, Icam1 forward: AGACGCAGAGGACCTTAACAG, Icam1 reverse: ACTGTGGGCTTCACACTTCAC, Tnfa forward: CATCTTCTCAAAATTCGAGTGACAA, Tnfa reverse: TGGGAGTAGACAAGGTACAACCC, Ifng forward: CACGGCACAGTCATTGAAAG, Ifng reverse: CATCCTTTTGCCAGTTCCTC

RESULTS

INCREASE IN ACUTE MYOCARDIAL VIRAL REPLICATION IN TNNI3K^{TG} MICE

We had previously identified the *Vms1* locus on distal chromosome 3 as a modifier of viral myocarditis(135, 188). Mice with the A/J allele of *Vms1* (*Vms1*^{a}) are less able to control viral replication, while expressing equivalent levels of type I interferon in the heart. A/J and *Vms1*^{a} hearts carry the same allele of *Tnni3k* as DBA2/J, C3H/HeJ, and BALB/c. These strains express carry a SNP (rs49812611^{g}) that is recognized by the nonsense mediated decay pathway resulting in extremely low levels of *Tnni3k* transcript(350, 353, 358). The C57BL/6, C57BL/10, 129, AKR and MRL strains carry the (rs49812611^{g}) version of *Tnni3k* and express the gene at normal levels exclusively within the myocardium. Cardiac specific overexpression (5-20X) of a human cDNA copy of TNNI3K (TNNI3K^{tg}) has been shown to recapitulate phenotypic aspects of rs49812611^{g}(350, 353). The coincidence of *Tnni3k* with the peak of genetic linkage to viral myocarditis, and the cardiac specificity of *Tnni3k* encouraged us to test whether overexpression of *Tnni3k* might modify the progression of viral myocarditis.

While A/J and DBA2/J are essentially a null for *Tnni3k* expression, and C57BL/6, C57BL/10 are normal expressers, TNNI3K^{tg} express between 5X and 20X normal levels of *Tnni3k*. If no *Tnni3k* expression in *Vms1*^{a} was causally related to higher viral replication relative to normal *Tnni3k* in *Vms1*^{b}, then it might be expected that overexpression of TNNI3K in TNNI3K^{tg} mice would confer even more resistance than the *Vms1*^{b} allele in inbred mice. At day 8 post infection, virus was cleared more effectively (T-Test P=0.0334) and in many mice to undetectable levels in TNNI3K^{tg} mice as compared to wildtype seeming to support our initial hypothesis (Supplemental Figure 1). However, phenotyping at earlier time points in a similar manner to experiments on *Vms1*^{a} vs. *Vms1*^{b} mice, revealed a more complex situation. Viral replication as measured by plaque assay was relatively low and virtually identical across days 2 and day 4 post infection; furthermore, the significance of the difference seen at day 8 did not survive correction for multiple testing (P=0.0784) [Figure 1A]. Since CVB3 genomic RNA is more abundant than fully infectious plaque forming units (PFU), we next sought

to confirm our plaque assay results by the more sensitive quantitative RT-PCR (qPCR) for CVB3 genome and also to include a time point 6 days post-infection to see if a trend emerged. Across the course of infection TNNI3K^{tg} mice have significantly higher viral RNA in their hearts than wildtype DBA2/J (P=0.0030). This difference was significantly different as early as 2 days post-infection (P=0.0094), and continued through days 4 (P=0.0008), and 6 (P<0.0001) post infection. These results taken together indicated that from early time points in infection, overexpression of TNNI3K led to increased levels of virus replication in the heart.

INCREASE IN SARCOLEMMAL DISRUPTION AND MYOCARDITIS IN TNNI3K^{TG} MICE

We had previously described significant correlation between viral replication and sarcolemmal disruption in [B10.A x A/J]F2 mice (Spearman ρ =0.61, p<0.0001)(188). *Tnni3k* expression has been found to decrease myocardial integrity under acute insults such as ischemia(349), and chronic insults such as transverse aortic constriction or calsequestrin overexpression (350, 352). Given a suggestive increase in viral replication as early as day 4, it was of interest to determine if sarcolemmal disruption would correlate with viral replication. It was found that while viral replication occurs at high levels four days post infection, very little sarcolemmal disruption occurred until six days post infection when it was significantly higher in TNNI3K^{tg} than in wild-type mice (P=0.0030) [figure 2]. This trend shifted by day 8 post infection where sarcolemmal disruption in TNNI3K^{tg} mice remained relatively high, but the mean difference compared to wildtype decreased from 7.2±2.0% at day 6, to 4.0±1.9 at day 8.

Inflammation in the heart was not clearly present on day 4 in either group [Figure 3]. Myocarditis score in TNNI3K^{tg} increased to an average score of 2.8±0.52 by day 6, and continued to worsen on day 8 at an average score of 3.2±0.28. Inflammation is comparatively mild in the wild-type DBA2/J mice with average myocarditis scores of 0.59±0.19 at day 6, and 1.33±0.25 at day 8. Both of these differences were highly significant (P<0.0001). No histological differences were observed in uninfected animals, and both TNNI3K^{tg} and wild-type DBA2/J exhibited occasional dystrophic calcification

[Supplemental figure 2](130-132). These results taken together with viral replication data indicate that TNNI3K overexpression leads to an early increase in replicating virus, followed by an increase in sarcolemmal damage, and fulminant inflammation of the sarcolemmal tissue.

MICROARRAY ANALYSIS OF DBA2/J AND TNNI3KTG REVEALS COMMON AND DIFFERENTIAL GENE EXPRESSION IN RESPONSE TO CVB3

By day 4 post infection there is no clear infiltration of the myocardium, or extensive necrosis [Figures 2 and 3], but viral replication has reached a high level and is differentially controlled between TNNI3K^{tg} and wild-type mice. We therefore chose this time point to use global transcription profiling to ascertain factors that might account for the intense necrosis and inflammation occurring at later time points. Genes with absolute fold changes following infection in both strains greater than 1.65 (corresponding to the top 106 probes, or 72 genes) were first analyzed using the DAVID bioinformatics tool. Functional annotation clustering identified “immune response” and “antigen processing and presentation” as being the most significant gene ontology (GO) terms present in the data (q=9e-13 and 6.1e-8 respectively). The strong up regulation of class I MHC molecules was consistent with interferon stimulus, so highly expressed genes were then analyzed with the Interferome bioinformatics tool. Of the 72 genes in the dataset, 42 were consistent with a type I or type II interferon response and 9 were consistent with a type I response only. This suggests the sensing and signaling pathways involved in generating and responding to a type I interferon signal are essentially intact in both DBA2/J and TNNI3K^{tg} mice. This is supported by no significant differences in qPCR results for *Ifnb1* across the course of infection [Supplemental Figure 3].

Differentially expressed genes were identified using a stepwise approach: only probes where mean expression in at least one condition was above the bottom 40% all probes were included, to reduce spurious results. Only genes where the ANOVA interaction term between strain and infection was significant were included. Only genes where either genotype was differentially expressed (1.5 fold change, $p<0.05$) were included.

Finally, genes were ranked by difference in strain means, and a threshold was set such that only genes in the top 5% of difference were included. This list was further incrementally simplified to remove genes where expression differences were parallel or where unlikely to be meaningful, as previously(188). A total of 65 genes were identified as preferentially expressed in TNNI3K^{tg} hearts. DAVID functional annotation clustering identified “immune response”, “defense response” and “inflammatory response” as the most significant GO terms within the gene list (q= 1.5e-5, 3.5=-5 and 7.9e-5 respectively). Interferome analysis of this genelist indicated that unlike the core expression program, which could be explained by type I interferon alone, TNNI3K^{tg} specific expression also pointed to type II interferon [Figure 5a]. This was refined further using Ingenuity Pathway Analysis upstream analysis tool which confirmed that a signature of interferon-ɣ was strongly present, but also TNF-α and IKK2/NF-κB signaling. Genes corresponding to these pathways and their corresponding fold changes are shown in [Figure 5b]. Selected cytokines, chemokines and adhesion molecules associated with inflammation were tested to both verify microarray results and further characterize response. The most differentially expressed cytokine, Cxcl1 (KC) from the microarray was found to be highly differentially expressed as early as day 4 post-infection. Also identified at day 4, were the adhesion molecules Sele (e-selectin) and Icam1 (ICAM-1). These were followed by Ifng (IFN- ɣ) and Tnfa (TNF-α) by day 6. Cxcl10 (IP10) expression was significantly increased across the entire infection (P=0.0082), but was not significantly different at any individual time point. These results taken together suggest that both DBA2/J and TNNI3K^{tg} are responsive to CVB3 infection in a number of equivalent ways, but that TNNI3K^{tg} hearts also respond with an early burst of KC as well as upregulation of adhesion molecules. This is followed by an increase in cytokine markers of inflammation at a time point when necrosis and inflammation becomes histologically apparent.

DIFFERENTIAL VIRAL REPLICATION AND INFLAMMATORY RESPONSE IN PRIMARY CARDIOMYOCYTES

In view of the discrepancy of phenotype between *Vms1^{b}* and TNNI3K^{tg} mice, we questioned the role of TNNI3K in virus replication and inflammatory response in primary

cardiomyocytes. The cardiomyocyte is known to be a TNF-α producing organ under stress conditions (359), and this occurs at least partially in a p38 dependent manner (360). Primary cardiomyocytes have also been convincingly demonstrated to produce IP10 upon treatment with type II interferon (259). To ensure that early elevation of *Cxcl1* and viral RNA were originating from cardiomyocytes expressing TNNI3K transgene rather than another cell-type contained within whole heart tissue, adult primary ventricular cardiomyocytes were isolated and infected with CVB3. In cardiomyocytes infected with CVB3, it was determined that TNNI3K^{tg} cells produce both more viral RNA following infection and also express more *Cxcl1*. The presence of TNNI3K^{tg} resulted in significantly increased CVB3 and *Cxcl1* across the observed 48-hour infection (P=0.0036, 0.0080), and in particular at 24 hours post infection (P=0.011, P=0.031). These data indicate that TNNI3K overexpression leads to increased viral replication and inflammation in cardiomyocytes.

DISCUSSION

The relationship between viral infection, myocarditis and cardiomyopathy is complex(41, 184, 185), and clearly heterogeneous(115, 175, 186, 361). Factors controlling experimental viral myocarditis include availability of viral receptor(45, 46, 53), innate sensing of virus (240, 244, 298, 362, 363), production of and response to cytokines(242, 243, 248, 299, 364-366), infiltrating immune cells(259, 367, 368), generation of an adaptive immune response, the development of autoimmunity(133, 186, 369) and more(184, 185, 267, 370, 371). Nonetheless, to date it remains unclear which host genetic factors describe the remarkable degree of clinical heterogeneity in dilated cardiomyopathy and myocarditis (177, 361). Multiple groups have analyzed natural variation in patients (372), and in model organisms(20, 118, 135, 143, 186, 188) to understand. So far, the role of the mouse major histocompatibility locus (*H2*)(25, 26), the T-cell receptor locus(143), and proximal chromosome 1 have all been genetically implicated(134, 369). We previously identified the viral myocarditis susceptibility 1 (*Vms1*) locus on mouse distal chromosome 3 as determining early viral replication, acute infiltration and sarcolemmal necrosis. The *Vms1* locus was confirmed by replication in two separate test crosses, [B10.A x A/J]F_2 (135), [B6x B6.chr3^{AA}]F_2 (188), and also using congenic lines of mice [unpublished data].

The leading candidate gene for the *Vms1* locus is the *Tnni3k* gene. Peak genetic linkage was found to correspond with the location of *Tnni3k*(135, 188). Tnni3k is expressed at different levels in inbred strains due to a SNP (rs49812611$^{g/a}$) that results in nonsense-mediated decay and extremely low levels of *Tnni3k* transcript(350, 353, 358). *Tnni3k* is expressed exclusively in the heart(349, 351, 353, 354), and appears to become activated under stress conditions including heart failure(349, 350, 353, 373-376). *Tnni3k* is known to modulate heart failure, hypertrophy, cardiomyocyte necrosis, ROS species and the p38 signaling cascade (349-354). The sub-cellular localization and function of TNNI3K is currently in dispute. One study demonstrated collocalization with the cardiomyocyte nucleus in neonatal rat ventricular cardiomyocytes by western blot and immunostaining (349). The other possible location of TNNI3K within the cell is in the sarcomeric Z-disc, within the desmin ring structures. This was also determined by

immunostaining but in DBA2/J, C57BL/6 and TNNI3K^{tg} adult mice (353). To test whether or not *Tnni3k* could play a role in viral myocarditis we investigated the response of DBA-TNNI3K^{tg} mice to infection with CVB3.

Using a *Tnni3k* humanized mouse for TNNI3K^{tg} model, we found that TNNI3K overexpression led to an increase in viral replication and inflammation in response to CVB3 infection at the level of isolated cardiomyocytes. This increase in viral replication was recapitulated at the organ level of the heart during acute infection. While highly significant differences in viral RNA were detected in the heart, differences were tempered at the level of viable plaque forming units. Furthermore, both TNNI3K^{tg} and wildtype mice appear to be able to clear virus from the heart, and though TNNI3K overexpression allows higher peak viral replication, TNNI3K^{tg} mice also cleared virus more rapidly by day 8 post-infection. This rapid clearance is associated with a high cost, as TNNI3K^{tg} mice also develop substantially greater necrosis and inflammation in the process.

The molecular mechanism underlying TNNI3K enhancement of inflammation is still unknown, but gene expression profiling combined with studies by other groups provides some clues. At basal conditions *Tnni3k* deficient and *Tnni3k* sufficient mice exhibit no apparent cardiac differences; however, under stress conditions *Tnni3k* sufficient or *TNNI3K* overexpressing mice develop severe pathology (349, 350, 353, 358, 377). TNNI3K is phosphorylated under stress conditions such as transverse aortic constriction(353). These results are consistent with a hypothesis that *Tnni3k* is a kinase activated via phosphorylation during cardiac stress. *Tnni3k* has been described to phosphorylate and thereby activate the p38-signaling pathway(349). The p38 kinase is a well-known modulator of both inflammation and cardiac hypertrophy(378, 379). TNNI3K modulation of p38 might serve to account for both cardiac hypertrophy seen in TNNI3K^{tg} mice(353), as well as the altered inflammation reported here.

Alternatively, the TNNI3K^{tg} expression program seen here might be the result of increased IKK2/NF-κB activity. Inhibitor of kappaB kinase beta (IKK2) activates NF-κB by phosphorylating the inhibitor IκB leading to its degradation and freeing NF-κB. IKK2 is itself activated when phosphorylated so it is also a potential direct or indirect target of

TNNI3K kinase activity(380). Remarkably CVB3 infection alone of HeLa cells is sufficient to activate NF-κB signaling by an apparently IκB independent and Akt dependent mechanism. In the context of CVB3 infection, blocking NF-κB activation markedly decreases infected cell viability and released viral particles. This suggests that the NF-κB pathway may be important for maintaining cellular survival during infection. However, sustained activation of NF-κB by TNF-α also leads to cell death, indicating that a delicate balance is required(303).

An apparent contradiction of phenotypes exists between of TNNI3K overexpression in TNNI3K^{tg} mice (high inflammation, high necrosis, high acute viral replication) and *Tnni3k* expressing *Vms1^{b}* mice (reduced inflammation, necrosis and viral replication). A number of factors may help to explain this: *Vms1^{b}* and TNNI3K^{tg} mice were studied on different genetic backgrounds, and background effects certainly play a role in experimental CVB3 infection. The TNNI3K transgene is expressed between 5-20X more than natural *Vms1^{b}* expression levels. Regulation of inflammation within the context of viral myocarditis is critical. If *Tnni3k* positively modulates innate cardiomyocyte driven inflammation, then normal expression may be beneficial whereas overexpression is conducive to excessive inflammation. A noteworthy example is the chemokine CXCL10, whose expression is significantly stimulated by the presence of the TNNI3K transgene. CXCL10 secretion by cardiomyocytes has been shown to be critical for the recruitment of NK cells and viral clearance at early time points during infection. However at later time-points the chemokine correlates with infiltration of activated thymocytes during the myocarditis phase without affect on virus load(259). Despite a significant initial benefit for virus growth, we have observed lower titers in hearts of TNNI3K^{tg} mice late in infection. Thus it would be of value to examine in more detail the ability of TNNI3K to elicit cell-mediated antiviral responses to better comprehend possible advantages of natural *Vms1^{b}* expression.

Comparatively greater viral replication may also be explained through a p38 specific mechanism, as recent *in vitro* based study demonstrated that p38 signaling was anti-apoptotic and conducive to increased viral replication(108). *In vivo* inhibition of p38 also enhanced viral replication as measured by *in situ* hybridization of virus in the heart (278).

Hence, activation of p38 could also explain the dramatic loss of cardiomyocyte membrane integrity typical of necrotic death revealed by Evans blue staining in hearts of in TNNI3K^{tg} mice as well as elevated virus progeny. CVB3, like other viruses, subvert host-signalling pathways for their own benefit. It is then reasonable to ask if the TNNI3K-mediated response, which is clearly of advantage for initial propagation of CVB3, is manipulated directly or indirectly by the virus itself.

Counterintuitive results in myocarditis studies are not unusual. Clinically it has been reported that patients who initially present with the most severe symptoms of myocarditis (fulminant myocarditis) recover more commonly than those with merely acute myocarditis (168). This result was replicated in a broader study, demonstrating that though fulminant myocarditis could be lethal if untreated, long-term prognosis was substantially better than for acute and chronic myocarditis (381).

It is clear that *Tnni3k* does play a role in viral myocarditis, in particular by permitting higher viral replication and leading to heightened inflammation. The role of *Tnni3k* in the context of specific signaling cascades, in particular p38 or NF-κB, and under different genetic backgrounds will require further studies.

ACKNOWLEDGEMENTS:

This work was supported by grants from the Canadian Institutes of Health Research (CIHR MOP-86592) S.A.W. and J.M. were supported by FRSQ Scholarships, and S.M.V. by the Canada Research Chair program.

FIGURE AND LEGENDS TO FIGURES:

FIGURE 1: ELEVATED VIRAL REPLICATION IN TNNI3K^{TG} MICE COMPARED TO WILD-TYPE

(a) No significant difference detected in viral replication as determined by plaque forming assay in TNNI3K^{tg} and wild-type DBA2/J mice at days 2, 6 and 8 post-infection (two-way ANOVA genotype effect P=0.5997). (b) Log10 of relative expression of CVB3 RNA is significantly higher in TNNI3K^{tg} mice across the course of infection (two-way ANOVA genotype effect P=0.003).

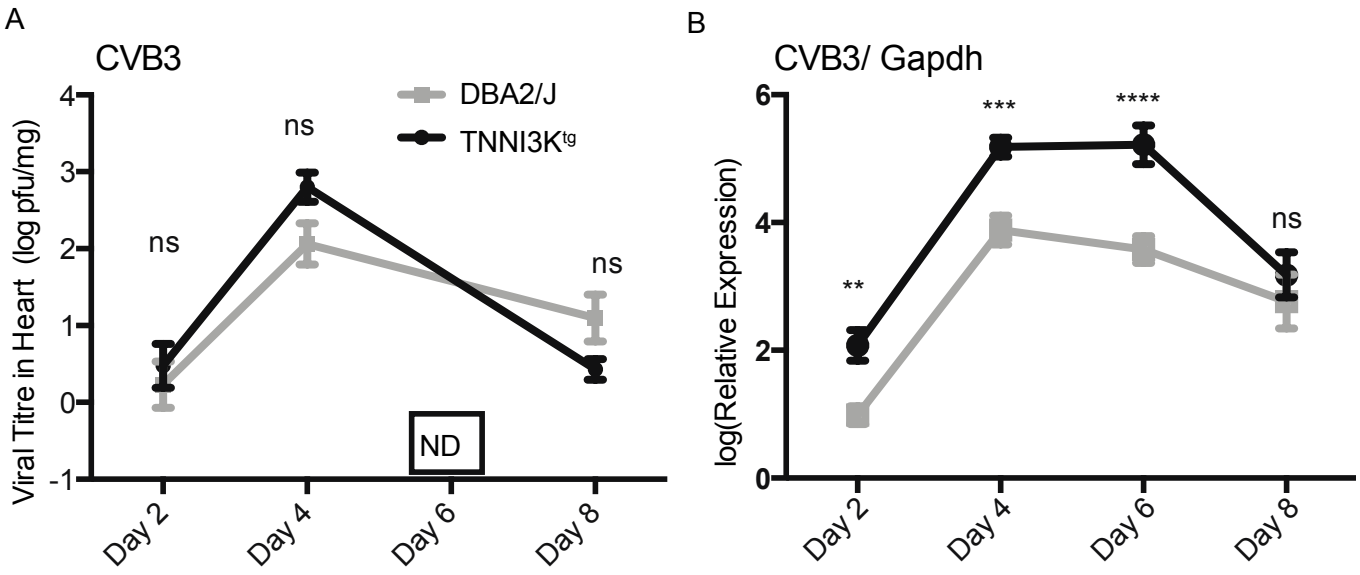
A
CVB3
DBA2/J
TNNI3K^tg
Viral Titre in Heart (log pfu/mg)
4
3
2
1
0
-1
ns
ns
ns
ND
Day 2
Day 4
Day 6
Day 8
B
CVB3/ Gapdh
log(Relative Expression)
6
4
2
0
**
***
****
ns
Day 2
Day 4
Day 6
Day 8

FIGURE 2: ELEVATED SARCOLEMMAL DISRUPTION IN TNNI3K^{TG} MICE

(a) Significantly higher sarcolemmal disruption in TNNI3K^{tg} is observed across the course of infection (two-way ANOVA genotype effect P=0.0009) at day 6 (P=0.0030) and suggestively at day 8 (P=0.1092). Values of sarcolemma disruption were calculated as the fraction of affected area relative to total myocardial surface area using Evans blue dye image analysis at the indicated times. Mean and standard error obtained for at least N=7 mice/time-point are shown. (b) Representative sections showing damaged myofibres in both DBA2/J and TNNI3K^{tg} mice at day 6: light areas correspond to fluorescence due to EBD uptake.

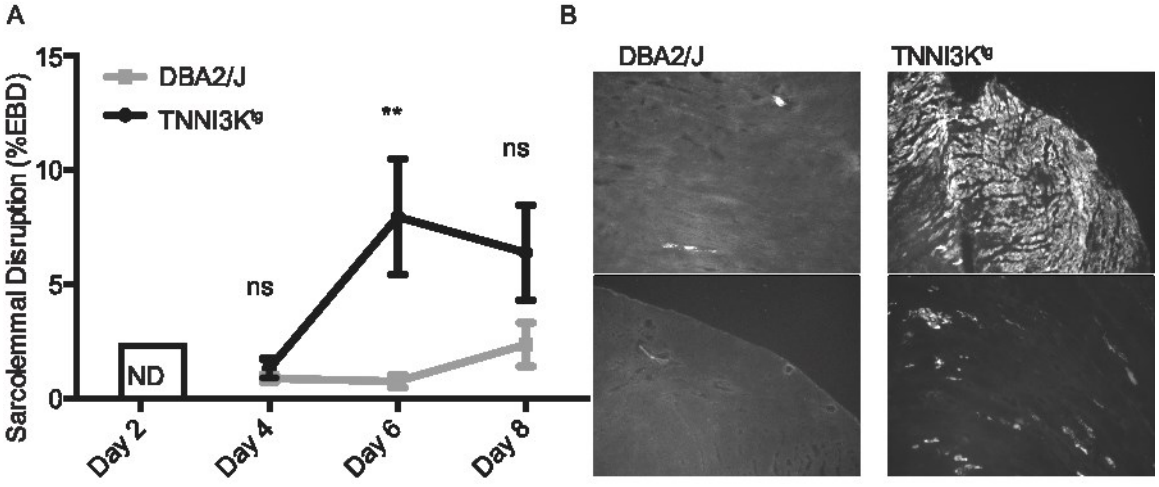
A
B
DBA2/J
TNNI3K^tg
Sarcolemmal Disruption (%EBD)
15
10
5
0
ND
ns
**
ns
Day 2
Day 4
Day 6
Day 8
DBA2/J
TNNI3K^tg

FIGURE 3: ELEVATED INFLAMMATION IN TNNI3K^{TG} MICE

(a) Greatly increased inflammation in TNNI3K^{tg} from days 6 to 8 post infection ($P<0.0001$). H&E stained sections were performed twice Day 8 once using cryosections as part of EBD image analysis, and a second time with paraffin embedded formaline fixed sections shown in (b). Data are shown as mean +/- standard error for at least N=7 mice per time point per group. Results were comparable by both embedding techniques but only the formaline fixed sections are shown in this figure. (b) Top: Representative sections showing intense necrosis, with large and diffuse leukocyte infiltration foci in TNNI3K^{tg} mice. DBA2/J mice have low to moderate focal myocarditis. Bottom: identically digitally magnified regions of inflammation are shown with arrows indicating corresponding region of original unmagnified image.

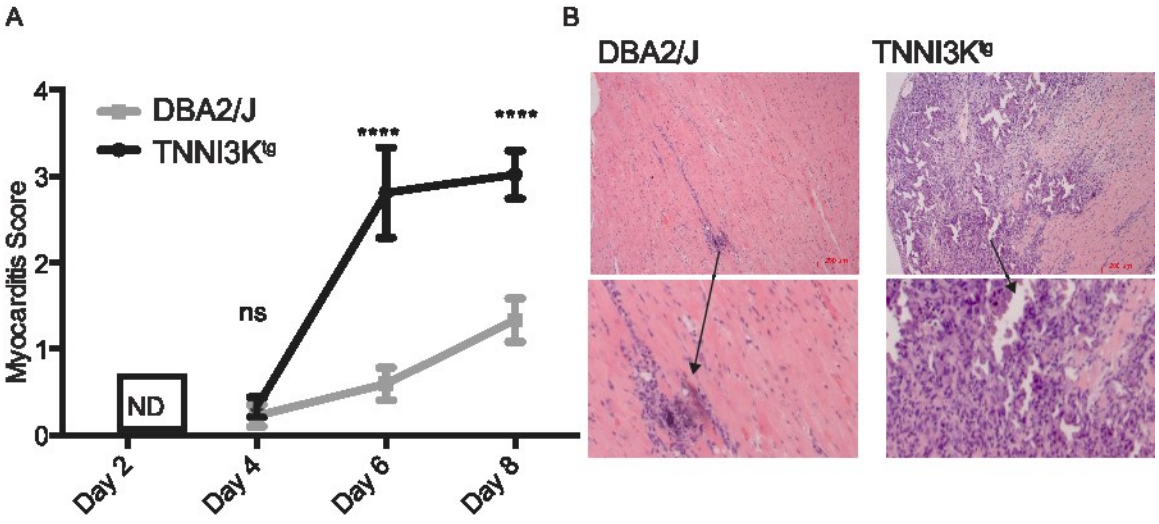
A
B
DBA2/J
TNNI3K^tg
Myocarditis Score
4
3
2
1
0
ND
ns
****
****
Day 2
Day 4
Day 6
Day 8
DBA2/J
TNNI3K^tg

FIGURE 4: INTERFERON RESPONSE COMMON BETWEEN TNNI3K^{TG} AND DBA2/J HEARTS FOLLOWING INFECTION

The core response program of genes highly (but not necessarily differentially) responding to CVB3 infection in TNNI3K^{tg} and DBA2/J hearts 4 days post-infection. All genes with fold changes of at least 1.65-fold (increase or decrease) in both TNNI3K^{tg} and DBA2/J mice (106 probes corresponding to 71 genes) were included. (b) Interferon sub-type analysis showing 48 of 71 genes identified as either responsive to Type-I or Type-II interferon by Interferome (357).

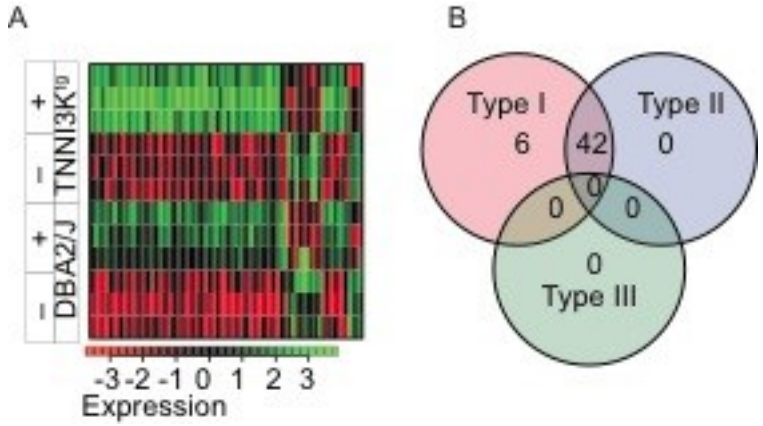
A
+
-
+
-
TNNI3K^19
DBA2/J
-3 -2 -1 0 1 2 3
Expression
B
Type I
6
42
Type II
0
0
0
0
0
Type III

FIGURE 5: UPSTREAM ANALYSIS INDICATIVE OF RESPONSE TO TNFA, IFNɣ AND NF-κB

Microarray fold changes of genes identified to be preferentially upregulated for TNNI3Ktg mice 4 days post-infection were further subsetted using IPA upstream analysis tool for the top 3 biologically relevant pathways: response to TNFA, IFNɣ and IKK2/NF-κB stimulus.

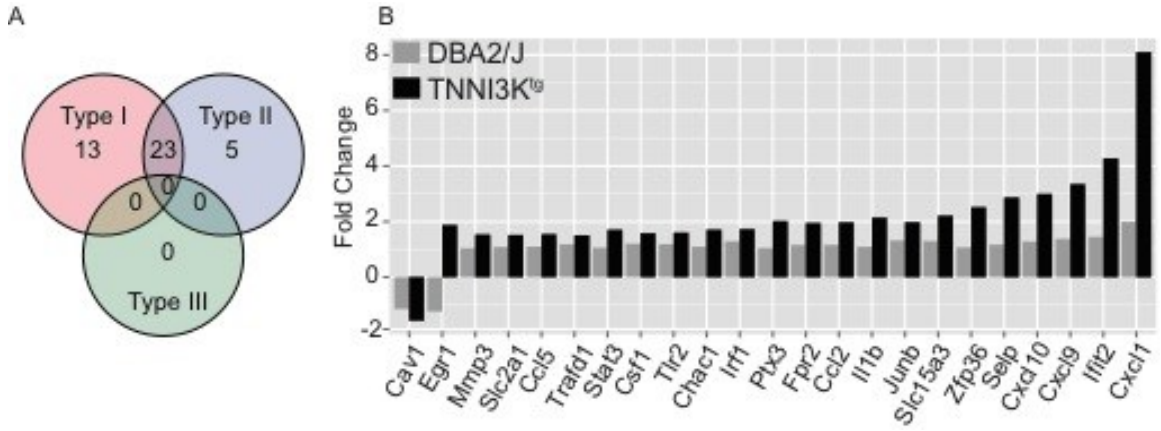
A
Type I
13
Type II
5
Type III
23
0
0
0
0
B
DBA2/J
TNNI3K^tg
Fold Change
8
6
4
2
0
-2
Cav1
Egr1
Mmp3
Slc2a1
Ccl5
Trafd1
Stat3
Csf1
Tlr2
Chac1
Irf1
Ptx3
Fpr2
Ccl2
Il1b
Junb
Slc15a3
Zfp36
Selp
Cxcl10
Cxcl9
Ifit2
Cxcl1

FIGURE 6: DIFFERENTIAL EXPRESSION OF CYTOKINES AND ADHESION MOLECULES

Quantitative RT-PCR (qPCR) comparing mRNA levels for differentially regulated genes in TNNI3Ktg and DBA2/J hearts at 2, 4,6 and 8 days post CVB3 infection. Normalized gene expression data are shown as mean +/- standard error for at least N=5 mice per mice per time point per group.

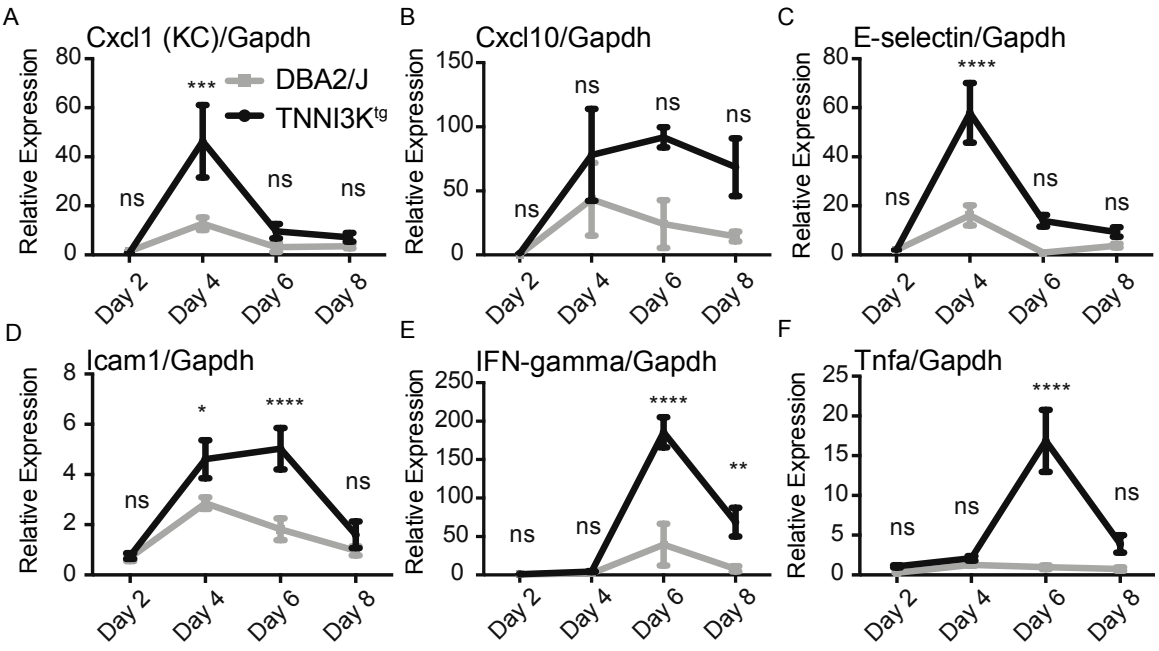
A
Cxcl1 (KC)/Gapdh
DBA2/J
TNNI3K^tg
Relative Expression
B
Cxcl10/Gapdh
C
E-selectin/Gapdh
D
Icam1/Gapdh
E
IFN-gamma/Gapdh
F
Tnfa/Gapdh
Day 2
Day 4
Day 6
Day 8
ns
*
**
***
****

FIGURE 7: DIFFERENTIAL EXPRESSION OF CYTOKINES AND ADHESION MOLECULES

Quantitative RT-PCR (qPCR) comparing CVB3 mRNA levels in primary cardiomyocytes isolated from TNNI3Ktg and DBA2/J hearts, and infected in vitro. Normalized gene expression data are shown as mean +/- standard deviation for at least N=5 mice per mice per time point per group.

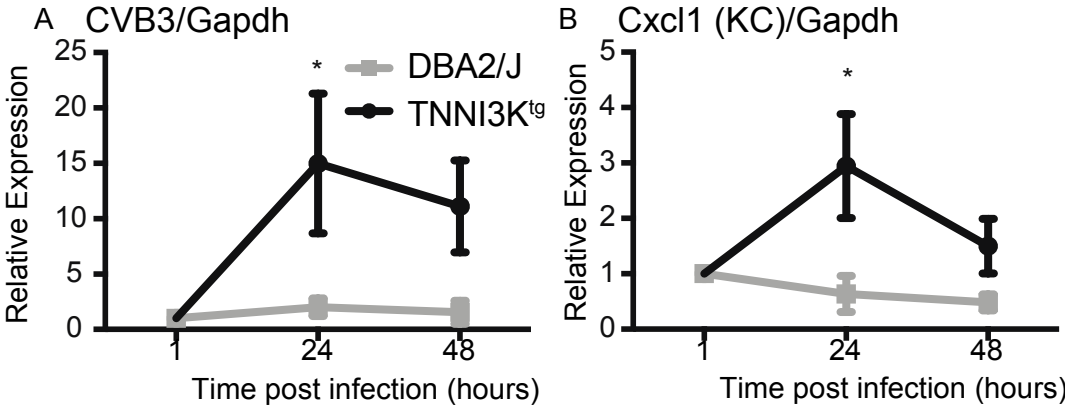
A
CVB3/Gapdh
Relative Expression
25
20
15
10
5
0
*
DBA2/J
TNNI3K^tg
1
24
48
Time post infection (hours)
B
Cxcl1 (KC)/Gapdh
Relative Expression
5
4
3
2
1
0
*
1
24
48
Time post infection (hours)

SUPPLEMENTAL FIGURE 1:

Viral replication at day 8 by plaque assay. Viral replication difference is significant by two-tailed T-test (P=0.0334).

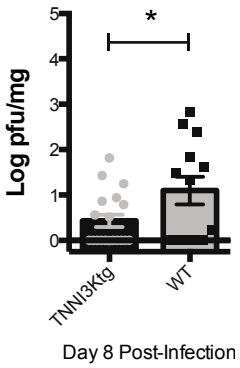

SUPPLEMENTAL FIGURE 2:

H&E staining in the Myocardium in uninfected animals showing no clear differences.

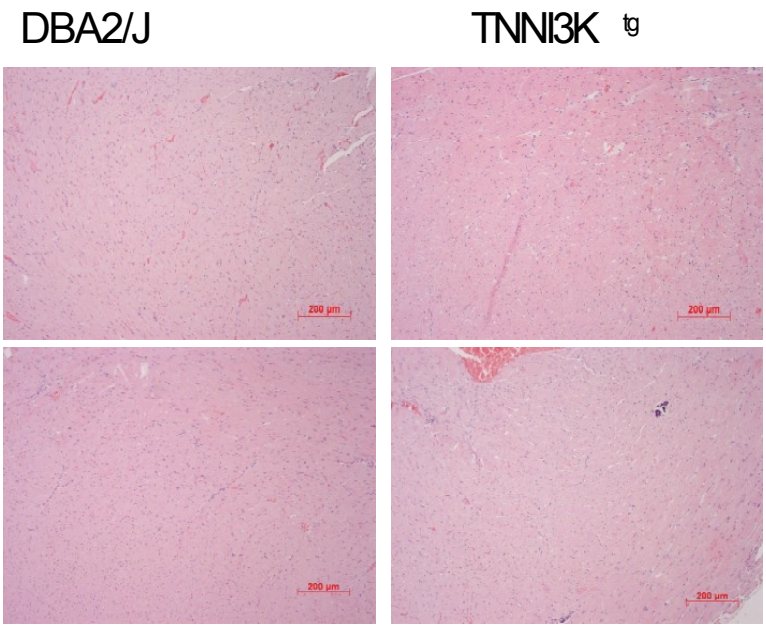

SUPPLEMENTAL FIGURE 3:

Interferon ß expression after infection, no significant differences between strains at any time point.

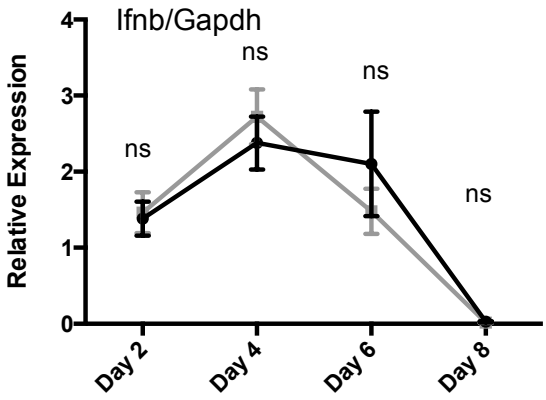

CONCLUSIONS AND GENERAL DISCUSSION

Coxsackievirus B (CVB) is an enterovirus, which spreads in mid to late summer. CVB infection is very common with estimates ranging between 9% of individuals up to 70% of individuals possessing serological evidence of previous exposure. Severe infection is less common though up to 5% of reported cases of CVB infection are fatal, suggesting that the majority of infections go unreported. Severe infections can result in fatal meningitis, pancreatitis, hepatitis or myocarditis (30, 31, 33-35, 43, 44). Multiple mechanisms have been proposed to account for differential virulence between infected hosts: differential virulence between individual isolates of CVB, genetically determined differential response of the host to infection, environmental factors in the context of infection, or simply bad luck. Which of these factors controls the severity and specific pathogenesis of any given CVB infection? After over 65 years of research on CVB infections (8), we can definitively say all of the above.

Bad luck: As an enterovirus, CVB replicates its genome as a quasi-species. Each replication produces on average, one base pair substitution. In other enterovirus species such as poliovirus, this diversity has been shown to be a key determinant of virulence. Genomic diversity and quasi-species repertoire are required for access within specific tissues, and lethality of infection (74-81). That quasi-species diversity, or that generation of virulent sub-strains of coxsackievirus within a single infection, lead to severe outcomes has yet to be formally demonstrated. However, even within a controlled environment, the inter-individual variability of phenotypic responses is considerable. This variability is high within a single experiment, under identical housing conditions, at identical ages, on identical diets, within a single genetically defined inbred mouse strain, even when starting with a clonal isolate of CVB (see chapter 2, Figure 1, and figure 2A, 2B from (135)). Though the quasi-species nature of CVB3 may be one mechanism to generate this variability, others surely exist. Similar intrastrain variability is also evident during experimental autoimmune myocarditis (see figure 1A, 1B from (133)), demonstrating that high variability in myocarditis phenotypes is not solely dependent on coxsackieviral infection. Stochastic phenomena beyond host and viral

genotype clearly play a substantial role in determining the course of pathogenesis during CVB3 infection and myocarditis.

Environment: The seasonal nature of coxsackievirus outbreaks is intriguing. What is it about late summer that leads to the epidemic spread of coxsackievirus? The virus is quite stable and resistant to inactivation (382). The mechanisms here are unknown, but the phenomenon of “summer grippe” or coxsackievirus infection has been reported since at least 1911(383). Perhaps enteroviruses are spread effectively in swimming water? It might also be possible that coxsackievirus infection is actually endemic within the population, but severity varies seasonally. Seasonal monitoring of immunoglobulin levels could be measured to ascertain whether recency of infection in the population as a whole coincides with late summer epidemics.

Keshan disease is a congestive form of cardiomyopathy that has been recognized in regions where soil is deficient in Selenium. Consuming selenium deficient grain leads to Selenium deficient individuals and this combined with coxsackievirus infection leads to cardiomyopathy. Coxsackievirus within selenium deficient infected mice is rapidly selected for cardiovirulence, indicating that host Selenium sufficiency is crucial in determining pathogenesis (384). Caloric intake has also been shown to clearly modify virulence, but again the precise mechanisms governing this phenomenon in CVB infection are unclear (17, 191). In our own studies, following a transfer between two facilities we noticed a profound shift of susceptibility between genetically defined strains. In an attempt to follow up on this effect, we have investigated the role of diet, and found a clear and reproducible effect of diet on multiple aspects of CVB3 pathogenesis. The mechanism of these effects will be more fully characterized in a future publication.

Viral factors: Original isolates of coxsackievirus were characterized based on their capacity to induce neurological symptoms: meningitis and flaccid or shaking paralysis. Intracerebral passage of the virus created isolates that would reproducibly induce these symptoms. Other isolates including the commonly used Woodruff lineage CVB3 isolates (M, W, NR, CG, H3 etc…) have been prepared by passaging virus from the heart (21). In both cases, internal pathologies caused by the virus are a probably a sideshow to its natural life cycle. The virus passes from person to person via a fecal oral route, so

replication within brain or heart is unlikely to lead to reproduction. Conversely, viral RNA persistence in the heart has been described experimentally, and observed in humans. Perhaps long term persistence within long-lived and quiescent cells such as the cardiomyocyte or neuron is a mechanism for establishing latency? If so, reactivation and passage of reactivated virus into the stool will still need to be demonstrated.

Virally genetically controlled mechanisms of cardiovirulence have been elucidated including mutation in the VP2 region (21, 22). Other mutations within the 5' untranslated region (UTR) of the CVB3 genome have also been shown to modulate virulence (23, 24, 385). Between highly related strains virulence is clearly variable between specific isolates. In our own studies, myocarditic strains (CVB3-CG and CVB3-H3) produced equivalent effects in inbred strains (CSS3 and C57BL/6)(188). To achieve this experimental outcome 400pfu/g (≈8000PFU) of CVB3-CG was required, but only 10pfu/g (≈200PFU) of CVB3-H3 was required. Working stocks of both viruses were prepared in HeLa cells, quantified in several aliquots across several plaque forming assays, and diluted in the same PBS prior to infection. Clearly some feature of the viral genome within these two isolates influences the ability of each virus to establish cardiovirulent infection (135, 188).

Host genetics: Surveys of genetically defined inbred strains have demonstrated a clear role for mouse background strain in determining susceptibility to infection (20). Specific genomic regions such as the major histocompatibility complex (*H2*) were able to modulate susceptibility within a single background. Comparison between different genetic backgrounds carrying the same *H2* allele revealed that while *H2* modulated disease severity, it did not account for most of interstrain differences observed (26, 118). In addition to *H2*, genetic mapping techniques used to study these innate differences have so far identified several genomic regions controlling susceptibility to viral myocarditis and related phenotypes: One gene (*Abcc6*) on chromosome 7 controls dystrophic calcification and necrosis (130-132); 3 QTL on chromosomes 1, 4 and 6 control experimental autoimmune myocarditis (133, 134, 369); 3 QTL control viral myocarditis on chromosomes 1, 3 and 4 (135); and 2 non-*H2* QTL on proximal chromosome 17 control viral autoimmune myocarditis on chromosome 17 (145). The

Eam and *Vms* QTL on chromosomes 1 and 4 were linked to non-overlapping regions, therefore to date at least 10 distinct genomic regions have been identified to contribute significantly to myocarditis and associated phenotypes.

Following screening the BcA/AcB recombinant congenic panel, we found that most strains were susceptible to lethal CVB3 infection. This was initially surprising, but this is actually in keeping with other complex traits, which have been determined to be highly polygenic and subject to pervasive epistasis (386). In a study of 90 phenotypic traits across CSS panels and within individual CSS mice, it was found that QTL often have larger effect sizes than expected. If each QTL contributed additively to the end phenotype, one would expect the sum of QTL effects to equal interstrain differences (i.e.: Q1 + Q2 +… QN ≤ A-B). What was found was that the average CSS phenotypic effect was actually 76% of the interstrain difference. Further studies determined that non-additive interactions must be a contributory factor. Our study of [B10.AxA/J]F_2 identified 8 suggestively or significantly linked regions, and the susceptibility to lethal CVB3 infection in most BcA strains is likely the result of similar phenomena.

The effects of depletion, abrogation or overexpression of specific components of the immune system in the context of coxsackievirus infection are increasingly well described (387). Control of survival during early infection is apparently dependent on a prototypical innate immune sensing circuit. Global gene knockouts for cytosolic RNA sensing MDA5, its cognate adapter MAVS, downstream gene product IFN-ß and its cognate receptor IFNAR1 all lead to early lethality temporally associated with hepatic necrosis and excessive hepatic viral replication (190, 235-237), showing this pathway is non-redundant in the control of early hepatic infection.

We found a phenotype in BcA86 mice reminiscent of a defect in this circuit: hepatic necrosis and early mortality. Linkage analysis identified a region on distal chromosome 13 that controlled some of this difference with numerous attractive candidate genes. Linkage to a background (non-A/J) segment of the BcA86 genome suggests the possibility of a *de novo* mutation within the BcA86 strain. That F_2 mice homozygous for the BcA86 genotype on distal chromosome 13 do not seem to have any problem

producing IFN-ß transcript suggests the causal mutation may be in one of the many downstream interferon stimulated genes.

Downstream of IFNAR1 signaling, signal transducer and activator of transcription 1 and 2 (STAT1, STAT2) combine with interferon regulatory factor 9 (IRF9) to form ISGF3 to bind interferon stimulated response elements (ISRE) and induce interferon stimulated genes (ISG) (214). At the time of writing, the list of genes which have been identified to be IFN type I stimulated at a fold change of greater than 2 and a p-value less than 0.05 is 1690 in the mouse, and 2156 in humans. Including both IFN-ɣ and IFN-λ increases the sum of ISGs to 2825 and 3747 in humans and mice (357). Recently, an IFNAR1, IFN-ß dependent and STAT1, IFNAR2 independent transcription program has also been described (388). Which of these transcription programs (STAT1 dependent or independent) and which of the approximately 3000 ISG is non-redundant in controlling early viral replication and hepatic necrosis in BcA86 mice is unclear. Located within the 1.5 LOD interval on distal chromosome 13 are 149 protein coding genes, at least 22 of which are ISG.

Consistent with the hypothesis that different type I IFN profiles and ISG contribute to protective responses to CVB, it has been shown that survival of pancreatic islets during CVB4 infection depends on at least two ISG. RNase L was found to be essential for *in vitro* survival of infection of cells that were stimulated with interferon-α, while PKR was required for survival in cells stimulated with IFN-ɣ. Unstimulated RNaseL and PKR global knockouts were highly susceptible to CVB4 infection *in vitro* and *in vivo* (389). Host genomes evolve mechanisms to limit viral replication, and viral genomes are selected to evade those many ISG effector mechanisms. It is therefore intuitive that a variety of the thousands of ISG will be involved in resisting and resolving viral infections.

Administration of type I IFN or IFN inducing TLR agonists is cardioprotective *in vivo* (273, 390). Moreover, unequivocal evidence that IFN-ß inhibits viral replication in the cardiomyocyte was presented *ex vivo* by treating primary adult cardiomyocytes with IFN-ß prior to infection (247). Nevertheless, whatever protections the type I IFN system may provide, during the course of infection it appears to be functionally redundant. In IFNAR1 and IFN-ß global gene knockouts no significant effect on viral replication or

inflammation in the heart was observed (190, 237). So which features of the host response to CVB3 infection are non-redundant, and which if any are intrinsic to the cardiomyocyte?

Sensing of CVB3 infection by TLR3 mediated mechanisms clearly plays a role. Absence of TLR3 during CVB3 infection leads to enhanced viral replication within the heart, delayed clearance of virus from the heart, and death. Lethal infection is associated with myocarditis, but not hepatitis in TLR3 knockout mice, and gene expression profiling indicate that an IL-12 and IFN-ɣ cytokine response is different in TLR3 mice(240). TLR3 itself does appear to be expressed within cardiomyocytes and the HL-1 cardiomyocyte-like cell line. However following the administration of a variety of ligands to the different toll-like receptors to HL-1 cells in vitro, only ligands to TLR2, TLR4 and TLR5 were able to induce an NF-κB response as measured by expression of IL-6, KC, and MIP2. Unfortunately, induction of IFN-γ was not measured so cardiac specific recognition of viral pathogen associated molecular pattern by TLR3 cannot be ruled out (391). Nonetheless, transfer of wild-type macrophages into TLR3 deficient mice reverted most of the effects of TLR3 deficiency suggesting that TLR3 recognition of dsRNA is cardiomyocyte independent (241).

Since TLR4 signals strongly activate NF-κB responses within the cardiomyocyte (391), it is interesting to closely examine the effects of TLR4 deficiency on the cardiomyocyte. TLR4 global knockout leads to very early increases of cardiac viral replication (day 2), long before infiltrating inflammation makes an appearance suggesting this is a cardiomyocyte intrinsic response. TLR4 deficiency also leads to decreased viral replication and inflammation at later time points in association with diminished IL-1ß and IL-18, indicating TLR4 recognition plays distinct roles during early and late infection (242). TLR4 uses two adaptors for signalling; MYD88 and TRIF, and these appear to play opposing roles in the cardiomyocyte response to CVB3 infection. MYD88 is clearly pathogenic: MYD88 deficiency leads to increased survival, decreased inflammation and, decreased viral replication at early time points (earliest measured is day 4) following CVB3 infection. TRIF is clearly protective: TRIF deletion leads to decreased survival, increased inflammation, and increased viral replication at very early time points (24

hours post infection). The study of TRIF in cardiomyocyte infection further demonstrated that this effect was cardiomyocyte intrinsic: viral replication in TRIF deficient embryonic primary cardiomyocytes was increased (243, 244). The importance of TRIF is underscored by viral $3C^{pro}$ targeting of TRIF for cleavage (238). Cardiomyocyte specific overexpression of SOCS1 and SOCS3 recapitulate aspects of this phenotype: enhanced inflammation and necrosis in the heart (247, 248). TLR4 expression in non-leukocytes has been reported to be strictly intracellular, namely within the Golgi complex (392), though its distribution within adult cardiomyocytes has not been demonstrated. What TLR4 is responding to during a CVB3 infection also remains to be demonstrated, as CVB3 infection does not produce the canonical TLR4 ligand: bacterial lipopolysaccharide (LPS). Many endogenous ligands have been proposed, though these remain controversial (199). Taken together, these studies indicate that at least one innate pathway within the cardiomyocyte, consisting of TLR4, signalling through TRIF under regulation of SOCS1 and SOCS3 controls myocarditis. What TLR4 is recognizing, and whether this is occurring at the surface of the cardiomyocyte or within, is very much an open question.

Non-redundant mechanisms of resistance outside of the cardiomyocyte have also been described. Getting back to TLR3, TLR3 sufficiency within the macrophage compartment was essential for protective production of IL-12 and IFN-ɣ, and global TLR3 overexpression was protective during infection(240, 241). Other IFN-ɣ producing cells non-redundant for control of early CVB3 replication include the NK cells. Depletion of NK cells greatly increases viral replication in the heart at early time points(19). NK cell activation by virally infected cells, and not uninfected cells implies specific recognition or cytokine activation (257). Abrogation of NK-inhibitory signal in the form of MHC class I surface expression potently reduced viral replication in the heart as well(258). Natural killer cells are clearly important for control of CVB3 infection, but how? Activated NK cell effector mechanisms include production of cytolytic granules, production of cytokines including IFN-ɣ, and direct killing by triggering TRAIL and FASL death receptors on infected cells (250). Other enzymes are contained within NK cytolytic granules, however the pore forming component perforin is apparently dispensable for control of viral replication in coxsackievirus infection (260). FAS and FASL deficient mice also show no

significant exaggeration of viral replication following CVB3 infection (393) and TRAIL mediated killing remains to be studied. Studies on TNF in CVB infection are limited, however in EMCV induced viral myocarditis, TNF-α deficient mice were less able to survive infection, and EMCV RNA was significantly higher than in wild type mice, though this was accompanied by less inflammation. Serum TNF-α peaked between 12 and 48 hours post infection (394). Whether IFN-ɣ itself is protective, or activates some other protective response is unclear. Pancreatic expression of IFN-ɣ was sufficient to lower viral replication of CVB4 systemically (262). IFN-ɣ itself has been demonstrated to induce cardiomyocytes to express the chemokine IP10. IP10 is chemotactic for cells expressing its receptor CXCR3 such as NK cells. By creating a kind of allelic series with IP10 knockouts, wild-type mice and transgenic overexpression, it was demonstrated that IP10 decreases viral replication by increasing recruitment of NK cells to the heart. Though interpretation of these results was complicated by having high or deficient IP10 expression on different mouse genetic backgrounds (259). A possible mechanism for cardiomyocyte protection by infiltrating NK cells producing high levels of IFN-ɣ is the induction of nitric oxide, which appears to be reproducibly, and highly protective (365, 395-397). Mechanistically, this may occur through inhibition of viral RNA synthesis, protein translation(398) and inactivation of viral proteins(276). The mechanism of recognition, and killing or control of viral replication by NK cells remains unclear, but their involvement seems to contribute to control of early replication, probably through perforin independent mechanisms.

Our results in the [B10.A/A/J]F_2 and [CSS3xB6]F_2 fit into this model as follows. A locus on distal chromosome 3 was identified, which contributes modestly to early control of viral replication, as well as to later control of viral replication, sarcolemmal necrosis and myocarditis. Candidate gene analysis and refined mapping identified three genes in particular which might underlie the *Vms1* phenotype: *H28*, *Tnni3k* and *Fpgt.*

H28, also known as interferon induced 44-like (IFI44L) is expressed in the *Vms1*^{s} genotype following infection but not in *Vms1*^{r}. *H28* has no known function and has only been previously described as being presented during allograft rejection between BALB.B (*H2*^{b}) and B6 mice. *H28* is an ISG, and has been demonstrated in vitro to

exhibit anti-viral activity towards several viruses including hepatitics C virus (HCV), yellow fever virus (YFV), Venezuelan equine encephalitis virus (VEEV), and West Nile virus (WNV); all of which are + stranded RNA viruses. During HCV infection IFI44L appears to inhibit protein translation, and act synergistically with other ISG proteins to inhibit viral replication(222). The closely related and nearby gene IFI44 from which IFI44L gets is name has been shown to bind and possibly tie up cellular pools of GTP(399). IFI44L activity might act in concert with other ISG to inhibit CVB3 infection.

No expression differences were noted in the *Fpgt* gene, however a coding non-synonymous SNP predicted to be damaging was present within the protein. FPGT catalyzes the formation of the fucosyl donor GDP-ß-fucose, as part of the fucose salvage pathway(345). L-fucose is a sugar present in glycoproteins involved in inflammation and immunity, e.g. sialyl-lewis X, the inflammatory ligand of selectins, contains L-fucose. Moreover, CVB3 infection alters the presence of fucosylated proteins at the cell surface (400), and this surface difference was proposed as a possible mechanism for NK cell recognition of CVB3 infected cells (257).

Finally TNNI3K, the best understood of our three candidate genes and the one we decided to pursue for further studies (349, 350, 353, 401). Several features of TNNI3K made it an attractive candidate for study. 1) TNNI3K appears to become activated and mediate effects during cardiac stress. 2) The localization of TNNI3K either in the Z-disc, or within the nucleus is a strong sign that TNNI3K connects cardiomyocyte functional state with downstream gene expression. 3) TNNI3K's reported increase of cellular reactive oxygen species reminded us the role of reactive (and antiviral) nitric oxide.

By studying an overexpressor of TNNI3K we expected an exaggerated phenotype, and we were not disappointed. TNNI3K overexpression leads to mild to moderate increases in viral replication at the cardiomyocyte level, and early on during infection. Though virus is cleared more effectively at late time points. This curious inversion of control of viral replication result has also been described for TLR4 deficient mice (242). TNNI3K leads to greatly increased sarcolemmal necrosis, and inflammation. Microarray analysis of TNNI3K hearts strongly suggests upstream NF-κB activity, and *ex vivo* infection of primary cardiomyocytes supported this.

TNNI3K dependent increases in NF-κB activity could account for the *Vms1* phenotypes observed. In a normal wild-type cell, under stressful conditions TNNI3K is phosphorylated, and initiates a signalling cascade which includes at least p38. This could amplify signalling through the TLR4-TRIF circuit as described above, leading to cardiomyocyte cytokine and chemokine expression such as TNF, KC. The heart is known as a TNF-α producing organ under stress conditions(359), and this occurs at least partially in a p38 dependent manner(360). This would lead to modestly increased expression of adhesion molecules, increasing infiltrating cells, and possibly inducing directly antiviral proteins. The activity of p38 in infected cells, would also favour cellular necrosis over apoptosis, releasing more viral particles (108, 278), but also more replicative intermediate dsRNA. Infiltrating macrophages expressing functional TLR3(240, 241, 372) could sense this dsRNA and begin an IL-12, STAT4, IFN-ɣ cascade (261). Macrophage IFN-ɣ on cardiomyocytes would induce expression of the NK cell attracting CXCL10 (259). NK cells arriving which would sense infected cells more directly, and kill cells either directly, by producing bursts of IFN-ɣ, and TNF-α, which induce both apoptosis (reversing the p38 pro-necrosis cell death phenotype), and nitric oxide production. This persists until infection can be cleared either by antibody mediated inhibition of new infection, or apoptotic killing of all infected cells. The proposed innate system is non-redundant because coxsackieviruses are very poor inducers of MHC class I dependent cellular immunity *in vivo*, CVB3 almost completely abrogates class I presentation (402).

In the context of TNNI3K overexpression, the proposed cascade begins similarly but somehow over-signals through the p38 and NF-κB pathways. Besides its role in promoting inflammation, NF-κB is a survival pathway, and keeps cells viable. *In vitro* experiments in the context of CVB3 infection have shown NF-κB activity is required to maintain cells alive long enough to replicate and inhibition of NF-κB blocks viral replication. If TNNI3K is upstream of NF-κB, then overexpression could ensure viral replication, this is consistent with our *ex vivo* observation of increased KC and CVB3 RNA in TNNI3K^{tg} cardiomyocytes. The reported TNNI3K induction of p38 map kinase signalling leading to increased cardiac superoxide levels, and necrosis(349) is consistent with enhanced viral replication and increased necrosis observed *in vivo* (108,

278). Inflammation responding to the resultant necrosis and overabundance of pathogen and damage associated molecular patterns (PAMPs and DAMPs) would be as severe as observed in CVB3 infected TNNI3K^{tg}. The effector mechanisms, whatever they might be are still functional within TNNI3K^{tg} mice, and so the infection is cleared with the heart sustaining heavy damage in the process.

This thesis was begun with the goal of further determining host genetic contributions to CVB3 between genetically inbred strains. We were also interested in whether we would be able to learn about host determinants of tissue specific pathology. Finally, we sought to provide insight on whether severe viral myocarditis was a result of unequal host immune responses to roughly equivalent infection, or if unequal control of control viral replication precedes unequal inflammation between strains.

We have learned that CVB3 myocarditis is genetically highly complex, and like other complex traits interstrain variation is accounted for by several non-overlapping loci. We have learned that a locus on chromosome 13 controls liver damage following CVB3 infection. We have learned that distal chromosome 3 controls inflammation, necrosis and viral replication following CVB3 infection. We have learned that in a *Vms1* context, heightened viral replication precedes cellular infiltration. In the TNNI3K model we also learned that unequal control of inflammation and unequal control of viral replication are more entangled than we initially suspected.

We are entering a phase of CVB3 research reminiscent of the pre-Gauntt era where Woodruff reported that strain of virus and host were both important but the latter has seen only little attention(15). In multiple laboratories, individual strains of mouse were being infected with individual viral isolates, and different phenotypic outcomes were reported. Like the Buddhist parable of blind monks and an elephant, this made cross comparison difficult.

Today, we face a similar problem (see table 1 in (387)), many genes, pathways or chemicals are being manipulated in several strains of mouse and then being infected with various strains of virus. Many have provided specific insight, but integration and synthesis is rendered tenuous when we know that different host, and virus combinations

produce non-linear results (26). Systems approaches such as genome wide RNA silencing of host genes (58), or applied predictive modeling on cell signaling (108) hold much promise. However if history is any guide, we will at some point require large *in vivo* screens interrogating multiple pathways with multiple viral isolates to learn the answers to our initial questions.

REFERENCES

1. Solomon T, Lewthwaite P, Perera D, Cardosa MJ, McMinn P, Ooi MH. Virology, epidemiology, pathogenesis, and control of enterovirus 71. Lancet Infect Dis. 2010;10(11):778-90.

2. Ooi MH, Wong SC, Lewthwaite P, Cardosa MJ, Solomon T. Clinical features, diagnosis, and management of enterovirus 71. Lancet Neurol. 2010;9(11):1097-105.

3. Xu W, Liu CF, Yan L, Li JJ, Wang LJ, Qi Y, et al. Distribution of enteroviruses in hospitalized children with hand, foot and mouth disease and relationship between pathogens and nervous system complications. Virol J. 2012;9:8.

4. Zhu FC, Liang ZL, Li XL, Ge HM, Meng FY, Mao QY, et al. Immunogenicity and safety of an enterovirus 71 vaccine in healthy Chinese children and infants: a randomised, double-blind, placebo-controlled phase 2 clinical trial. Lancet. 2013;381(9871):1037-45.

5. Li YP, Liang ZL, Gao Q, Huang LR, Mao QY, Wen SQ, et al. Safety and immunogenicity of a novel human Enterovirus 71 (EV71) vaccine: a randomized, placebo-controlled, double-blind, Phase I clinical trial. Vaccine. 2012;30(22):3295-303.

6. Chang JY, Chang CP, Tsai HH, Lee CD, Lian WC, Ih Jen S, et al. Selection and characterization of vaccine strain for Enterovirus 71 vaccine development. Vaccine. 2012;30(4):703-11.

7. Dalldorf, Sickles. An Unidentified, Filtrable Agent Isolated From the Feces of Children With Paralysis. Science (New York, NY). 1948;108(2794):61-2.

8. Melnick JL, Shaw EW, Curnen EC. A virus isolated from patients diagnosed as non-paralytic poliomyelitis or aseptic meningitis. Proceedings of the Society for Experimental Biology and Medicine Society for Experimental Biology and Medicine. 1949;71(3):344-9.

9. Dalldorf G. The Coxsackie viruses. Bulletin of the New York Academy of Medicine. 1950;26(5):329-35.

10. Melnick JL. The poliomyelitis, encephalomyocarditis, and coxsackie groups of viruses. Bacteriol Rev. 1950;14(3):233-44.

11. Shaw EW, Melnick JL, Curnen EC. Infection of laboratory workers with coxsackie viruses. Annals of internal medicine. 1950;33(1):32-40.

12. Melnick JL, LEDINKO N. Immunological reactions of the Coxsackie viruses. I. The neutralization test; technic and application. The Journal of experimental medicine. 1950;92(5):463-82.

13. Melnick JL, Godman GC. Pathogenesis of coxsackie virus infection; multiplication of virus and evolution of the muscle lesion in mice. J Exp Med. 1951;93(3):247-66.

14. Fechner RE, Smith MG, Middlekamp JN. Coxsackie B virus infection of the newborn. Am J Pathol. 1963;42:493-505.

15. Woodruff JF. Viral myocarditis. A review. Am J Pathol. 1980;101(2):425-84.

16. Woodruff JF, Kilbourne ED. The influence of quantitated post-weaning undernutrition on coxsackievirus B3 infection of adult mice. I. Viral persistence and increased severity of lesions. J Infect Dis. 1970;121(2):137-63.

17. Woodruff JF. The influence of quantitated post-weaning undernutrition on coxsackievirus B3 infection of adult mice. II. Alteration of host defense mechanisms. The Journal of infectious diseases. 1970;121(2):164-81.

18. Woodruff JF. Lack of correlation between neutralizing antibody production and suppression of coxsackievirus B-3 replication in target organs: evidence for involvement of mononuclear inflammatory cells in host defense. Journal of immunology (Baltimore, Md : 1950). 1979;123(1):31-6.

19. Godeny E, Gauntt C. Involvement of natural killer cells in coxsackievirus B3-induced murine myocarditis. Journal of immunology (Baltimore, Md : 1950). 1986;137(5):1695-702.

20. Gauntt C, Gomez P, Duffey P, Grant J, Trent D, Witherspoon S, et al. Characterization and myocarditic capabilities of coxsackievirus B3 variants in selected mouse strains. Journal of virology. 1984;52(2):598-605.

21. Van Houten N, Bouchard P, Moraska A, Huber S. Selection of an attenuated Coxsackievirus B3 variant, using a monoclonal antibody reactive to myocyte antigen. Journal of virology. 1991;65(3):1286-90.

22. Knowlton KU, Jeon ES, Berkley N, Wessely R, Huber S. A mutation in the puff region of VP2 attenuates the myocarditic phenotype of an infectious cDNA of the Woodruff variant of coxsackievirus B3. Journal of virology. 1996;70(11):7811-8.

23. Gauntt CJ, Trousdale MD, LaBadie DR, Paque RE, Nealon T. Properties of coxsackievirus B3 variants which are amyocarditic or myocarditic for mice. J Med Virol. 1979;3(3):207-20.

24. Trousdale MD, Paque RE, Gauntt CJ. Isolation of Coxsackievirus B3 temperture-sensitive mutants and their assignment to complementation groups. Biochem Biophys Res Commun. 1976;76(2):368-75.

25. Herskowitz A, Wolfgram L, Rose NR, Beisel K. Coxsackievirus B3 murine myocarditis: a pathologic spectrum of myocarditis in genetically defined inbred strains. Journal of the American College of Cardiology. 1987;9(6):1311-9.

26. Wolfgram L, Beisel K, Herskowitz A, Rose NR. Variations in the susceptibility to Coxsackievirus B3-induced myocarditis among different strains of mice. Journal of immunology (Baltimore, Md : 1950). 1986;136(5):1846-52.

27. Chow LH, Gauntt CJ, McManus BM. Differential effects of myocarditic variants of Coxsackievirus B3 in inbred mice. A pathologic characterization of heart tissue damage. Lab Invest. 1991;64(1):55-64.

28. Centers for Disease C, Prevention. Nonpolio enterovirus and human parechovirus surveillance --- United States, 2006-2008. MMWR Morbidity and mortality weekly report. 2010;59(48):1577-80.

29. Roth B, Enders M, Arents A, Pfitzner A, Terletskaia-Ladwig E. Epidemiologic aspects and laboratory features of enterovirus infections in Western Germany, 2000-2005. J Med Virol. 2007;79(7):956-62.

30. Khetsuriani N, Lamonte-Fowlkes A, Oberst S, Pallansch MA, Centers for Disease C, Prevention. Enterovirus surveillance--United States, 1970-2005. MMWR Surveill Summ. 2006;55(8):1-20.

31. Tseng FC, Huang HC, Chi CY, Lin TL, Liu CC, Jian JW, et al. Epidemiological survey of enterovirus infections occurring in Taiwan between 2000 and 2005: analysis of sentinel physician surveillance data. J Med Virol. 2007;79(12):1850-60.

32. Chu PY, Ke GM, Chen YS, Lu PL, Chen HL, Lee MS, et al. Molecular epidemiology of Coxsackievirus B3. Infect Genet Evol. 2010;10(6):777-84.

33. Cheng LL, Ng PC, Chan PK, Wong HL, Cheng FW, Tang JW. Probable intrafamilial transmission of coxsackievirus b3 with vertical transmission, severe early-onset neonatal hepatitis, and prolonged viral RNA shedding. Pediatrics. 2006;118(3):e929-33.

34. Tseng F-C, Huang H-C, Chi C-Y, Lin T-L, Liu C-C, Jian J-W, et al. Epidemiological survey of enterovirus infections occurring in Taiwan between 2000 and 2005: analysis of sentinel physician surveillance data. Journal of medical virology. 2007;79(12):1850-60.

35. Wang SM, Liu CC, Yang YJ, Yang HB, Lin CH, Wang JR. Fatal coxsackievirus B infection in early infancy characterized by fulminant hepatitis. The Journal of infection. 1998;37(3):270-3.

36. Tao Z, Song Y, Li Y, Liu Y, Jiang P, Lin X, et al. Coxsackievirus B3, Shandong Province, China, 1990-2010. Emerg Infect Dis. 2012;18(11):1865-7.

37. Cioc AM, Nuovo GJ. Histologic and in situ viral findings in the myocardium in cases of sudden, unexpected death. Modern pathology : an official journal of the United States and Canadian Academy of Pathology, Inc. 2002;15(9):914-22.

38. Gaaloul II, Riabi S, Harrath R, Evans M, H Salem N, Mlayeh S, et al. Sudden unexpected death related to enterovirus myocarditis: histopathology, immunohistochemstry and molecular pathology diagnosis at post-mortem. BMC infectious diseases. 2012;12(1):212.

39. Ward C. Severe arrhythmias in Coxsackievirus B3 myopericarditis. Arch Dis Child. 1978;53(2):174-6.

40. Pauschinger M, Doerner A, Kuehl U, Schwimmbeck P, Poller W, Kandolf R, et al. Enteroviral RNA replication in the myocardium of patients with left ventricular dysfunction and clinically suspected myocarditis. Circulation. 1999;99(7):889-95.

41. Spotnitz MD, Lesch M. Idiopathic dilated cardiomyopathy as a late complication of healed viral (Coxsackie B virus) myocarditis: historical analysis, review of the literature, and a postulated unifying hypothesis. Progress in cardiovascular diseases. 2006;49(1):42-57.

42. Spanakis N, Manolis E, Tsakris A, Tsiodras S, Panagiotopoulos T, Saroglou G, et al. Coxsackievirus B3 sequences in the myocardium of fatal cases in a cluster of acute myocarditis in Greece. J Clin Pathol. 2005;58(4):357-60.

43. Mavrouli MD, Spanakis N, Levidiotou S, Politi C, Alexiou S, Tseliou P, et al. Serologic prevalence of coxsackievirus group B in Greece. Viral Immunol. 2007;20(1):11-8.

44. Gkrania-Klotsas E, Langenberg C, Tauriainen S, Sharp SJ, Luben R, Forouhi NG, et al. The association between prior infection with five serotypes of Coxsackievirus B and incident type 2 diabetes mellitus in the EPIC-Norfolk study. Diabetologia. 2012;55(4):967-70.

45. Bergelson J, Cunningham J, Droguett G, Kurt-Jones E, Krithivas A, Hong J, et al. Isolation of a common receptor for Coxsackie B viruses and adenoviruses 2 and 5. Science (New York, NY). 1997;275(5304):1320-3.

46. Tomko R, Xu R, Philipson L. HCAR and MCAR: the human and mouse cellular receptors for subgroup C adenoviruses and group B coxsackieviruses. Proceedings of the National Academy of Sciences of the United States of America. 1997;94(7):3352-6.

47. Cohen CJ, Shieh JT, Pickles RJ, Okegawa T, Hsieh JT, Bergelson JM. The coxsackievirus and adenovirus receptor is a transmembrane component of the tight junction. Proc Natl Acad Sci U S A. 2001;98(26):15191-6.

48. Chen JW, Zhou B, Yu QC, Shin SJ, Jiao K, Schneider MD, et al. Cardiomyocyte-specific deletion of the coxsackievirus and adenovirus receptor results in hyperplasia of the embryonic left ventricle and abnormalities of sinuatrial valves. Circ Res. 2006;98(7):923-30.

49. Dorner AA, Wegmann F, Butz S, Wolburg-Buchholz K, Wolburg H, Mack A, et al. Coxsackievirus-adenovirus receptor (CAR) is essential for early embryonic cardiac development. J Cell Sci. 2005;118(Pt 15):3509-21.

50. Kashimura T, Kodama M, Hotta Y, Hosoya J, Yoshida K, Ozawa T, et al. Spatiotemporal changes of coxsackievirus and adenovirus receptor in rat hearts during postnatal development and in cultured cardiomyocytes of neonatal rat. Virchows Archiv : an international journal of pathology. 2004;444(3):283-92.

51. Lim B-K, Xiong D, Dorner A, Youn T-J, Yung A, Liu TI, et al. Coxsackievirus and adenovirus receptor (CAR) mediates atrioventricular-node function and connexin 45 localization in the murine heart. The Journal of clinical investigation. 2008;118(8):2758-70.

52. Lisewski U, Shi Y, Wrackmeyer U, Fischer R, Chen C, Schirdewan A, et al. The tight junction protein CAR regulates cardiac conduction and cell-cell communication. J Exp Med. 2008;205(10):2369-79.

53. Martino T, Petric M, Brown M, Aitken K, Gauntt C, Richardson C, et al. Cardiovirulent coxsackieviruses and the decay-accelerating factor (CD55) receptor. Virology. 1998;244(2):302-14.

54. Coyne CB, Bergelson JM. Virus-induced Abl and Fyn kinase signals permit coxsackievirus entry through epithelial tight junctions. Cell. 2006;124(1):119-31.

55. Bergelson JM. Intercellular junctional proteins as receptors and barriers to virus infection and spread. Cell host & microbe. 2009;5(6):517-21.

56. Coyne CB, Shen L, Turner JR, Bergelson JM. Coxsackievirus entry across epithelial tight junctions requires occludin and the small GTPases Rab34 and Rab5. Cell host & microbe. 2007;2(3):181-92.

57. Patel KP, Coyne CB, Bergelson JM. Dynamin- and lipid raft-dependent entry of decay-accelerating factor (DAF)-binding and non-DAF-binding coxsackieviruses into nonpolarized cells. Journal of virology. 2009;83(21):11064-77.

58. Coyne CB, Bozym R, Morosky SA, Hanna SL, Mukherjee A, Tudor M, et al. Comparative RNAi Screening Reveals Host Factors Involved in Enterovirus Infection of Polarized Endothelial Monolayers. Cell host & microbe. 2011;9(1):70-82.

59. Hyypia T, Hovi T, Knowles NJ, Stanway G. Classification of enteroviruses based on molecular and biological properties. J Gen Virol. 1997;78 (Pt 1):1-11.

60. Beales LP, Holzenburg A, Rowlands DJ. Viral internal ribosome entry site structures segregate into two distinct morphologies. J Virol. 2003;77(11):6574-9.

61. Hellen CU, Sarnow P. Internal ribosome entry sites in eukaryotic mRNA molecules. Genes & development. 2001;15(13):1593-612.

62. Whitton JL, Cornell CT, Feuer R. Host and virus determinants of picornavirus pathogenesis and tropism. Nature reviews Microbiology. 2005;3(10):765-76.

63. Levine B, Klionsky DJ. Development by self-digestion: molecular mechanisms and biological functions of autophagy. Dev Cell. 2004;6(4):463-77.

64. Kudchodkar SB, Levine B. Viruses and autophagy. Rev Med Virol. 2009;19(6):359-78.

65. Richards AL, Jackson WT. How positive-strand RNA viruses benefit from autophagosome maturation. J Virol. 2013;87(18):9966-72.

66. Luo H, McManus BM. Is autophagy an avenue to modulate coxsackievirus replication and pathogenesis? Future Microbiol. 2012;7(8):921-4.

67. Wong J, Zhang J, Si X, Gao G, Mao I, McManus BM, et al. Autophagosome supports coxsackievirus B3 replication in host cells. J Virol. 2008;82(18):9143-53.

68. Kemball CC, Alirezaei M, Flynn CT, Wood MR, Harkins S, Kiosses WB, et al. Coxsackievirus infection induces autophagy-like vesicles and megaphagosomes in pancreatic acinar cells in vivo. J Virol. 2010;84(23):12110-24.

69. Alirezaei M, Flynn CT, Wood MR, Whitton JL. Pancreatic acinar cell-specific autophagy disruption reduces coxsackievirus replication and pathogenesis in vivo. Cell host & microbe. 2012;11(3):298-305.

70. Richards AL, Jackson WT. Intracellular vesicle acidification promotes maturation of infectious poliovirus particles. PLoS Pathog. 2012;8(11):e1003046.

71. Hsu NY, Ilnytska O, Belov G, Santiana M, Chen YH, Takvorian PM, et al. Viral Reorganization of the Secretory Pathway Generates Distinct Organelles for RNA Replication. Cell. 2010;141(5):799-811.

72. Sasaki J, Ishikawa K, Arita M, Taniguchi K. ACBD3-mediated recruitment of PI4KB to picornavirus RNA replication sites. Embo J. 2012;31(3):754-66.

73. Ilnytska O, Santiana M, Hsu NY, Du WL, Chen YH, Viktorova EG, et al. Enteroviruses harness the cellular endocytic machinery to remodel the host cell cholesterol landscape for effective viral replication. Cell host & microbe. 2013;14(3):281-93.

74. Malpica JM, Fraile A, Moreno I, Obies CI, Drake JW, García-Arenal F. The rate and character of spontaneous mutation in an RNA virus. Genetics. 2002;162(4):1505-11.

75. Drake JW, Holland JJ. Mutation rates among RNA viruses. Proceedings of the National Academy of Sciences of the United States of America. 1999;96(24):13910-3.

76. Drake JW. Rates of spontaneous mutation among RNA viruses. Proceedings of the National Academy of Sciences of the United States of America. 1993;90(9):4171-5.

77. Codoñer FM, Darós J-A, Solé RV, Elena SF. The fittest versus the flattest: experimental confirmation of the quasispecies effect with subviral pathogens. PLoS pathogens. 2006;2(12):e136.

78. Anderson JP, Daifuku R, Loeb LA. Viral error catastrophe by mutagenic nucleosides. Annual review of microbiology. 2004;58:183-205.

79. Crotty S, Cameron CE, Andino R. RNA virus error catastrophe: direct molecular test by using ribavirin. Proceedings of the National Academy of Sciences of the United States of America. 2001;98(12):6895-900.

80. Vignuzzi M, Wendt E, Andino R. Engineering attenuated virus vaccines by controlling replication fidelity. Nature medicine. 2008;14(2):154-61.

81. Vignuzzi M, Stone JK, Arnold JJ, Cameron CE, Andino R. Quasispecies diversity determines pathogenesis through cooperative interactions in a viral population. Nature. 2006;439(7074):344-8.

82. Eigen M. Error catastrophe and antiviral strategy. Proceedings of the National Academy of Sciences of the United States of America. 2002;99(21):13374-6.

83. Etchison D, Milburn SC, Edery I, Sonenberg N, Hershey JWB. Inhibition of Hela-Cell Protein-Synthesis Following Poliovirus Infection Correlates with the Proteolysis of a 220,000-Dalton Polypeptide Associated with Eukaryotic Initiation Factor-Iii and a Cap Binding-Protein Complex. Journal of Biological Chemistry. 1982;257(24):4806-10.

84. Belsham GJ, Sonenberg N. RNA-Protein interactions in regulation of picornavirus RNA translation. Microbiol Rev. 1996;60(3):499-&.

85. Carthy CM, Granville DJ, Watson KA, Anderson DR, Wilson JE, Yang D, et al. Caspase activation and specific cleavage of substrates after coxsackievirus B3-induced cytopathic effect in HeLa cells. J Virol. 1998;72(9):7669-75.

86. Joachims M, Van Breugel PC, Lloyd RE. Cleavage of poly(A)-binding protein by enterovirus proteases concurrent with inhibition of translation in vitro. Journal of Virology. 1999;73(1):718-27.

87. Kuyumcu-Martinez NM, Joachims M, Lloyd RE. Efficient cleavage of ribosome-associated poly(A)-binding protein by enterovirus 3C protease. Journal of Virology. 2002;76(5):2062-74.

88. Bonderoff JM, Larey JL, Lloyd RE. Cleavage of poly(A)-binding protein by poliovirus 3C proteinase inhibits viral internal ribosome entry site-mediated translation. Journal of Virology. 2008;82(19):9389-99.

89. Weidman MK, Sharma R, Raychaudhuri S, Kundu P, Tsai W, Dasgupta A. The interaction of cytoplasmic RNA viruses with the nucleus. Virus Research. 2003;95(1-2):75-85.

90. Sharma R, Raychaudhuri S, Dasgupta A. Nuclear entry of poliovirus protease-polymerase precursor 3CD: implications for host cell transcription shut-off. Virology. 2004;320(2):195-205.

91. Clark ME, Lieberman PM, Berk AJ, Dasgupta A. Direct Cleavage of Human Tata-Binding Protein by Poliovirus Protease 3c Invivo and Invitro. Molecular and Cellular Biology. 1993;13(2):1232-7.

92. Yalamanchili P, Datta U, Dasgupta A. Inhibition of host cell transcription by poliovirus: Cleavage of transcription factor CREB by poliovirus-encoded protease 3C(pro). Journal of Virology. 1997;71(2):1220-6.

93. vanKuppeveld FJM, Hoenderop JGJ, Smeets RLL, Willems PHGM, Dijkman HBPM, Galama JMD, et al. Coxsackievirus protein 2B modifies endoplasmic reticulum membrane and plasma membrane permeability and facilitates virus release. Embo J. 1997;16(12):3519-32.

94. VanKuppeveld FJM, Melchers WJG, Kirkegaard K, Doedens JR. Structure-function analysis of coxsackie B3 virus protein 2B. Virology. 1997;227(1):111-8.

95. Agirre A, Barco A, Carrasco L, Nieva JL. Viroporin-mediated membrane permeabilization - Pore formation by nonstructural poliovirus 2B protein. Journal of Biological Chemistry. 2002;277(43):40434-41.

96. de Jong AS, Wessels E, Dijkman HBPM, Galama JMD, Melchers WJG, Willems PHGM, et al. Determinants for membrane association and permeabilization of the coxsackievirus 2B protein and the identification of the Golgi complex as the target organelle. Journal of Biological Chemistry. 2003;278(2):1012-21.

97. Campanella M, de Jong AS, Lanke KWH, Melchers WJG, Willems PHGM, Pinton P, et al. The coxsackievirus 2B protein suppresses apoptotic host cell responses by manipulating intracellular Ca2+ homeostasis. Journal of Biological Chemistry. 2004;279(18):18440-50.

98. Badorff C, Lee G, Lamphear B, Martone M, Campbell K, Rhoads R, et al. Enteroviral protease 2A cleaves dystrophin: evidence of cytoskeletal disruption in an acquired cardiomyopathy. Nature medicine. 1999;5(3):320-6.

99. Davies KE, Nowak KJ. Molecular mechanisms of muscular dystrophies: old and new players. Nature Reviews Molecular Cell Biology. 2006;7(10):762-73.

100. Xiong D, Yajima T, Lim B, Stenbit A, Dublin A, Dalton N, et al. Inducible cardiac-restricted expression of enteroviral protease 2A is sufficient to induce dilated cardiomyopathy. Circulation. 2007;115(1):94-102.

101. Whelan RS, Kaplinskiy V, Kitsis RN. Cell death in the pathogenesis of heart disease: mechanisms and significance. Annu Rev Physiol. 2010;72:19-44.

102. Vanden Berghe T, Vanlangenakker N, Parthoens E, Deckers W, Devos M, Festjens N, et al. Necroptosis, necrosis and secondary necrosis converge on similar cellular disintegration features. Cell Death Differ. 2010;17(6):922-30.

103. Vandenabeele P, Galluzzi L, Vanden Berghe T, Kroemer G. Molecular mechanisms of necroptosis: an ordered cellular explosion. Nature reviews Molecular cell biology. 2010;11(10):700-14.

104. Zhang Q, Raoof M, Chen Y, Sumi Y, Sursal T, Junger W, et al. Circulating mitochondrial DAMPs cause inflammatory responses to injury. Nature. 2010;464(7285):104-7.

105. Yuan JP, Zhao W, Wang HT, Wu KY, Li T, Guo XK, et al. Coxsackievirus B3-induced apoptosis and caspase-3. Cell Res. 2003;13(3):203-9.

106. Chau DH, Yuan J, Zhang H, Cheung P, Lim T, Liu Z, et al. Coxsackievirus B3 proteases 2A and 3C induce apoptotic cell death through mitochondrial injury and cleavage of eIF4GI but not DAP5/p97/NAT1. Apoptosis : an international journal on programmed cell death. 2007;12(3):513-24.

107. Bozym RA, Patel K, White C, Cheung K-H, Bergelson JM, Morosky SA, et al. Calcium signals and calpain-dependent necrosis are essential for release of coxsackievirus B from polarized intestinal epithelial cells. Molecular biology of the cell. 2011;22(17):3010-21.

108. Jensen KJ, Garmaroudi FS, Zhang J, Lin J, Boroomand S, Zhang M, et al. An ERK-p38 Subnetwork Coordinates Host Cell Apoptosis and Necrosis during Coxsackievirus B3 Infection. Cell host & microbe. 2013;13(1):67-76.

109. Tam PE, Messner RP. Molecular mechanisms of coxsackievirus persistence in chronic inflammatory myopathy: viral RNA persists through formation of a double-stranded complex without associated genomic mutations or evolution. J Virol. 1999;73(12):10113-21.

110. Klingel K, Hohenadl C, Canu A, Albrecht M, Seemann M, Mall G, et al. Ongoing enterovirus-induced myocarditis is associated with persistent heart muscle infection: quantitative analysis of virus replication, tissue damage, and inflammation. Proceedings of the National Academy of Sciences of the United States of America. 1992;89(1):314-8.

111. Feuer R, Mena I, Pagarigan R, Slifka MK, Whitton JL. Cell cycle status affects coxsackievirus replication, persistence, and reactivation in vitro. J Virol. 2002;76(9):4430-40.

112. Harrath R, Bourlet T, Delezay O, Douche-Aourik F, Omar S, Aouni M, et al. Coxsackievirus B3 replication and persistence in intestinal cells from mice infected orally and in the human CaCo-2 cell line. J Med Virol. 2004;74(2):283-90.

113. Baboonian C, Treasure T. Meta-analysis of the association of enteroviruses with human heart disease. Heart (British Cardiac Society). 1997;78(6):539-43.

114. Maisch B, Ristic A, Portig I, Pankuweit S. Human viral cardiomyopathy. Front Biosci. 2003;8:s39-67.

115. Kühl U, Pauschinger M, Noutsias M, Seeberg B, Bock T, Lassner D, et al. High prevalence of viral genomes and multiple viral infections in the myocardium of adults with "idiopathic" left ventricular dysfunction. Circulation. 2005;111(7):887-93.

116. Held J. Appropriate animal models. Annals of the New York Academy of Sciences. 1983;406:13-9.

117. Silver LM. Mouse Genetics Concepts and Applications http://www.informatics.jax.org/silver/: Oxford University Press; 1995 [cited 2014].

118. Chow L, Gauntt C, McManus B. Differential effects of myocarditic variants of Coxsackievirus B3 in inbred mice. A pathologic characterization of heart tissue damage. Lab Invest. 1991;64(1):55-64.

119. Leduc MS, Lyons M, Darvishi K, Walsh K, Sheehan S, Amend S, et al. The mouse QTL map helps interpret human genome-wide association studies for HDL cholesterol. Journal of lipid research. 2011;52(6):1139-49.

120. Lander E, Kruglyak L. Genetic dissection of complex traits: guidelines for interpreting and reporting linkage results. Nature genetics. 1995;11(3):241-7.

121. Lander E, Botstein D. Mapping mendelian factors underlying quantitative traits using RFLP linkage maps. Genetics. 1989;121(1):185-99.

122. Stylianou I, Tsaih S, DiPetrillo K, Ishimori N, Li R, Paigen B, et al. Complex genetic architecture revealed by analysis of high-density lipoprotein cholesterol in chromosome substitution strains and F2 crosses. Genetics. 2006;174(2):999-1007.

123. Su Z, Ishimori N, Chen Y, Leiter EH, Churchill GA, Paigen B, et al. Four additional mouse crosses improve the lipid QTL landscape and identify Lipg as a QTL gene. Journal of lipid research. 2009;50(10):2083-94.

124. Wang X, Paigen B. Genetics of variation in HDL cholesterol in humans and mice. Circulation research. 2005;96(1):27-42.

125. Wang X, Ishimori N, Korstanje R, Rollins J, Paigen B. Identifying novel genes for atherosclerosis through mouse-human comparative genetics. Am J Hum Genet. 2005;77(1):1-15.

126. Berghout J, Min-Oo G, Tam M, Gauthier S, Stevenson MM, Gros P. Identification of a novel cerebral malaria susceptibility locus (Berr5) on mouse chromosome 19. Genes and immunity. 2010;11(4):310-8.

127. Boivin GA, Pothlichet J, Skamene E, Brown EG, Loredo-Osti JC, Sladek R, et al. Mapping of clinical and expression quantitative trait loci in a sex-dependent effect of host susceptibility to mouse-adapted influenza H3N2/HK/1/68. Journal of immunology (Baltimore, Md : 1950). 2012;188(8):3949-60.

128. Soller M, Brody T, Genizi A. On the power of experimental designs for the detection of linkage between marker loci and quantitative loci in crosses between inbred lines. TAG Theoretical and applied genetics Theoretische und angewandte Genetik. 1976;47(1):35-9.

129. Broman K, Wu H, Sen S, Churchill G. R/qtl: QTL mapping in experimental crosses. Bioinformatics (Oxford, England). 2003;19(7):889-90.

130. Ivandic BT, Qiao JH, Machleder D, Liao F, Drake TA, Lusis AJ. A locus on chromosome 7 determines myocardial cell necrosis and calcification (dystrophic cardiac calcinosis) in mice. Proc Natl Acad Sci U S A. 1996;93(11):5483-8.

131. Meng H, Vera I, Che N, Wang X, Wang SS, Ingram-Drake L, et al. Identification of Abcc6 as the major causal gene for dystrophic cardiac calcification in mice through integrative genomics. Proc Natl Acad Sci U S A. 2007;104(11):4530-5.

132. Aherrahrou Z, Doehring LC, Ehlers EM, Liptau H, Depping R, Linsel-Nitschke P, et al. An alternative splice variant in Abcc6, the gene causing dystrophic calcification, leads to protein deficiency in C3H/He mice. J Biol Chem. 2008;283(12):7608-15.

133. Guler M, Ligons D, Wang Y, Bianco M, Broman K, Rose NR. Two autoimmune diabetes loci influencing T cell apoptosis control susceptibility to experimental autoimmune myocarditis. Journal of immunology (Baltimore, Md : 1950). 2005;174(4):2167-73.

134. Ligons D, Guler M, Li H, Rose N. A locus on chromosome 1 promotes susceptibility of experimental autoimmune myocarditis and lymphocyte cell death. Clinical immunology (Orlando, Fla). 2008.

135. Aly M, Wiltshire SA, Chahrour G, Osti J-CL, Vidal SM. Complex genetic control of host susceptibility to coxsackievirus B3-induced myocarditis. Genes and immunity. 2007;8(3):193-204.

136. Bailey DW. Recombinant-inbred strains. An aid to finding identity, linkage, and function of histocompatibility and other genes. Transplantation. 1971;11(3):325-7.

137. Demant P, Hart A. Recombinant congenic strains--a new tool for analyzing genetic traits determined by more than one gene. Immunogenetics. 1986;24(6):416-22.

138. Nadeau JH, Singer JB, Matin A, Lander ES. Analysing complex genetic traits with chromosome substitution strains. Nature genetics. 2000;24(3):221-5.

139. Burgess-Herbert S, Cox A, Tsaih S, Paigen B. Practical Applications of the Bioinformatics Toolbox for Narrowing Quantitative Trait Loci. Genetics. 2008.

140. Fortin A, Diez E, Henderson JE, Mogil JS, Gros P, Skamene E. The AcB/BcA recombinant congenic strains of mice: strategies for phenotype dissection, mapping and cloning of quantitative trait genes. Novartis Foundation symposium. 2007;281:141-53; discussion 53-5, 208-9.

141. Li R, Lyons MA, Wittenburg H, Paigen B, Churchill GA. Combining data from multiple inbred line crosses improves the power and resolution of quantitative trait loci mapping. Genetics. 2005;169(3):1699-709.

142. Flint J, Valdar W, Shifman S, Mott R. Strategies for mapping and cloning quantitative trait genes in rodents. Nature reviews Genetics. 2005;6(4):271-86.

143. Traystman MD, Chow LH, McManus BM, Herskowitz A, Nesbitt MN, Beisel KW. Susceptibility to Coxsackievirus B3-induced chronic myocarditis maps near the murine Tcr alpha and Myhc alpha loci on chromosome 14. Am J Pathol. 1991;138(3):721-6.

144. Traystman MD, Beisel KW. Genetic control of Coxsackievirus B3-induced heart-specific autoantibodies associated with chronic myocarditis. Clin Exp Immunol. 1991;86(2):291-8.

145. Poffenberger MC, Shanina I, Aw C, El Wharry N, Straka N, Fang D, et al. Novel nonmajor histocompatibility complex-linked loci from mouse chromosome 17 confer susceptibility to viral-mediated chronic autoimmune myocarditis. Circulation Cardiovascular genetics. 2010;3(5):399-408.

146. Lindenmann J, LANE CA, HOBSON D. THE RESISTANCE OF A2G MICE TO MYXOVIRUSES. Journal of immunology (Baltimore, Md : 1950). 1963;90:942-51.

147. Staeheli P, Pravtcheva D, Lundin LG, Acklin M, Ruddle F, Lindenmann J, et al. Interferon-regulated influenza virus resistance gene Mx is localized on mouse chromosome 16. Journal of virology. 1986;58(3):967-9.

148. Staeheli P, Haller O, Boll W, Lindenmann J, Weissmann C. Mx protein: constitutive expression in 3T3 cells transformed with cloned Mx cDNA confers selective resistance to influenza virus. Cell. 1986;44(1):147-58.

149. Collaborative Cross C. The genome architecture of the Collaborative Cross mouse genetic reference population. Genetics. 2012;190(2):389-401.

150. Aylor DL, Valdar W, Foulds-Mathes W, Buus RJ, Verdugo RA, Baric RS, et al. Genetic analysis of complex traits in the emerging Collaborative Cross. Genome Res. 2011;21(8):1213-22.

151. Churchill GA, Airey DC, Allayee H, Angel JM, Attie AD, Beatty J, et al. The Collaborative Cross, a community resource for the genetic analysis of complex traits. Nat Genet. 2004;36(11):1133-7.

152. Ferris MT, Aylor DL, Bottomly D, Whitmore AC, Aicher LD, Bell TA, et al. Modeling host genetic regulation of influenza pathogenesis in the collaborative cross. PLoS Pathog. 2013;9(2):e1003196.

153. Shusterman A, Salyma Y, Nashef A, Soller M, Wilensky A, Mott R, et al. Genotype is an important determinant factor of host susceptibility to periodontitis in the Collaborative Cross and inbred mouse populations. BMC genetics. 2013;14:68.

154. Shusterman A, Durrant C, Mott R, Polak D, Schaefer A, Weiss EI, et al. Host susceptibility to periodontitis: mapping murine genomic regions. Journal of dental research. 2013;92(5):438-43.

155. Durrant C, Tayem H, Yalcin B, Cleak J, Goodstadt L, de Villena FP, et al. Collaborative Cross mice and their power to map host susceptibility to Aspergillus fumigatus infection. Genome Res. 2011;21(8):1239-48.

156. Bottomly D, Ferris MT, Aicher LD, Rosenzweig E, Whitmore A, Aylor DL, et al. Expression quantitative trait Loci for extreme host response to influenza a in pre-collaborative cross mice. G3. 2012;2(2):213-21.

157. Schmidtke, Merkle, Klingel, Hammerschmidt, Zautner, Wutzler. The viral genetic background determines the outcome of coxsackievirus B3 infection in outbred NMRI mice. Journal of medical virology. 2007;79(9):1334-42.

158. Merkle I, Tonew M, Glück B, Schmidtke M, Egerer R, Stelzner A. Coxsackievirus B3-induced chronic myocarditis in outbred NMRI mice. Journal of human virology. 1999;2(6):369-79.

159. Laflamme MA, Murry CE. Heart regeneration. Nature. 2011;473(7347):326-35.

160. Bergmann O, Bhardwaj RD, Bernard S, Zdunek S, Barnabe-Heider F, Walsh S, et al. Evidence for Cardiomyocyte Renewal in Humans. Science. 2009;324(5923):98-102.

161. Clark KA, McElhinny AS, Beckerle MC, Gregorio CC. Striated muscle cytoarchitecture: An intricate web of form and function. Annual Review of Cell and Developmental Biology. 2002;18:637-706.

162. Lehman W, Craig R, Vibert P. Ca2+-Induced Tropomyosin Movement in Limulus Thin-Filaments Revealed by 3-Dimensional Reconstruction. Nature. 1994;368(6466):65-7.

163. Sohl G, Willecke K. Gap junctions and the connexin protein family. Cardiovascular Research. 2004;62(2):228-32.

164. Kumar NM, Gilula NB. The gap junction communication channel. Cell. 1996;84(3):381-8.

165. Sanders V. Viral Myocarditis. Am Heart J. 1963;66:707-13.

166. Aretz H. Myocarditis: the Dallas criteria. Hum Pathol. 1987;18(6):619-24.

167. Baughman K. Diagnosis of myocarditis: death of Dallas criteria. Circulation. 2006;113(4):593-5.

168. Lieberman EB, Hutchins GM, Herskowitz A, Rose NR, Baughman KL. Clinicopathologic description of myocarditis. J Am Coll Cardiol. 1991;18(7):1617-26.

169. McCarthy RE, Boehmer JP, Hruban RH, Hutchins GM, Kasper EK, Hare JM, et al. Long-term outcome of fulminant myocarditis as compared with acute (nonfulminant) myocarditis. The New England journal of medicine. 2000;342(10):690-5.

170. Kindermann I, Barth C, Mahfoud F, Ukena C, Lenski M, Yilmaz A, et al. Update on myocarditis. J Am Coll Cardiol. 2012;59(9):779-92.

171. Kindermann I, Kindermann M, Kandolf R, Klingel K, Bultmann B, Muller T, et al. Predictors of outcome in patients with suspected myocarditis. Circulation. 2008;118(6):639-48.

172. Kindermann I, Kindermann M, Kandolf R, Klingel K, Bültmann B, Müller T, et al. Predictors of Outcome in Patients With Suspected Myocarditis. Circulation. 2008.

173. Chang AN, Potter JD. Sarcomeric protein mutations in dilated cardiomyopathy. Heart Fail Rev. 2005;10(3):225-35.

174. Poller W, Kühl U, Tschoepe C, Pauschinger M, Fechner H, Schultheiss H-P. Genome-environment interactions in the molecular pathogenesis of dilated cardiomyopathy. Journal of molecular medicine (Berlin, Germany). 2005;83(8):579-86.

175. Moimas S, Zacchigna S, Merlo M, Buiatti A, Anzini M, Dreas L, et al. Idiopathic dilated cardiomyopathy and persistent viral infection: Lack of association in a controlled study using a quantitative assay. Heart, lung & circulation. 2012.

176. D'Ambrosio A, Patti G, Manzoli A, Sinagra G, Di Lenarda A, Silvestri F, et al. The fate of acute myocarditis between spontaneous improvement and evolution to dilated cardiomyopathy: a review. Heart. 2001;85(5):499-504.

177. Ruppert V, Meyer T, Pankuweit S, Möller E, Funck RC, Grimm W, et al. Gene expression profiling from endomyocardial biopsy tissue allows distinction between subentities of dilated cardiomyopathy. The Journal of thoracic and cardiovascular surgery. 2008;136(2):360-9.e1.

178. DeBiasi RL, Robinson BA, Sherry B, Bouchard R, Brown RD, Rizeq M, et al. Caspase inhibition protects against reovirus-induced myocardial injury in vitro and in vivo. J Virol. 2004;78(20):11040-50.

179. Sherry B, Baty CJ, Blum MA. Reovirus-induced acute myocarditis in mice correlates with viral RNA synthesis rather than generation of infectious virus in cardiac myocytes. J Virol. 1996;70(10):6709-15.

180. Sherry B, Schoen FJ, Wenske E, Fields BN. Derivation and characterization of an efficiently myocarditic reovirus variant. J Virol. 1989;63(11):4840-9.

181. Carocci M, Bakkali-Kassimi L. The encephalomyocarditis virus. Virulence. 2012;3(4):351-67.

182. Carocci M, Cordonnier N, Huet H, Romey A, Relmy A, Gorna K, et al. Encephalomyocarditis virus 2A protein is required for viral pathogenesis and inhibition of apoptosis. J Virol. 2011;85(20):10741-54.

183. Hardarson HS, Baker JS, Yang Z, Purevjav E, Huang CH, Alexopoulou L, et al. Toll-like receptor 3 is an essential component of the innate stress response in virus-induced cardiac injury. American journal of physiology Heart and circulatory physiology. 2007;292(1):H251-8.

184. Gauntt C, Huber S. Coxsackievirus experimental heart diseases. Front Biosci. 2003;8:e23-35.

185. Yajima T, Knowlton KU. Viral myocarditis: from the perspective of the virus. Circulation. 2009;119(19):2615-24.

186. Li HS, Ligons DL, Rose NR. Genetic complexity of autoimmune myocarditis. Autoimmunity reviews. 2008;7(3):168-73.

187. Fairweather D, Kaya Z, Shellam GR, Lawson CM, Rose NR. From infection to autoimmunity. Journal of autoimmunity. 2001;16(3):175-86.

188. Wiltshire SA, Leiva-Torres GA, Vidal SM. Quantitative trait locus analysis, pathway analysis, and consomic mapping show genetic variants of Tnni3k, Fpgt, or H28 control susceptibility to viral myocarditis. Journal of immunology (Baltimore, Md : 1950). 2011;186(11):6398-405.

189. Weinzierl AO, Szalay G, Wolburg H, Sauter M, Rammensee H-G, Kandolf R, et al. Effective chemokine secretion by dendritic cells and expansion of cross-presenting CD4-/CD8+ dendritic cells define a protective phenotype in the mouse model of coxsackievirus myocarditis. Journal of virology. 2008;82(16):8149-60.

190. Deonarain R, Cerullo D, Fuse K, Liu P, Fish E. Protective role for interferon-beta in coxsackievirus B3 infection. Circulation. 2004;110(23):3540-3.

191. Woodruff JF, Woodruff JJ. Modification of severe coxsackievirus B 3 infection in marasmic mice by transfer of immune lymphoid cells. Proceedings of the National Academy of Sciences of the United States of America. 1971;68(9):2108-11.

192. Lim B, Shin J, Choe S, Choi S, Jeong J, Seong I, et al. Myocardial injury occurs earlier than myocardial inflammation in acute experimental viral myocarditis. Exp Mol Med. 2005;37(1):51-7.

193. Yajima T, Murofushi Y, Zhou H, Park S, Housman J, Zhong Z-H, et al. Absence of SOCS3 in the Cardiomyocyte Increases Mortality in a gp130-Dependent Manner Accompanied by Contractile Dysfunction and Ventricular Arrhythmias. Circulation. 2011.

194. Hoffmann JA. The immune response of Drosophila. Nature. 2003;426(6962):33-8.

195. Lemaitre B, Nicolas E, Michaut L, Reichhart JM, Hoffmann JA. The dorsoventral regulatory gene cassette spätzle/Toll/cactus controls the potent antifungal response in Drosophila adults. Cell. 1996;86(6):973-83.

196. Medzhitov R, Preston-Hurlburt P, Janeway CA. A human homologue of the Drosophila Toll protein signals activation of adaptive immunity. Nature. 1997;388(6640):394-7.

197. Qureshi ST, Larivière L, Leveque G, Clermont S, Moore KJ, Gros P, et al. Endotoxin-tolerant mice have mutations in Toll-like receptor 4 (Tlr4). The Journal of experimental medicine. 1999;189(4):615-25.

198. Poltorak A, He X, Smirnova I, Liu MY, Van Huffel C, Du X, et al. Defective LPS signaling in C3H/HeJ and C57BL/10ScCr mice: mutations in Tlr4 gene. Science (New York, NY). 1998;282(5396):2085-8.

199. Erridge C. Endogenous ligands of TLR2 and TLR4: agonists or assistants? J Leukoc Biol. 2010;87(6):989-99.

200. Kurt-Jones EA, Popova L, Kwinn L, Haynes LM, Jones LP, Tripp RA, et al. Pattern recognition receptors TLR4 and CD14 mediate response to respiratory syncytial virus. Nat Immunol. 2000;1(5):398-401.

201. Lund J, Sato A, Akira S, Medzhitov R, Iwasaki A. Toll-like receptor 9-mediated recognition of Herpes simplex virus-2 by plasmacytoid dendritic cells. The Journal of experimental medicine. 2003;198(3):513-20.

202. Hemmi H, Takeuchi O, Kawai T, Kaisho T, Sato S, Sanjo H, et al. A Toll-like receptor recognizes bacterial DNA. Nature. 2000;408(6813):740-5.

203. Beutler B, Jiang Z, Georgel P, Crozat K, Croker B, Rutschmann S, et al. Genetic analysis of host resistance: Toll-like receptor signaling and immunity at large. Annu Rev Immunol. 2006;24:353-89.

204. O'Neill LA, Bowie AG. The family of five: TIR-domain-containing adaptors in Toll-like receptor signalling. Nat Rev Immunol. 2007;7(5):353-64.

205. Beutler B, Eidenschenk C, Crozat K, Imler JL, Takeuchi O, Hoffmann JA, et al. Genetic analysis of resistance to viral infection. Nat Rev Immunol. 2007;7(10):753-66.

206. Hoebe K, Du X, Georgel P, Janssen E, Tabeta K, Kim SO, et al. Identification of Lps2 as a key transducer of MyD88-independent TIR signalling. Nature. 2003;424(6950):743-8.

207. Yamamoto M, Sato S, Mori K, Hoshino K, Takeuchi O, Takeda K, et al. Cutting edge: a novel Toll/IL-1 receptor domain-containing adapter that preferentially activates the IFN-beta promoter in the Toll-like receptor signaling. Journal of immunology (Baltimore, Md : 1950). 2002;169(12):6668-72.

208. Diebold SS, Montoya M, Unger H, Alexopoulou L, Roy P, Haswell LE, et al. Viral infection switches non-plasmacytoid dendritic cells into high interferon producers. Nature. 2003;424(6946):324-8.

209. Kato H, Takeuchi O, Sato S, Yoneyama M, Yamamoto M, Matsui K, et al. Differential roles of MDA5 and RIG-I helicases in the recognition of RNA viruses. Nature. 2006;441(7089):101-5.

210. Yoneyama M, Kikuchi M, Natsukawa T, Shinobu N, Imaizumi T, Miyagishi M, et al. The RNA helicase RIG-I has an essential function in double-stranded RNA-induced innate antiviral responses. Nature Immunology. 2004;5(7):730-7.

211. Pichlmair A, Sousa CRE. Innate recognition of viruses. Immunity. 2007;27(3):370-83.

212. Gitlin L, Barchet W, Gilfillan S, Cella M, Beutler B, Flavell RA, et al. Essential role of mda-5 in type I IFN responses to polyriboinosinic:polyribocytidylic acid and encephalomyocarditis picornavirus. Proc Natl Acad Sci U S A. 2006;103(22):8459-64.

213. Wu B, Peisley A, Richards C, Yao H, Zeng XH, Lin C, et al. Structural Basis for dsRNA Recognition, Filament Formation, and Antiviral Signal Activation by MDA5. Cell. 2013;152(1-2):276-89.

214. Kaufmann SHE, Rouse BT, Sacks DL. The immune response to infection. Washington, DC: ASM Press; 2011. xiii, 666 p. p.

215. Keating SE, Baran M, Bowie AG. Cytosolic DNA sensors regulating type I interferon induction. Trends Immunol. 2011;32(12):574-81.

216. Takaoka A, Wang Z, Choi MK, Yanai H, Negishi H, Ban T, et al. DAI (DLM-1/ZBP1) is a cytosolic DNA sensor and an activator of innate immune response. Nature. 2007;448(7152):501-5.

217. Burdette DL, Monroe KM, Sotelo-Troha K, Iwig JS, Eckert B, Hyodo M, et al. STING is a direct innate immune sensor of cyclic di-GMP. Nature. 2011;478(7370):515-8.

218. Wu J, Sun L, Chen X, Du F, Shi H, Chen C, et al. Cyclic GMP-AMP is an endogenous second messenger in innate immune signaling by cytosolic DNA. Science (New York, NY). 2013;339(6121):826-30.

219. Sun L, Wu J, Du F, Chen X, Chen ZJ. Cyclic GMP-AMP synthase is a cytosolic DNA sensor that activates the type I interferon pathway. Science (New York, NY). 2013;339(6121):786-91.

220. ISAACS A, Lindenmann J. Virus interference. I. The interferon. Proceedings of the Royal Society of London Series B, Containing papers of a Biological character Royal Society (Great Britain). 1957;147(927):258-67.

221. Sadler AJ, Williams BR. Interferon-inducible antiviral effectors. Nat Rev Immunol. 2008;8(7):559-68.

222. Schoggins JW, Wilson SJ, Panis M, Murphy MY, Jones CT, Bieniasz P, et al. A diverse range of gene products are effectors of the type I interferon antiviral response. Nature. 2011.

223. MacMicking JD. IFN-inducible GTPases and immunity to intracellular pathogens. Trends Immunol. 2004;25(11):601-9.

224. Perelygin AA, Scherbik SV, Zhulin IB, Stockman BM, Li Y, Brinton MA. Positional cloning of the murine flavivirus resistance gene. Proceedings of the National Academy of Sciences of the United States of America. 2002;99(14):9322-7.

225. Mashimo T, Lucas M, Simon-Chazottes D, Frenkiel M, Montagutelli X, Ceccaldi P, et al. A nonsense mutation in the gene encoding 2'-5'-oligoadenylate synthetase/L1

isoform is associated with West Nile virus susceptibility in laboratory mice. Proceedings of the National Academy of Sciences of the United States of America. 2002;99(17):11311-6.

226. Clemens MJ, Williams BR. Inhibition of cell-free protein synthesis by pppA2'p5'A2'p5'A: a novel oligonucleotide synthesized by interferon-treated L cell extracts. Cell. 1978;13(3):565-72.

227. Silverman RH. Viral encounters with 2',5'-oligoadenylate synthetase and RNase L during the interferon antiviral response. Journal of virology. 2007;81(23):12720-9.

228. Malathi K, Dong B, Gale M, Silverman RH. Small self-RNA generated by RNase L amplifies antiviral innate immunity. Nature. 2007;448(7155):816-9.

229. Morales DJ, Lenschow DJ. The antiviral activities of ISG15. Journal of molecular biology. 2013;425(24):4995-5008.

230. KewalRamani VN, Coffin JM. Virology. Weapons of mutational destruction. Science. 2003;301(5635):923-5.

231. Shi H, Kokoeva MV, Inouye K, Tzameli I, Yin H, Flier JS. TLR4 links innate immunity and fatty acid-induced insulin resistance. The Journal of clinical investigation. 2006;116(11):3015-25.

232. Strowig T, Henao-Mejia J, Elinav E, Flavell R. Inflammasomes in health and disease. Nature. 2012;481(7381):278-86.

233. Saleh M. The machinery of Nod-like receptors: refining the paths to immunity and cell death. Immunological Reviews. 2011;243:235-46.

234. Davis BK, Wen HT, Ting JPY. The Inflammasome NLRs in Immunity, Inflammation, and Associated Diseases. Annual Review of Immunology, Vol 29. 2011;29:707-35.

235. Wang JP, Cerny A, Asher DR, Kurt-Jones EA, Bronson RT, Finberg RW. MDA5 and MAVS mediate type I interferon responses to coxsackie B virus. J Virol. 2010;84(1):254-60.

236. Huhn MH, McCartney SA, Lind K, Svedin E, Colonna M, Flodstrom-Tullberg M. Melanoma differentiation-associated protein-5 (MDA-5) limits early viral replication but is not essential for the induction of type 1 interferons after Coxsackievirus infection. Virology. 2010;401(1):42-8.

237. Wessely R, Klingel K, Knowlton K, Kandolf R. Cardioselective infection with coxsackievirus B3 requires intact type I interferon signaling: implications for mortality and early viral replication. Circulation. 2001;103(5):756-61.

238. Mukherjee A, Morosky SA, Delorme-Axford E, Dybdahl-Sissoko N, Oberste MS, Wang T, et al. The Coxsackievirus B 3C Protease Cleaves MAVS and TRIF to Attenuate Host Type I Interferon and Apoptotic Signaling. PLoS pathogens. 2011;7(3):e1001311.

239. Feng Q, Langereis MA, Lork M, Nguyen M, Hato SV, Lanke K, et al. Enteroviruses 2Apro targets MDA5 and MAVS in infected cells. J Virol. 2014.

240. Negishi H, Osawa T, Ogami K, Ouyang X, Sakaguchi S, Koshiba R, et al. A critical link between Toll-like receptor 3 and type II interferon signaling pathways in antiviral innate immunity. Proceedings of the National Academy of Sciences of the United States of America. 2008;105(51):20446-51.

241. Richer MJ, Lavallee DJ, Shanina I, Horwitz MS. Toll-like receptor 3 signaling on macrophages is required for survival following coxsackievirus B4 infection. PLoS One. 2009;4(1):e4127.

242. Fairweather D, Yusung S, Frisancho S, Barrett M, Gatewood S, Steele R, et al. IL-12 receptor beta 1 and Toll-like receptor 4 increase IL-1 beta- and IL-18-associated myocarditis and coxsackievirus replication. Journal of immunology (Baltimore, Md : 1950). 2003;170(9):4731-7.

243. Fuse K, Chan G, Liu P, Gudgeon P, Husain M, Chen M, et al. Myeloid differentiation factor-88 plays a crucial role in the pathogenesis of Coxsackievirus B3-induced myocarditis and influences type I interferon production. Circulation. 2005;112(15):2276-85.

244. Riad A, Westermann D, Zietsch C, Savvatis K, Becher PM, Bereswill S, et al. TRIF Is a Critical Survival Factor in Viral Cardiomyopathy. Journal of immunology (Baltimore, Md : 1950). 2011.

245. Abston ED, Coronado MJ, Bucek A, Bedja D, Shin J, Kim JB, et al. Th2 Regulation of Viral Myocarditis in Mice: Different Roles for TLR3 versus TRIF in Progression to Chronic Disease. Clinical & developmental immunology. 2012;2012:129486.

246. Yoshimura A, Naka T, Kubo M. SOCS proteins, cytokine signalling and immune regulation. Nature reviews Immunology. 2007;7(6):454-65.

247. Yajima T, Yasukawa H, Jeon E, Xiong D, Dorner A, Iwatate M, et al. Innate defense mechanism against virus infection within the cardiac myocyte requiring gp130-STAT3 signaling. Circulation. 2006;114(22):2364-73.

248. Yasukawa H, Yajima T, Duplain H, Iwatate M, Kido M, Hoshijima M, et al. The suppressor of cytokine signaling-1 (SOCS1) is a novel therapeutic target for enterovirus-induced cardiac injury. The Journal of clinical investigation. 2003;111(4):469-78.

249. Spits H, Artis D, Colonna M, Diefenbach A, Di Santo JP, Eberl G, et al. Innate lymphoid cells--a proposal for uniform nomenclature. Nature reviews Immunology. 2013;13(2):145-9.

250. Lee SH, Miyagi T, Biron CA. Keeping NK cells in highly regulated antiviral warfare. Trends Immunol. 2007;28(6):252-9.

251. Pyzik M, Gendron-Pontbriand E-M, Fodil-Cornu N, Vidal SM. Self or nonself? That is the question: sensing of cytomegalovirus infection by innate immune receptors. Mamm Genome. 2011;22(1-2):6-18.

252. Kielczewska A, Pyzik M, Sun T, Krmpotic A, Lodoen MB, Munks MW, et al. Ly49P recognition of cytomegalovirus-infected cells expressing H2-Dk and CMV-encoded m04 correlates with the NK cell antiviral response. The Journal of experimental medicine. 2009;206(3):515-23.

253. Pyzik M, Kielczewska A, Vidal S. NK cell receptors and their MHC class I ligands in host response to cytomegalovirus: Insights from the mouse genome. Seminars in immunology. 2008.

254. Reiner SL. Decision making during the conception and career of CD4+ T cells. Nature reviews Immunology. 2009;9(2):81-2.

255. Janeway C, Travers P, Walport M, Shlomchik M. Immunobiology 5 : the immune system in health and disease. 5th ed. New York: Garland Pub.; 2001. xviii, 732 p. p.

256. Godeny EK, Gauntt CJ. In situ immune autoradiographic identification of cells in heart tissues of mice with coxsackievirus B3-induced myocarditis. Am J Pathol. 1987;129(2):267-76.

257. Godeny E, Gauntt C. Murine natural killer cells limit coxsackievirus B3 replication. Journal of immunology (Baltimore, Md : 1950). 1987;139(3):913-8.

258. Henke A, Huber S, Stelzner A, Whitton JL. The role of CD8+ T lymphocytes in coxsackievirus B3-induced myocarditis. J Virol. 1995;69(11):6720-8.

259. Yuan J, Liu Z, Lim T, Zhang H, He J, Walker E, et al. CXCL10 Inhibits Viral Replication Through Recruitment of Natural Killer Cells in Coxsackievirus B3-Induced Myocarditis. Circulation research. 2009.

260. Gebhard JR, Perry CM, Harkins S, Lane T, Mena I, Asensio VC, et al. Coxsackievirus B3-induced myocarditis: perforin exacerbates disease, but plays no detectable role in virus clearance. Am J Pathol. 1998;153(2):417-28.

261. Fairweather D, Frisancho-Kiss S, Yusung S, Barrett M, Davis S, Steele R, et al. IL-12 protects against coxsackievirus B3-induced myocarditis by increasing IFN-gamma and macrophage and neutrophil populations in the heart. Journal of immunology (Baltimore, Md : 1950). 2005;174(1):261-9.

262. Horwitz MS, Krahl T, Fine C, Lee J, Sarvetnick N. Protection from lethal coxsackievirus-induced pancreatitis by expression of gamma interferon. J Virol. 1999;73(3):1756-66.

263. Woodruff JF. Involvement of T lymphocytes in the pathogenesis of coxsackie virus B3 heart disease. Journal of immunology (Baltimore, Md : 1950). 1974;113(6):1726-34.

264. Wong CY, Woodruff JJ, Woodruff JF. Generation of cytotoxic T lymphocytes during coxsackievirus B-3 infection. I. Model and viral specificity1. Journal of immunology (Baltimore, Md : 1950). 1977;118(4):1159-64.

265. Rose NR. Life amidst the contrivances. Nature immunology. 2006;7(10):1009-11.

266. Wolfgram L, Beisel K, Rose NR. Heart-specific autoantibodies following murine coxsackievirus B3 myocarditis. The Journal of experimental medicine. 1985;161(5):1112-21.

267. Opavsky A, Penninger J, Aitken K, Wen W, Dawood F, Mak T, et al. Susceptibility to myocarditis is dependent on the response of alphabeta T lymphocytes to coxsackieviral infection. Circulation research. 1999;85(6):551-8.

268. Barnard DL. Current status of anti-picornavirus therapies. Current pharmaceutical design. 2006;12(11):1379-90.

269. Romero JR. Pleconaril: a novel antipicornaviral drug. Expert opinion on investigational drugs. 2001;10(2):369-79.

270. Bauer S, Gottesman G, Sirota L, Litmanovitz I, Ashkenazi S, Levi I. Severe Coxsackie virus B infection in preterm newborns treated with pleconaril. European journal of pediatrics. 2002;161(9):491-3.

271. Schmidtke M, Hammerschmidt E, Schuler S, Zell R, Birch-Hirschfeld E, Makarov VA, et al. Susceptibility of coxsackievirus B3 laboratory strains and clinical isolates to the capsid function inhibitor pleconaril: antiviral studies with virus chimeras demonstrate the crucial role of amino acid 1092 in treatment. J Antimicrob Chemother. 2005;56(4):648-56.

272. Matsumori A, Tomioka N, Kawai C. Protective effect of recombinant alpha interferon on coxsackievirus B3 myocarditis in mice. Am Heart J. 1988;115(6):1229-32.

273. Padalko E, Nuyens D, De Palma A, Verbeken E, Aerts J, De Clercq E, et al. The interferon inducer ampligen [poly(I)-poly(C12U)] markedly protects mice against coxsackie B3 virus-induced myocarditis. Antimicrob Agents Chemother. 2004;48(1):267-74.

274. Heim A, Canu A, Kirschner P, Simon T, Mall G, Hofschneider PH, et al. Synergistic interaction of interferon-beta and interferon-gamma in coxsackievirus B3-infected carrier cultures of human myocardial fibroblasts. J Infect Dis. 1992;166(5):958-65.

275. Kishimoto C, Crumpacker CS, Abelmann WH. Ribavirin treatment of murine coxsackievirus B3 myocarditis with analyses of lymphocyte subsets. J Am Coll Cardiol. 1988;12(5):1334-41.

276. Zell R, Markgraf R, Schmidtke M, Gorlach M, Stelzner A, Henke A, et al. Nitric oxide donors inhibit the coxsackievirus B3 proteinases 2A and 3C in vitro, virus production in cells, and signs of myocarditis in virus-infected mice. Med Microbiol Immunol. 2004;193(2-3):91-100.

277. Merl S, Michaelis C, Jaschke B, Vorpahl M, Seidl S, Wessely R. Targeting 2A protease by RNA interference attenuates coxsackieviral cytopathogenicity and promotes survival in highly susceptible mice. Circulation. 2005;111(13):1583-92.

278. Marchant D, Dou Y, Luo H, Garmaroudi FS, McDonough JE, Si X, et al. Bosentan enhances viral load via endothelin-1 receptor type-A-mediated p38 mitogen-activated protein kinase activation while improving cardiac function during coxsackievirus-induced myocarditis. Circ Res. 2009;104(6):813-21.

279. Gatmaitan BG, Chason JL, Lerner AM. Augmentation of the virulence of murine coxsackie-virus B-3 myocardiopathy by exercise. The Journal of experimental medicine. 1970;131(6):1121-36.

280. V de Noronha S, Sharma S, Papadakis M, Desai S, Whyte G, Sheppard M. Exercise Related Sudden Cardiac Death: The Experience of a Tertiary Referral Pathology Centre in the United Kingdom. Heart (British Cardiac Society). 2009.

281. Melnick JL, GODMAN GC. Pathogenesis of coxsackie virus infection; multiplication of virus and evolution of the muscle lesion in mice. The Journal of experimental medicine. 1951;93(3):247-66.

282. Wessely R, Klingel K, Knowlton KU, Kandolf R. Cardioselective infection with coxsackievirus B3 requires intact type I interferon signaling: implications for mortality and early viral replication. Circulation. 2001;103(5):756-61.

283. Fortin A, Diez E, Rochefort D, Laroche L, Malo D, Rouleau G, et al. Recombinant congenic strains derived from A/J and C57BL/6J: a tool for genetic dissection of complex traits. Genomics. 2001;74(1):21-35.

284. Aly M, Wiltshire S, Chahrour G, Osti JC, Vidal SM. Complex genetic control of host susceptibility to coxsackievirus B3-induced myocarditis. Genes Immun. 2007;8(3):193-204.

285. Rozen S, Skaletsky H. Primer3 on the WWW for general users and for biologist programmers. Methods Mol Biol. 2000;132:365-86.

286. Livak KJ, Schmittgen TD. Analysis of relative gene expression data using real-time quantitative PCR and the 2(-Delta Delta C(T)) Method. Methods (San Diego, Calif). 2001;25(4):402-8.

287. Yang H, Ding Y, Hutchins L, Szatkiewicz J, Bell T, Paigen B, et al. A customized and versatile high-density genotyping array for the mouse. Nature methods. 2009.

288. Xia Y, Won S, Du X, Lin P, Ross C, La Vine D, et al. Bulk segregation mapping of mutations in closely related strains of mice. Genetics. 2010;186(4):1139-46.

289. Box G CD. An Analysis of Transformations. Journal of the Royal Statistical Society Series B (Methodological). 1964:211-52.

290. Wiltshire SA, Diez E, Miao Q, Dubé M-P, Gagné M, Paquette O, et al. Genetic control of high density lipoprotein-cholesterol in AcB/BcA recombinant congenic strains of mice. Physiological genomics. 2012;44(17):843-52.

291. Min-Oo G, Fortin A, Tam M, Nantel A, Stevenson M, Gros P. Pyruvate kinase deficiency in mice protects against malaria. Nature genetics. 2003;35(4):357-62.

292. Bongfen SE, Rodrigue-Gervais I-G, Berghout J, Torre S, Cingolani P, Wiltshire SA, et al. An N-Ethyl-N-Nitrosourea (ENU)-Induced Dominant Negative Mutation in the JAK3 Kinase Protects against Cerebral Malaria. PLoS ONE. 2012;7(2):e31012.

293. Khetsuriani N, Lamonte-Fowlkes A, Oberst S, Pallansch M. Enterovirus surveillance--United States, 1970-2005. MMWR Surveill Summ. 2006;55(8):1-20.

294. CDC CfDCaP. Nonpolio enterovirus and human parechovirus surveillance --- United States, 2006--2008. MMWR Morbidity and mortality weekly report. 2010;59(48):1577-80.

295. Stadnick E, Dan M, Sadeghi A, Chantler JK. Attenuating mutations in coxsackievirus B3 map to a conformational epitope that comprises the puff region of VP2 and the knob of VP3. Journal of virology. 2004;78(24):13987-4002.

296. Schmidtke M, Merkle I, Klingel K, Hammerschmidt E, Zautner AE, Wutzler P. The viral genetic background determines the outcome of coxsackievirus B3 infection in outbred NMRI mice. J Med Virol. 2007;79(9):1334-42.

297. Gay RT, Belisle S, Beck MA, Meydani SN. An aged host promotes the evolution of avirulent coxsackievirus into a virulent strain. Proceedings of the National Academy of Sciences of the United States of America. 2006;103(37):13825-30.

298. Frisancho-Kiss S, Davis SE, Nyland JF, Frisancho JA, Cihakova D, Barrett MA, et al. Cutting Edge: Cross-regulation by TLR4 and T cell Ig mucin-3 determines sex differences in inflammatory heart disease. 2007;178(11):6710-4.

299. Frisancho-Kiss S, Nyland JF, Davis SE, Frisancho JA, Barrett MA, Rose NR, et al. Sex differences in coxsackievirus B3-induced myocarditis: IL-12Rbeta1 signaling and IFN-gamma increase inflammation in males independent from STAT4. Brain research. 2006;1126(1):139-47.

300. Boivin GA, Pothlichet J, Skamene E, Brown EG, Loredo-Osti JC, Sladek R, et al. Mapping of clinical and expression quantitative trait loci in a sex-dependent effect of host susceptibility to mouse-adapted influenza H3N2/HK/1/68. Journal of immunology. 2012;188(8):3949-60.

301. Coyne CB, Bozym R, Morosky SA, Hanna SL, Mukherjee A, Tudor M, et al. Comparative RNAi screening reveals host factors involved in enterovirus infection of polarized endothelial monolayers. Cell host & microbe. 2011;9(1):70-82.

302. Antoniak S, Owens AP, 3rd, Baunacke M, Williams JC, Lee RD, Weithauser A, et al. PAR-1 contributes to the innate immune response during viral infection. J Clin Invest. 2013;123(3):1310-22.

303. Esfandiarei M, Boroomand S, Suarez A, Si X, Rahmani M, McManus B. Coxsackievirus B3 activates nuclear factor kappa B transcription factor via a phosphatidylinositol-3 kinase/protein kinase B-dependent pathway to improve host cell viability. Cell Microbiol. 2007;9(10):2358-71.

304. Esfandiarei M, Luo H, Yanagawa B, Suarez A, Dabiri D, Zhang J, et al. Protein kinase B/Akt regulates coxsackievirus B3 replication through a mechanism which is not caspase dependent. J Virol. 2004;78(8):4289-98.

305. Diez E, Lee SH, Gauthier S, Yaraghi Z, Tremblay M, Vidal S, et al. Birc1e is the gene within the Lgn1 locus associated with resistance to Legionella pneumophila. Nat Genet. 2003;33(1):55-60.

306. Bortoluci KR, Medzhitov R. Control of infection by pyroptosis and autophagy: role of TLR and NLR. Cell Mol Life Sci. 2010;67(10):1643-51.

307. Suppiah V, Moldovan M, Ahlenstiel G, Berg T, Weltman M, Abate ML, et al. IL28B is associated with response to chronic hepatitis C interferon-alpha and ribavirin therapy. Nat Genet. 2009;41(10):1100-4.

308. Cooper LT, Jr. Myocarditis. N Engl J Med. 2009;360(15):1526-38.

309. Klingel K, Hohenadl C, Canu A, Albrecht M, Seemann M, Mall G, et al. Ongoing enterovirus-induced myocarditis is associated with persistent heart muscle infection: quantitative analysis of virus replication, tissue damage, and inflammation. Proceedings of the National Academy of Sciences of the United States of America. 1992;89(1):314-8.

310. Maisch B, Ristic AD, Portig I, Pankuweit S. Human viral cardiomyopathy. Front Biosci. 2003;8:s39-67.

311. Ligons DL, Guler ML, Li HS, Rose NR. A locus on chromosome 1 promotes susceptibility of experimental autoimmune myocarditis and lymphocyte cell death. Clin Immunol. 2009;130(1):74-82.

312. Xiong D, Yajima T, Lim BK, Stenbit A, Dublin A, Dalton ND, et al. Inducible cardiac-restricted expression of enteroviral protease 2A is sufficient to induce dilated cardiomyopathy. Circulation. 2007;115(1):94-102.

313. Garcia-Sastre A, Biron CA. Type 1 interferons and the virus-host relationship: a lesson in detente. Science. 2006;312(5775):879-82.

314. Biron CA, Nguyen KB, Pien GC, Cousens LP, Salazar-Mather TP. Natural killer cells in antiviral defense: function and regulation by innate cytokines. Annu Rev Immunol. 1999;17:189-220.

315. Negishi H, Osawa T, Ogami K, Ouyang X, Sakaguchi S, Koshiba R, et al. A critical link between Toll-like receptor 3 and type II interferon signaling pathways in antiviral innate immunity. Proc Natl Acad Sci U S A. 2008;105(51):20446-51.

316. Deonarain R, Cerullo D, Fuse K, Liu PP, Fish EN. Protective role for interferon-beta in coxsackievirus B3 infection. Circulation. 2004;110(23):3540-3.

317. Yuan J, Liu Z, Lim T, Zhang H, He J, Walker E, et al. CXCL10 inhibits viral replication through recruitment of natural killer cells in coxsackievirus B3-induced myocarditis. Circ Res. 2009;104(5):628-38.

318. Wolfgram LJ, Beisel KW, Herskowitz A, Rose NR. Variations in the susceptibility to Coxsackievirus B3-induced myocarditis among different strains of mice. J Immunol. 1986;136(5):1846-52.

319. Gorbea C, Makar KA, Pauschinger M, Pratt G, Bersola JL, Varela J, et al. A role for Toll-like receptor 3 variants in host susceptibility to enteroviral myocarditis and dilated cardiomyopathy. The Journal of biological chemistry. 2010;285(30):23208-23.

320. Nadeau JH, Singer JB, Matin A, Lander ES. Analysing complex genetic traits with chromosome substitution strains. Nat Genet. 2000;24(3):221-5.

321. Knowlton KU, Jeon ES, Berkley N, Wessely R, Huber S. A mutation in the puff region of VP2 attenuates the myocarditic phenotype of an infectious cDNA of the Woodruff variant of coxsackievirus B3. J Virol. 1996;70(11):7811-8.

322. Broman KW, Wu H, Sen S, Churchill GA. R/qtl: QTL mapping in experimental crosses. Bioinformatics. 2003;19(7):889-90.

323. Ng PC, Henikoff S. Accounting for human polymorphisms predicted to affect protein function. Genome Res. 2002;12(3):436-46.

324. de Veer MJ, Holko M, Frevel M, Walker E, Der S, Paranjape JM, et al. Functional classification of interferon-stimulated genes identified using microarrays. J Leukoc Biol. 2001;69(6):912-20.

325. Samarajiwa SA, Forster S, Auchettl K, Hertzog PJ. INTERFEROME: the database of interferon regulated genes. Nucleic Acids Res. 2009;37(Database issue):D852-7.

326. Huang da W, Sherman BT, Lempicki RA. Systematic and integrative analysis of large gene lists using DAVID bioinformatics resources. Nat Protoc. 2009;4(1):44-57.

327. Michal Blazejczyk MM, Robert Nadon. FlexArray: A statistical data analysis software for gene expression microarrays. Montreal: Genome Quebec; 2007.

328. Baldi P, Long AD. A Bayesian framework for the analysis of microarray expression data: regularized t -test and statistical inferences of gene changes. Bioinformatics. 2001;17(6):509-19.

329. Wheeler FC, Tang H, Marks OA, Hadnott TN, Chu PL, Mao L, et al. Tnni3k modifies disease progression in murine models of cardiomyopathy. PLoS Genet. 2009;5(9):e1000647.

330. Baig E, Fish EN. Distinct signature type I interferon responses are determined by the infecting virus and the target cell. Antivir Ther. 2008;13(3):409-22.

331. Yajima T, Knowlton KU. Viral myocarditis: from the perspective of the virus. Circulation. 2009;119(19):2615-24.

332. Yasukawa H, Yajima T, Duplain H, Iwatate M, Kido M, Hoshijima M, et al. The suppressor of cytokine signaling-1 (SOCS1) is a novel therapeutic target for enterovirus-induced cardiac injury. J Clin Invest. 2003;111(4):469-78.

333. Melnick JL. The poliomyelitis, encephalomyocarditis, and coxsackie groups of viruses. Bacteriol Rev. 1950;14(3):233-44.

334. Spanakis N, Manolis EN, Tsakris A, Tsiodras S, Panagiotopoulos T, Saroglou G, et al. Coxsackievirus B3 sequences in the myocardium of fatal cases in a cluster of acute myocarditis in Greece. J Clin Pathol. 2005;58(4):357-60.

335. Xia Y, Won S, Du X, Lin P, Ross C, La Vine D, et al. Bulk Segregation Mapping of Mutations in Closely Related Strains of Mice. Genetics. 2010.

336. Drake JW. The distribution of rates of spontaneous mutation over viruses, prokaryotes, and eukaryotes. Ann N Y Acad Sci. 1999;870:100-7.

337. Duffy S, Shackelton LA, Holmes EC. Rates of evolutionary change in viruses: patterns and determinants. Nat Rev Genet. 2008;9(4):267-76.

338. Barth AS, Kuner R, Buness A, Ruschhaupt M, Merk S, Zwermann L, et al. Identification of a common gene expression signature in dilated cardiomyopathy across independent microarray studies. J Am Coll Cardiol. 2006;48(8):1610-7.

339. Szalay G, Meiners S, Voigt A, Lauber J, Spieth C, Speer N, et al. Ongoing coxsackievirus myocarditis is associated with increased formation and activity of myocardial immunoproteasomes. Am J Pathol. 2006;168(5):1542-52.

340. Taylor LA, Carthy CM, Yang D, Saad K, Wong D, Schreiner G, et al. Host gene regulation during coxsackievirus B3 infection in mice: assessment by microarrays. Circ Res. 2000;87(4):328-34.

341. Jakel S, Kuckelkorn U, Szalay G, Plotz M, Textoris-Taube K, Opitz E, et al. Differential interferon responses enhance viral epitope generation by myocardial immunoproteasomes in murine enterovirus myocarditis. Am J Pathol. 2009;175(2):510-8.

342. Kozak CA, Su Y, Raj NB, Pitha PM. Identification and genetic mapping of differentially expressed genes in mice differing at the If1 interferon regulatory locus. Mamm Genome. 1999;10(9):853-7.

343. Verdino P, Witherden DA, Havran WL, Wilson IA. The molecular interaction of CAR and JAML recruits the central cell signal transducer PI3K. Science. 2010;329(5996):1210-4.

344. Huber SA, Moraska A, Choate M. T cells expressing the gamma delta T-cell receptor potentiate coxsackievirus B3-induced myocarditis. J Virol. 1992;66(11):6541-6.

345. Pastuszak I, Ketchum C, Hermanson G, Sjoberg EJ, Drake R, Elbein AD. GDP-L-fucose pyrophosphorylase. Purification, cDNA cloning, and properties of the enzyme. The Journal of biological chemistry. 1998;273(46):30165-74.

346. Zhao Y, Meng XM, Wei YJ, Zhao XW, Liu DQ, Cao HQ, et al. Cloning and characterization of a novel cardiac-specific kinase that interacts specifically with cardiac troponin I. J Mol Med. 2003;81(5):297-304.

347. Lai ZF, Chen YZ, Feng LP, Meng XM, Ding JF, Wang LY, et al. Overexpression of TNNI3K, a cardiac-specific MAP kinase, promotes P19CL6-derived cardiac myogenesis and prevents myocardial infarction-induced injury. Am J Physiol Heart Circ Physiol. 2008;295(2):H708-16.

348. Xiong D, Lee G, Badorff C, Dorner A, Lee S, Wolf P, et al. Dystrophin deficiency markedly increases enterovirus-induced cardiomyopathy: a genetic predisposition to viral heart disease. Nature medicine. 2002;8(8):872-7.

349. Vagnozzi RJ, Gatto GJ, Kallander LS, Hoffman NE, Mallilankaraman K, Ballard VLT, et al. Inhibition of the Cardiomyocyte-Specific Kinase TNNI3K Limits Oxidative Stress, Injury, and Adverse Remodeling in the Ischemic Heart. Science translational medicine. 2013;5(207):207ra141.

350. Wheeler FC, Tang H, Marks OA, Hadnott TN, Chu P-L, Mao L, et al. Tnni3k modifies disease progression in murine models of cardiomyopathy. PLoS genetics. 2009;5(9):e1000647.

351. Zhao Y, Meng X, Wei Y, Zhao X, Liu D, Cao H, et al. Cloning and characterization of a novel cardiac-specific kinase that interacts specifically with cardiac troponin I. Journal of molecular medicine (Berlin, Germany). 2003;81(5):297-304.

352. Wang X, Wang J, Su M, Wang C, Chen J, Wang H, et al. TNNI3K, a Cardiac-Specific Kinase, Promotes Physiological Cardiac Hypertrophy in Transgenic Mice. PLoS ONE. 2013;8(3).

353. Tang H, Xiao K, Mao L, Rockman HA, Marchuk DA. Overexpression of TNNI3K, a cardiac-specific MAPKKK, promotes cardiac dysfunction. Journal of molecular and cellular cardiology. 2013;54:101-11.

354. Wang H, Chen C, Song X, Chen J, Zhen Y, Sun K, et al. Mef2c is an essential regulatory element required for unique expression of the cardiac-specific CARK gene. Journal of cellular and molecular medicine. 2008;12(1):304-15.

355. Hamer PW, McGeachie JM, Davies MJ, Grounds MD. Evans Blue Dye as an in vivo marker of myofibre damage: optimising parameters for detecting initial myofibre membrane permeability. Journal of anatomy. 2002;200(Pt 1):69-79.

356. Schneider CA, Rasband WS, Eliceiri KW. NIH Image to ImageJ: 25 years of image analysis. Nat Methods. 2012;9(7):671-5.

357. Rusinova I, Forster S, Yu S, Kannan A, Masse M, Cumming H, et al. Interferome v2.0: an updated database of annotated interferon-regulated genes. Nucleic Acids Res. 2013;41(Database issue):D1040-6.

358. Wheeler F, Fernandez L, Carlson K, Wolf M, Rockman H, Marchuk D. QTL mapping in a mouse model of cardiomyopathy reveals an ancestral modifier allele affecting heart function and survival. Mamm Genome. 2005;16(6):414-23.

359. Kapadia S, Lee J, Torre-Amione G, Birdsall HH, Ma TS, Mann DL. Tumor necrosis factor-alpha gene and protein expression in adult feline myocardium after endotoxin administration. J Clin Invest. 1995;96(2):1042-52.

360. Peng T, Lu X, Lei M, Moe GW, Feng Q. Inhibition of p38 MAPK decreases myocardial TNF-alpha expression and improves myocardial function and survival in endotoxemia. Cardiovasc Res. 2003;59(4):893-900.

361. Klugman D, Berger J, Sable C, He J, Khandelwal S, Slonim A. Pediatric Patients Hospitalized with Myocarditis: A Multi-Institutional Analysis. Pediatric cardiology. 2009.

362. Wang JP, Asher DR, Chan M, Kurt-Jones EA, Finberg RW. Cutting Edge: Antibody-mediated TLR7-dependent recognition of viral RNA. Journal of immunology (Baltimore, Md : 1950). 2007;178(6):3363-7.

363. Triantafilou K, Triantafilou M. Coxsackievirus B4-induced cytokine production in pancreatic cells is mediated through toll-like receptor 4. Journal of virology. 2004;78(20):11313-20.

364. Poffenberger MC, Straka N, El Warry N, Fang D, Shanina I, Horwitz MS. Lack of IL-6 during coxsackievirus infection heightens the early immune response resulting in increased severity of chronic autoimmune myocarditis. PLoS ONE. 2009;4(7):e6207.

365. Jarasch N, Martin U, Kamphausen E, Zell R, Wutzler P, Henke A. Interferon-gamma-induced activation of nitric oxide-mediated antiviral activity of macrophages caused by a recombinant coxsackievirus B3. Viral immunology. 2005;18(2):355-64.

366. Kishimoto C, Kawamata H, Sakai S, Shinohara H, Ochiai H. Role of MIP-2 in coxsackievirus B3 myocarditis. Journal of molecular and cellular cardiology. 2000;32(4):631-8.

367. Luo H, Wong J, Wong B. Protein degradation systems in viral myocarditis leading to dilated cardiomyopathy. Cardiovascular research. 2009.

368. Shen Y, Xu W, Chu Y-W, Wang Y, Liu Q-S, Xiong S-D. Coxsackievirus group B type 3 infection upregulates expression of monocyte chemoattractant protein 1 in cardiac myocytes, which leads to enhanced migration of mononuclear cells in viral myocarditis. Journal of virology. 2004;78(22):12548-56.

369. Li HS, Ligons DL, Rose NR, Guler ML. Genetic differences in bone marrow-derived lymphoid lineages control susceptibility to experimental autoimmune myocarditis. Journal of immunology (Baltimore, Md : 1950). 2008;180(11):7480-4.

370. Kemball CC, Harkins S, Whitmire JK, Flynn CT, Feuer R, Whitton JL. Coxsackievirus B3 inhibits antigen presentation in vivo, exerting a profound and selective effect on the MHC class I pathway. PLoS pathogens. 2009;5(10):e1000618.

371. Mena I, Perry C, Harkins S, Rodriguez F, Gebhard J, Whitton J. The role of B lymphocytes in coxsackievirus B3 infection. The American journal of pathology. 1999;155(4):1205-15.

372. Gorbea C, Makar KA, Pauschinger M, Pratt G, Bersola JLF, Varela J, et al. A role for Toll-like receptor 3 variants in host susceptibility to enteroviral myocarditis and dilated cardiomyopathy. The Journal of biological chemistry. 2010;285(30):23208-23.

373. Nagueh SF, Shah G, Wu Y, Torre-Amione G, King NM, Lahmers S, et al. Altered titin expression, myocardial stiffness, and left ventricular function in patients with dilated cardiomyopathy. Circulation. 2004;110(2):155-62.

374. Zolk O, Frohme M, Maurer A, Kluxen FW, Hentsch B, Zubakov D, et al. Cardiac ankyrin repeat protein, a negative regulator of cardiac gene expression, is augmented in human heart failure. Biochem Biophys Res Commun. 2002;293(5):1377-82.

375. Zou Y, Evans S, Chen J, Kuo HC, Harvey RP, Chien KR. CARP, a cardiac ankyrin repeat protein, is downstream in the Nkx2-5 homeobox gene pathway. Development. 1997;124(4):793-804.

376. Barth AS, Kuner R, Buness A, Ruschhaupt M, Merk S, Zwermann L, et al. Identification of a common gene expression signature in dilated cardiomyopathy across independent microarray studies. Journal of the American College of Cardiology. 2006;48(8):1610-7.

377. Suzuki M, Carlson K, Marchuk D, Rockman H. Genetic modifier loci affecting survival and cardiac function in murine dilated cardiomyopathy. Circulation. 2002;105(15):1824-9.

378. Ono K, Han J. The p38 signal transduction pathway: activation and function. Cellular signalling. 2000;12(1):1-13.

379. Cuenda A, Rousseau S. p38 MAP-kinases pathway regulation, function and role in human diseases. Biochim Biophys Acta. 2007;1773(8):1358-75.

380. Scheidereit C. IkappaB kinase complexes: gateways to NF-kappaB activation and transcription. Oncogene. 2006;25(51):6685-705.

381. McCarthy RE, 3rd, Boehmer JP, Hruban RH, Hutchins GM, Kasper EK, Hare JM, et al. Long-term outcome of fulminant myocarditis as compared with acute (nonfulminant) myocarditis. N Engl J Med. 2000;342(10):690-5.

382. Sattar SA, Springthorpe VS, Karim Y, Loro P. Chemical disinfection of non-porous inanimate surfaces experimentally contaminated with four human pathogenic viruses. Epidemiology and infection. 1989;102(3):493-505.

383. Michel JB, Shen YK, Aiden AP, Veres A, Gray MK, Google Books T, et al. Quantitative analysis of culture using millions of digitized books. Science. 2011;331(6014):176-82.

384. Beck MA, Levander OA, Handy J. Selenium deficiency and viral infection. The Journal of nutrition. 2003;133(5 Suppl 1):1463S-7S.

385. Lee C, Maull E, Chapman N, Tracy S, Gauntt C. Genomic regions of coxsackievirus B3 associated with cardiovirulence. Journal of medical virology. 1997;52(3):341-7.

386. Shao H, Burrage LC, Sinasac DS, Hill AE, Ernest SR, O'Brien W, et al. Genetic architecture of complex traits: large phenotypic effects and pervasive epistasis. Proceedings of the National Academy of Sciences of the United States of America. 2008;105(50):19910-4.

387. Corsten MF, Schroen B, Heymans S. Inflammation in viral myocarditis: friend or foe? Trends Mol Med. 2012;18(7):426-37.

388. de Weerd NA, Vivian JP, Nguyen TK, Mangan NE, Gould JA, Braniff SJ, et al. Structural basis of a unique interferon-beta signaling axis mediated via the receptor IFNAR1. Nat Immunol. 2013;14(9):901-7.

389. Flodström-Tullberg M, Hultcrantz M, Stotland A, Maday A, Tsai D, Fine C, et al. RNase L and double-stranded RNA-dependent protein kinase exert complementary roles in islet cell defense during coxsackievirus infection. Journal of immunology (Baltimore, Md : 1950). 2005;174(3):1171-7.

390. Wang YX, da Cunha V, Vincelette J, White K, Velichko S, Xu Y, et al. Antiviral and myocyte protective effects of murine interferon-beta and -{alpha}2 in coxsackievirus B3-induced myocarditis and epicarditis in Balb/c mice. American journal of physiology Heart and circulatory physiology. 2007;293(1):H69-76.

391. Boyd JH, Mathur S, Wang Y, Bateman RM, Walley KR. Toll-like receptor stimulation in cardiomyoctes decreases contractility and initiates an NF-kappaB dependent inflammatory response. Cardiovasc Res. 2006;72(3):384-93.

392. Hornef MW, Frisan T, Vandewalle A, Normark S, Richter-Dahlfors A. Toll-like receptor 4 resides in the Golgi apparatus and colocalizes with internalized lipopolysaccharide in intestinal epithelial cells. J Exp Med. 2002;195(5):559-70.

393. Huber S, Shi C, Budd RC. Gammadelta T cells promote a Th1 response during coxsackievirus B3 infection in vivo: role of Fas and Fas ligand. J Virol. 2002;76(13):6487-94.

394. Wada H, Saito K, Kanda T, Kobayashi I, Fujii H, Fujigaki S, et al. Tumor necrosis factor-alpha (TNF-alpha) plays a protective role in acute viralmyocarditis in mice: A study using mice lacking TNF-alpha. Circulation. 2001;103(5):743-9.

395. Lowenstein CJ, Hill SL, Lafond-Walker A, Wu J, Allen G, Landavere M, et al. Nitric oxide inhibits viral replication in murine myocarditis. J Clin Invest. 1996;97(8):1837-43.

396. Zaragoza C, Ocampo C, Saura M, Leppo M, Wei X, Quick R, et al. The role of inducible nitric oxide synthase in the host response to Coxsackievirus myocarditis. Proceedings of the National Academy of Sciences of the United States of America. 1998;95(5):2469-74.

397. Flodstrom M, Horwitz MS, Maday A, Balakrishna D, Rodriguez E, Sarvetnick N. A critical role for inducible nitric oxide synthase in host survival following coxsackievirus B4 infection. Virology. 2001;281(2):205-15.

398. Zaragoza C, Ocampo CJ, Saura M, McMillan A, Lowenstein CJ. Nitric oxide inhibition of coxsackievirus replication in vitro. J Clin Invest. 1997;100(7):1760-7.

399. Hallen LC, Burki Y, Ebeling M, Broger C, Siegrist F, Oroszlan-Szovik K, et al. Antiproliferative activity of the human IFN-alpha-inducible protein IFI44. Journal of interferon & cytokine research : the official journal of the International Society for Interferon and Cytokine Research. 2007;27(8):675-80.

400. Lutton CW, Gauntt CJ. Coxsackievirus B3 infection alters plasma membrane of neonatal skin fibroblasts. J Virol. 1986;60(1):294-6.

401. Lai Z-F, Chen Y-Z, Feng L-P, Meng X-M, Ding J-F, Wang L-Y, et al. Overexpression of TNNI3K, a cardiac-specific MAP kinase, promotes P19CL6-derived cardiac myogenesis and prevents myocardial infarction-induced injury. American journal of physiology Heart and circulatory physiology. 2008;295(2):H708-16.

402. Kemball CC, Harkins S, Whitmire JK, Flynn CT, Feuer R, Whitton JL. Coxsackievirus B3 inhibits antigen presentation in vivo, exerting a profound and selective effect on the MHC class I pathway. PLoS Pathog. 2009;5(10):e1000618.